Linear-Response Theory of Spin Transport

Diplomarbeit

von Michael Andreas Sentef

Universität Augsburg
Lehrstuhl für Theoretische Physik III
Elektronische Korrelationen und Magnetismus

24. April 2006

Erstgutachter: Prof. Dr. Arno P. Kampf

Zweitgutachter: Prof. Dr. Thilo Kopp

Inhaltsverzeichnis

KAPITEL 1

Introduction

The application of spin-polarized currents for new electronic devices has recently become a topic of high interest [**1**–**4**]. The motivation is to use not only the charge of the electrons, but also their spin degree of freedom for information processing. In this context, the spin diffusion length appears as an important characteristic of materials. It is the length scale on which the spin polarization of currents decays. The spin diffusion coefficient, on the other hand, is directly related to the spin conductivity [**5**] of the material.

In this thesis we give a precise definition of the term *spin conductivity*. We derive a Kubo formula for its calculation *without* relying on the analogy to charge transport, as it is the case for example in Ref. [**6**], and proceed to evaluate it for two-dimensional antiferromagnetic insulators.

Outline of this thesis: Chapter 2 provides an introduction to the physics of Heisenberg antiferromagnets. We show how the quantum spin system can be treated approximately by means of a spin-wave approximation.

In Chapter 3 a definition of spin currents is given. We consider a Heisenberg system in an inhomogeneous magnetic field and apply linear-response theory to derive a Kubo formula for the spin conductivity. In addition, the influence of a time-dependent electric field on spin currents is examined. Finally, we discuss a possible setup to determine a Hall effect for spin transport.

The purpose of Chapter 4 is the evaluation of the spin conductivity via spin-wave theory. We use many-body techniques (Green functions and diagrammatic methods) to include dominant spin-wave scattering processes, which turn out to be important in order to remove unphysical singularities from linear (noninteracting) spin-wave results.

The results are summarized in Chapter 5 which focusses on the two-dimensional Heisenberg antiferromagnet with spins $S = \frac{1}{2}$.

KAPITEL 2

Spin Waves in Heisenberg Antiferromagnets

2.1. The XXZ Heisenberg Antiferromagnet

The Heisenberg antiferromagnet (HAFM) is a model for magnetic insulators, i. e., for systems with fixed spins of spin length S on a lattice. We study the XXZ model, where the parameter Δ takes into account anisotropies of the exchange interaction. $\Delta = 1$ models the isotropic HAFM, whereas the antiferromagnetic Ising model is recovered for $\Delta \to \infty$ (with a proper scaling of the exchange coupling J such that $J\Delta = \text{const}$).

The isotropic HAFM has been intensely studied, especially since the discovery of high-temperature superconductivity in the cuprates. Its behavior depends on the number of spatial dimensions d. In $d = 3$ the ground-state of the nearest-neighbor Heisenberg model on bipartite lattices has antiferromagnetic long-range order (LRO) for all values of S [**7**, **8**]. For $d = 2$ the Mermin-Wagner theorem [**9**, **10**] implies that no LRO can exist for any $T > 0$ if the LRO breaks a continuous symmetry. On the other hand, it has been shown that for $S \geq 1$ at $T = 0$ LRO exists on the square lattice [**11**] and on the hexagonal lattice [**12**]. For $S = \frac{1}{2}$ a rigorous proof is still missing (see [**13**] for a detailed review). There is, however, strong evidence for a long-range ordered ground state [**14**]. In the anisotropic regime with $\Delta > 1$ magnetic order may also occur at finite temperatures, since the anisotropic HAFM falls into the same universality class as the Ising model. For the 2D Ising model ($\Delta \to \infty$) Onsager [**15**] showed that there is a finite-temperature phase transition.

The Heisenberg Hamiltonian models the antiferromagnetic phase of several materials fairly well. A prominent example are the parent compounds of high-T_C superconducting cuprates, where copper-oxide planes are quasi-2D antiferromagnets [**13**]. The insulating phase of La_2CuO_4 (a high-temperature superconductor when properly doped with Sr or Ba) can be modeled by a 2D spin $S = \frac{1}{2}$ HAFM. We should mention that there are, however, some problems with this description. As an example, calculations of the Raman line shape [**16**] show that the experimental spectra are not exactly reproduced. This implies either a failure of the approximative spin-wave approach, or that the Heisenberg model itself is not sufficient to describe the excitation spectrum of the system. However, spin-wave calculations for more complicated models (e. g., including ring exchange [**17**]) reproduce experimental spectra more appropriately. For a more detailed discussion of the topic, see also Ref. [**18**]. As another example, K_2NiF_4 is well-described by a 2D spin $S = 1$ HAFM within spin-wave theory [**19, 20**]. We thus conclude that spin-wave theory yields at least qualitatively correct results for the HAFM [**13**], and that the HAFM model itself is capable of describing dominant low-energy excitations of a large class of materials.

The general XXZ Heisenberg antiferromagnet (with arbitrary exchange couplings $J_{ij} > 0$, an anisotropy parameter Δ and local spin operators $\boldsymbol{S}_i$ with $\boldsymbol{S}_i^2 = S(S+1)$) reads

$$\mathcal{H}_{\text{general}} = \sum_{ij} J_{ij} \left[\frac{1}{2}(S_i^+ S_j^- + S_i^- S_j^+) + \Delta S_i^z S_j^z \right]. \tag{2.1}$$

We are going to focus on the "simple" nearest-neighbor Heisenberg model, where the exchange couplings J_{ij} are zero for lattice sites i and j which are not nearest neighbors, and $J_{ij} = J$ for nearest neighbors i and j. The Hamiltonian is given by

$$\mathcal{H}_{\text{HAFM}} = J \sum_{\langle ij \rangle} \left[\frac{1}{2}(S_i^+ S_j^- + S_i^- S_j^+) + \Delta S_i^z S_j^z \right]. \tag{2.2}$$

It can be rewritten as

$$\mathcal{H}_{\text{HAFM}} = \mathcal{H}_{\text{XY}} + \Delta \mathcal{H}_{\text{ZZ}} \tag{2.3}$$

with

$$\mathcal{H}_{\text{XY}} = J \sum_{\langle ij \rangle} \frac{1}{2}(S_i^+ S_j^- + S_i^- S_j^+) \tag{2.4}$$

and

$$\mathcal{H}_{\text{ZZ}} = J \sum_{\langle ij \rangle} S_i^z S_j^z. \tag{2.5}$$

The sum $\langle ij \rangle$ runs over bonds in a bipartite lattice (avoiding double counting of pairs i, j). For simplicity, we assume a simple hypercubic lattice with lattice constant $a = 1$, i. e., a square lattice in the two-dimensional case or a simple cubic (sc) lattice in three dimensions. Sites i belong to the sublattice A and sites j belong to the sublattice B. The total number of sites is N. The parameter Δ allows to include anisotropies. Special cases are $\Delta = 1$ (isotropic case, "standard" Heisenberg magnet), $\Delta = 0$ (XY model) and $\Delta \to \infty$ (Ising model). The units are chosen such that $J > 0$ has dimensions of an energy and the spin operators are dimensionless.

In order to apply standard many-body techniques we will use spin-wave theory, which requires a long-range ordered ground state. There are several slightly different ways to do this. One possibility is the Holstein-Primakoff representation [**21**] which has been extended to the HAFM by Anderson [**22**], Kubo [**23**] and Oguchi [**24**]. We will use the Dyson-Maleev (DM) transformation [**25, 26**]. The different representations are equivalent as long as spin-wave interactions are ignored, but the DM formalism is more convenient if one needs to go beyond linear spin-wave theory within a perturbation scheme. The disadvantage of the DM transformation is its non-Hermiticity. In principle, this may cause some problems, but the computation of physical observables is usually unhampered (see Ref. [**16**] and references therein).

2.2. Spin Waves

2.2.1. Standard Definition of Dyson-Maleev Spin Waves. We follow Canali and Girvin [**16**] who used the Dyson-Maleev representation [**25**, **26**] for the calculation of the Raman line shape of a two-dimensional HAFM including spin-wave interactions.

The Dyson-Maleev representation, which is non-Hermitian ($S^- \neq (S^+)^\dagger$), reads

$$\begin{aligned} S_i^z &= S - a_i^\dagger a_i, \\ S_i^+ &= \sqrt{2S}\left[1 - \frac{a_i^\dagger a_i}{2S}\right] a_i, \\ S_i^- &= \sqrt{2S} a_i^\dagger, \end{aligned} \tag{2.6}$$

for sublattice A, and

$$\begin{aligned} S_j^z &= -S + b_j^\dagger b_j, \\ S_j^+ &= \sqrt{2S} b_j^\dagger \left[1 - \frac{b_j^\dagger b_j}{2S}\right], \\ S_j^- &= \sqrt{2S} b_j, \end{aligned} \tag{2.7}$$

for sublattice B. The correct spin algebra is preserved if the a's and b's obey bosonic commutation relations and $[a^\dagger, b] = 0$.

The physical picture for this representation is the following: Consider a spin $S = \frac{1}{2}$ on site i. In the classical Néel state, the spin is in an eigenstate of the S_i^z operator with eigenvalue $+\frac{1}{2}$ ("up", $\uparrow$). The operator S_i^- flips the spin into a state with eigenvalue $-\frac{1}{2}$ ("down", $\downarrow$). In the linear spin-wave approximation (where $1 - \frac{a_i^\dagger a_i}{2S} \approx 1$) one boson is created ($a_i^\dagger$). The physical states are those with $\langle n \rangle \leq 2S$, where n is the number operator for a or b bosons, $n_i = a_i^\dagger a_i$ or $n_j = b_j^\dagger b_j$. Other states are unphysical since more bosons in one state would lead to a spin state with $\langle S_i^z \rangle > S$. We will come back to this point at the end of this section.

The spin Hamiltonian is turned into the following non-Hermitian bosonic Hamiltonian:

$$\mathcal{H}_{\mathrm{DM}} = E_0' + H_0' + V_{\mathrm{DM}}' \tag{2.8}$$

where

$$E'_0 = -\frac{N}{2}\Delta J S^2 z, \tag{2.9}$$

$$H'_0 = \Delta J S z \left[\sum_i a_i^\dagger a_i + \sum_j b_j^\dagger b_j\right] + JS\sum_{\langle ij\rangle}\left(a_i^\dagger b_j^\dagger + a_i b_j\right), \tag{2.10}$$

$$V'_{\mathrm{DM}} = -J\sum_{\langle ij\rangle}\left[\Delta a_i^\dagger a_i b_j^\dagger b_j + \frac{1}{2}\left(a_i^\dagger a_i a_i b_j + a_i^\dagger b_j^\dagger b_j^\dagger b_j\right)\right]. \tag{2.11}$$

Here z is the coordination number of the lattice, e. g., $z = 4$ for a two-dimensional square lattice.

We introduce the Fourier transform of the boson operators in the way it is usually written [**27**], namely with different signs in the exponentials for the two sublattices:

$$a_i = \sqrt{\frac{2}{N}}\sum_{\boldsymbol{k}} e^{-i\boldsymbol{k}\cdot\boldsymbol{R}_i} a_{\boldsymbol{k}}, \tag{2.12}$$

$$b_j = \sqrt{\frac{2}{N}}\sum_{\boldsymbol{k}} e^{+i\boldsymbol{k}\cdot\boldsymbol{R}_j} b_{\boldsymbol{k}}, \tag{2.13}$$

where $\boldsymbol{k}$ runs over the (antiferro-)magnetic Brillouin zone (MBZ, see Fig. 2.1). The

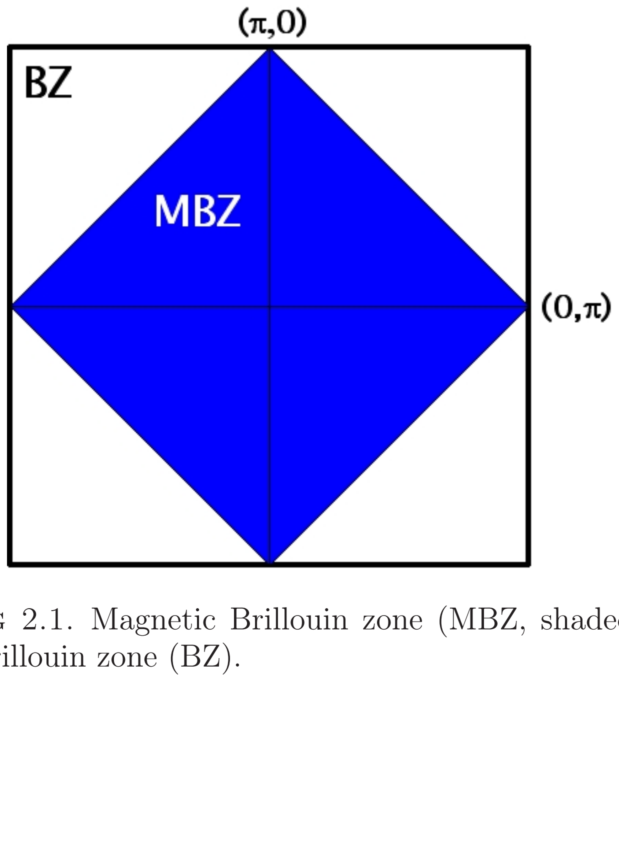

ABBILDUNG 2.1. Magnetic Brillouin zone (MBZ, shaded area) and standard Brillouin zone (BZ).

quadratic part H_0' is then given by

$$H_0' = E_0'' + H_0'', \tag{2.14}$$

$$E_0'' = -\frac{N}{2}\Delta JSz, \tag{2.15}$$

$$H_0'' = JSz\sum_{\boldsymbol{k}}\left[\gamma_{\boldsymbol{k}}(a_{\boldsymbol{k}}b_{\boldsymbol{k}} + b_{\boldsymbol{k}}^\dagger a_{\boldsymbol{k}}^\dagger) + \Delta(a_{\boldsymbol{k}}a_{\boldsymbol{k}}^\dagger + b_{\boldsymbol{k}}^\dagger b_{\boldsymbol{k}})\right], \tag{2.16}$$

where we have defined

$$\gamma_{\boldsymbol{k}} \equiv \frac{1}{z}\sum_{\delta} e^{ia\boldsymbol{k}\cdot\delta} = \frac{1}{d}\sum_{\alpha=1}^{d}\cos(k_\alpha a), \tag{2.17}$$

the sum over δ is over the z unit vectors connecting a given site with its nearest neighbors, d is the number of spatial dimensions and a the lattice constant (which will be set equal to 1 in the following).

For a two-dimensional square lattice we have $\delta = \pm\boldsymbol{x}, \pm\boldsymbol{y}$, where $\boldsymbol{x}$ and $\boldsymbol{y}$ are the x- and y-directions along the bonds of the square lattice. In this case,

$$\gamma_{\boldsymbol{k}} = \frac{\cos(k_x) + \cos(k_y)}{2}. \tag{2.18}$$

Let us introduce a matrix notation for H_0'':

$$H_0'' = JSz\sum_{\boldsymbol{k}}\begin{bmatrix} a_{\boldsymbol{k}}, & b_{\boldsymbol{k}}^\dagger \end{bmatrix}\begin{bmatrix} \Delta & -\gamma_{\boldsymbol{k}} \\ \gamma_{\boldsymbol{k}} & -\Delta \end{bmatrix}\begin{bmatrix} a_{\boldsymbol{k}}^\dagger \\ -b_{\boldsymbol{k}} \end{bmatrix}. \tag{2.19}$$

We can now diagonalize the matrix, which leads to the eigenvalues

$$\lambda_{\boldsymbol{k}} = \pm\sqrt{\Delta^2 - \gamma_{\boldsymbol{k}}^2}. \tag{2.20}$$

The corresponding eigenvectors are $[u_{\boldsymbol{k}}, v_{\boldsymbol{k}}]$, where

$$u_{\boldsymbol{k}} = \sqrt{\frac{\Delta + \lambda_{\boldsymbol{k}}}{2\lambda_{\boldsymbol{k}}}}, \tag{2.21}$$

$$v_{\boldsymbol{k}} = -\mathrm{sgn}(\gamma_{\boldsymbol{k}})\sqrt{\frac{\Delta - \lambda_{\boldsymbol{k}}}{2\lambda_{\boldsymbol{k}}}}. \tag{2.22}$$

These coefficients obey

$$u_{\boldsymbol{k}}^2 - v_{\boldsymbol{k}}^2 = 1, \tag{2.23}$$

$$u_{\boldsymbol{k}}^2 + v_{\boldsymbol{k}}^2 = \frac{\Delta}{\lambda_{\boldsymbol{k}}}, \tag{2.24}$$

$$u_{\boldsymbol{k}} v_{\boldsymbol{k}} = -\frac{\gamma_{\boldsymbol{k}}}{2\lambda_{\boldsymbol{k}}}. \tag{2.25}$$

We can write H_0'' in the following way:

$$\begin{aligned} H_0'' &= JSz \sum_{\boldsymbol{k}} \begin{bmatrix} a_{\boldsymbol{k}}, & b_{\boldsymbol{k}}^\dagger \end{bmatrix} \mathcal{U}\mathcal{U}^{-1} \begin{bmatrix} \Delta & -\gamma_{\boldsymbol{k}} \\ \gamma_{\boldsymbol{k}} & -\Delta \end{bmatrix} \mathcal{U}\mathcal{U}^{-1} \begin{bmatrix} a_{\boldsymbol{k}}^\dagger \\ -b_{\boldsymbol{k}} \end{bmatrix} \\ &= JSz \sum_{\boldsymbol{k}} \begin{bmatrix} \alpha_{\boldsymbol{k}}, & \beta_{\boldsymbol{k}}^\dagger \end{bmatrix} \begin{bmatrix} \lambda_{\boldsymbol{k}} & 0 \\ 0 & -\lambda_{\boldsymbol{k}} \end{bmatrix} \begin{bmatrix} \alpha_{\boldsymbol{k}}^\dagger \\ -\beta_{\boldsymbol{k}} \end{bmatrix}, \end{aligned}$$

where we have introduced

$$\mathcal{U} = \begin{bmatrix} u_{\boldsymbol{k}} & v_{\boldsymbol{k}} \\ v_{\boldsymbol{k}} & u_{\boldsymbol{k}} \end{bmatrix}, \tag{2.26}$$

$$\mathcal{U}^{-1} = \begin{bmatrix} u_{\boldsymbol{k}} & -v_{\boldsymbol{k}} \\ -v_{\boldsymbol{k}} & u_{\boldsymbol{k}} \end{bmatrix}. \tag{2.27}$$

The new operators $\alpha_{\boldsymbol{k}}$ and $\beta_{\boldsymbol{k}}$ are defined by

$$a_{\boldsymbol{k}} = u_{\boldsymbol{k}}\alpha_{\boldsymbol{k}} + v_{\boldsymbol{k}}\beta_{\boldsymbol{k}}^\dagger, \tag{2.28}$$

$$b_{\boldsymbol{k}} = u_{\boldsymbol{k}}\beta_{\boldsymbol{k}} + v_{\boldsymbol{k}}\alpha_{\boldsymbol{k}}^\dagger. \tag{2.29}$$

We obtain

$$\mathcal{H}_{\mathrm{DM}} = E_0''' + H_0''' + V_{\mathrm{DM}}', \tag{2.30}$$

where

$$E_0''' = -\frac{N}{2}\Delta JS(S+1)z + JSz\sum_{\boldsymbol{k}} \lambda_{\boldsymbol{k}}, \tag{2.31}$$

$$H_0''' = JSz\sum_{\boldsymbol{k}} \lambda_{\boldsymbol{k}}(\alpha_{\boldsymbol{k}}^\dagger\alpha_{\boldsymbol{k}} + \beta_{\boldsymbol{k}}^\dagger\beta_{\boldsymbol{k}}). \tag{2.32}$$

When V'_{DM} is written in terms of α's and β's via (2.28, 2.29), one gets a sum of quartic terms. If they are normal-ordered, the result is [**16**]

$$V'_{\mathrm{DM}} = -\frac{N}{2}\Delta J S^2 \left[\frac{r}{2S}\right]^2 z + JSz\frac{r}{2S}\sum_{\boldsymbol{k}} \lambda_{\boldsymbol{k}}(\alpha^\dagger_{\boldsymbol{k}}\alpha_{\boldsymbol{k}} + \beta^\dagger_{\boldsymbol{k}}\beta_{\boldsymbol{k}}) + V_{\mathrm{DM}}, \tag{2.33}$$

where the numerical constant r is defined as

$$r \equiv 1 - \frac{2}{N}\sum_{\boldsymbol{k}} \frac{\lambda_{\boldsymbol{k}}}{\Delta}. \tag{2.34}$$

For $d = 2$ and $\Delta = 1$ it is approximately equal to 0.158.

The normal-ordered interaction part V_{DM} reads

$$\boxed{\begin{aligned} V_{\mathrm{DM}} &\equiv \; : V'_{\mathrm{DM}} : \\ &= -\Delta J \tfrac{z}{4}\tfrac{2}{N}\textstyle\sum_{(1234)} \delta_{\boldsymbol{G}}(1+2-3-4) \\ &\times \Big[V^{(1)}_{(1234)}\alpha^\dagger_1\alpha^\dagger_2\alpha_3\alpha_4 + V^{(2)}_{(1234)}\alpha^\dagger_1\beta_2\alpha_3\alpha_4 + V^{(3)}_{(1234)}\alpha^\dagger_1\alpha^\dagger_2\beta^\dagger_3\alpha_4 \\ &\quad + V^{(4)}_{(1234)}\alpha^\dagger_1\alpha_3\beta^\dagger_4\beta_2 + V^{(5)}_{(1234)}\beta^\dagger_4\alpha_3\beta_2\beta_1 + V^{(6)}_{(1234)}\beta^\dagger_4\beta^\dagger_3\alpha^\dagger_2\beta_1 \\ &\quad + V^{(7)}_{(1234)}\alpha^\dagger_1\alpha^\dagger_2\beta^\dagger_3\beta^\dagger_4 + V^{(8)}_{(1234)}\beta_1\beta_2\alpha_3\alpha_4 + V^{(9)}_{(1234)}\beta^\dagger_4\beta^\dagger_3\beta_2\beta_1 \Big]. \end{aligned}} \tag{2.35}$$

Before we comment on the interaction part V_{DM}, we give the final result for the Dyson-Maleev Hamiltonian. Putting Equations (2.30), (2.31), (2.32) and (2.33) together, we can rewrite $\mathcal{H}_{\mathrm{DM}}$ in the following way:

$$\boxed{\mathcal{H}_{\mathrm{DM}} = E_0 + H_0 + V_{\mathrm{DM}},} \tag{2.36}$$

where the energy E_0 of the magnon vacuum is given by

$$\boxed{E_0 = -\frac{N}{2}\Delta J S^2[\alpha(S)]^2 z,} \tag{2.37}$$

where

$$\alpha(S) \equiv 1 + \frac{r}{2S}, \tag{2.38}$$

which is approximately equal to 1.158 for $d = 2$, $S = \frac{1}{2}$ and $\Delta = 1$. The contributions to the constant and quadratic parts coming from the normal-ordering are known as Oguchi corrections [**24**] to the ground-state energy and the spin-wave dispersion, respectively.

The quadratic part H_0 describes a gas of noninteracting magnons of two different species (α and β) with the same dispersion[1]:

$$\boxed{H_0 = \sum_{\boldsymbol{k}} \hbar\Omega_{\boldsymbol{k}}(\alpha^\dagger_{\boldsymbol{k}}\alpha_{\boldsymbol{k}} + \beta^\dagger_{\boldsymbol{k}}\beta_{\boldsymbol{k}}),} \tag{2.39}$$

where the spin-wave dispersion is

$$\Omega_{\boldsymbol{k}} = \frac{JS\alpha(S)z}{\hbar}\lambda_{\boldsymbol{k}} = \frac{JS\alpha(S)z}{\hbar}\sqrt{\Delta^2 - \gamma^2_{\boldsymbol{k}}}. \tag{2.40}$$

Note that it becomes imaginary for small $\boldsymbol{k}$ if we consider $|\Delta| < 1$ (XY regime). This is unphysical and can be regarded as a consequence of the low-energy physics of the XY regime which differs qualitatively from the regime $\Delta > 1$ since there are not only spin waves, but also vortex excitations.

The maximum magnon energy is

$$E_{\max} = \hbar\Omega_{\max} = \Delta JS\alpha(S)z. \tag{2.41}$$

It is important to note that the magnon vacuum (corresponding to the energy E_0) is *not* the ground state of the interacting system. When we calculate expectation values at $T = 0$ ($\langle\ldots\rangle = \langle\Psi_0|\ldots|\Psi_0\rangle$) we may identify the magnon vacuum with the ground state $|\Psi_0\rangle$ only in the noninteracting-magnon approximation.

Furthermore, the magnon vacuum is *not* the classical Néel state from which we have started. This can be easily seen from $E_0 = -\frac{N}{2}\Delta JS^2[\alpha(S)]^2 z < -\frac{N}{2}\Delta JS^2 z = E_{\mathrm{Neel}}$. Mathematically speaking, this is due to the Bogoliubov transformation which combines a- and b-type bosons to α- and β-magnons with a different vacuum state. The physical picture is that the magnon vacuum is a superposition of states with several numbers of "flipped bonds" with respect to the Néel state, i. e., bonds where the $\uparrow$-spin is flipped down and the $\downarrow$-spin is flipped up (see Fig. 2.2). Although the Néel state has the lowest possible energy with respect to the Ising term H_{ZZ}, the superposition including states with higher H_{ZZ}-energy leads to a lowering of the total energy due to the spin-flip term H_{XY}. The quantum-mechanical superposition (which is just a linear combination of quantum states) is not an eigenstate of any

[1]We will generally use $\hbar = 1$, but nevertheless $\hbar$ will appear in some formulae for clarity reasons. A detailed dicussion of dimensions is given in Appendix A.

given local spin operator S_i^z. One therefore says that the magnon vacuum contains quantum fluctuations.

The quartic interaction V_{DM} given in Equation (2.35) contains nine terms. The coefficients $V_{(1234)}^{(i)}$, $i = 1, \ldots, 9$, can be calculated by applying the Bogoliubov transformation (2.28), (2.29) to the Fourier transform of (2.11) and subsequent normal ordering. We will need to do this in order to calculate the spin conductivity at $T = 0$. We will then have to compute a spin-current correlation function in Dyson-Maleev representation, something comparable to a two-particle propagator in the language of many-particle theory. We will see that, at the lowest order including interactions, we will only have to compute the vertex function $V_{(1234)}^{(4)}$ explicitly, which will be done once needed. For the moment, it is enough to know that the $V_{(1234)}^{(i)}$ are functions of u's, v's and γ's with arguments containing the wave vectors $\boldsymbol{k}_1, \boldsymbol{k}_2, \boldsymbol{k}_3, \boldsymbol{k}_4$ abbreviated by $1, 2, 3, 4$.

In Equation (2.35), the Kronecker delta, $\delta_{\boldsymbol{G}}(1+2-3-4)$, expresses the conservation of momentum to within a reciprocal-lattice vector $\boldsymbol{G}$. It has to be interpreted as follows:

$$\delta_{\boldsymbol{G}}(1+2-3-4) \Rightarrow \boldsymbol{k}_4 = \boldsymbol{k}_1 + \boldsymbol{k}_2 - \boldsymbol{k}_3 + \boldsymbol{G}. \tag{2.42}$$

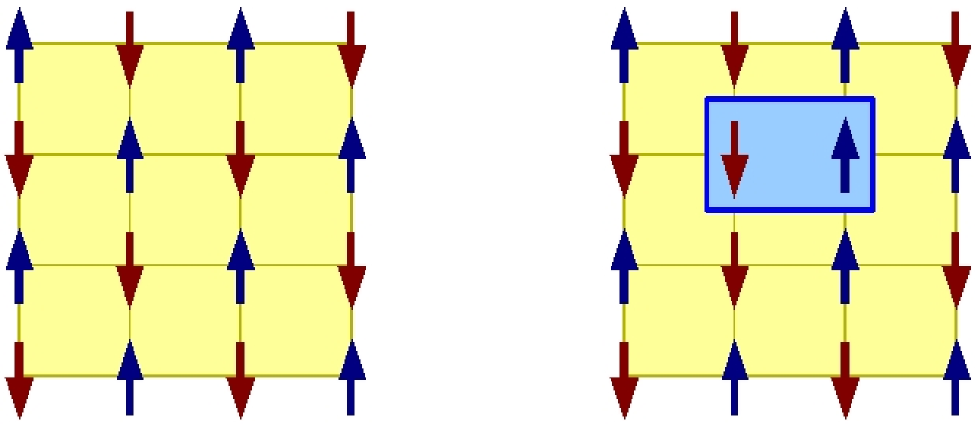

ABBILDUNG 2.2. Néel state (left) and state with a flipped bond (right). Each arrow schematically depicts the local magnetic moment on a lattice site.

Thus, $\boldsymbol{k}_1, \boldsymbol{k}_2, \boldsymbol{k}_3$ vary freely inside the HAFM Brillouin zone and $\boldsymbol{G}$ is the vector of the reciprocal lattice which "umklapps" the sum $\boldsymbol{k}_1 + \boldsymbol{k}_2 - \boldsymbol{k}_3$ back to the HAFM Brillouin zone, and $\boldsymbol{G}$ is equal to zero whenever the sum is already inside the HAFM Brillouin zone.

One should note that V_{DM} is not simply a two-body interaction since there are terms, like $V^{(7)}_{(1234)}\alpha^\dagger_1\alpha^\dagger_2\beta^\dagger_3\beta^\dagger_4$, describing the simultaneous creation of four magnons. Furthermore, it is nonlocal since the vertex functions $V^{(i)}_{(1234)}$ depend not only on the momentum transfer between particles, but also on their momenta separately. Finally, V_{DM} is non-Hermitian, so one should avoid implicitly assuming $V_{\mathrm{DM}} = V^\dagger_{\mathrm{DM}}$.

The whole spin-wave scheme only works if there is LRO, since the spin waves are excitations around a long-range ordered ground state. The procedure can be regarded as an expansion in $1/S$. One might ask if it is allowed to do this for $S = \frac{1}{2}$. We have seen that the bosonic representation requires $n_i \leq 2S = 1$. We can calculate the expectation value $\langle n_i \rangle$ of the number operator. In $d = 2$ at $T = 0$ (and for noninteracting magnons) the result is

$$\langle n_i \rangle = \frac{1}{2}\left(\left[\frac{2}{N}\sum_{\boldsymbol{k}} \frac{\Delta}{\lambda_{\boldsymbol{k}}}\right] - 1\right) \overset{\Delta=1}{\approx} 0.197. \tag{2.43}$$

This can be interpreted as an *a posteriori* justification for the spin-wave approximation in 2D at zero temperature even for $S = \frac{1}{2}$.

2.2.2. Alternative Definition of Dyson-Maleev Spin Waves. In order to determine the symmetry properties of the DM spin-current operator we now change the sign in the Fourier transformation (2.12) on sublattice A,

$$a_i = \sqrt{\frac{2}{N}} \sum_{\boldsymbol{k}} e^{+i\boldsymbol{k}\cdot\boldsymbol{R}_i} a_{\boldsymbol{k}}. \tag{2.44}$$

Then, Equation (2.19) becomes

$$H''_0 = JSz \sum_{\boldsymbol{k}} \begin{bmatrix} a_{\boldsymbol{k}}, & b^\dagger_{-\boldsymbol{k}} \end{bmatrix} \begin{bmatrix} \Delta & -\gamma_{\boldsymbol{k}} \\ \gamma_{\boldsymbol{k}} & -\Delta \end{bmatrix} \begin{bmatrix} a^\dagger_{\boldsymbol{k}} \\ -b_{-\boldsymbol{k}} \end{bmatrix}, \tag{2.45}$$

where, due to the inversion symmetry of $\gamma_{\boldsymbol{k}}$, we could also put the $-\boldsymbol{k}$-arguments on the a's instead of the b's. The eigenvalues (2.20) and the u's (2.21) and v's (2.22) are unaffected, but the Bogoliubov transformation (2.28, 2.29) now reads

$$a_{\boldsymbol{k}} = u_{\boldsymbol{k}}\alpha_{\boldsymbol{k}} - v_{\boldsymbol{k}}\beta^\dagger_{-\boldsymbol{k}}, \tag{2.46}$$

$$b_{\boldsymbol{k}} = u_{\boldsymbol{k}}\beta_{\boldsymbol{k}} - v_{\boldsymbol{k}}\alpha^\dagger_{-\boldsymbol{k}}. \tag{2.47}$$

The Hamiltonian (2.36) does not change, but the selection rules for the spin-current operator are easier to detect in the alternative representation (see Section 3.6).

2.3. Magnon Dispersion and Density of States

The normalized magnon dispersion

$$\varepsilon_{\boldsymbol{k}} = \Omega_{\boldsymbol{k}}/\Omega_{\max} = \sqrt{1-(\gamma_{\boldsymbol{k}}/\Delta)^2} \tag{2.48}$$

is displayed in Figure 2.3 for dimension $d = 2$. The corresponding density of states (DOS) for noninteracting magnons is shown in Figure 2.4 and calculated in Appendix B,

$$\boxed{\begin{aligned} \mathcal{N}_2(x) \quad &= \quad \frac{8}{\pi^2}\frac{\Delta x}{\sqrt{1-x^2}(\Delta\sqrt{1-x^2}+1)} \\ &\quad\times K\left(\frac{1-\Delta\sqrt{1-x^2}}{\Delta\sqrt{1-x^2}+1}\right)\ \Theta\left(x\in[\varepsilon_{\min},1]\right), \end{aligned}} \tag{2.49}$$

where $x = \omega/\Omega_{\max}$ and $\varepsilon_{\min} = \sqrt{1-1/\Delta^2}$. There is a van-Hove singularity (logarithmic due to the elliptic integral K and square root due to the prefactor) at $x = 1$. It corresponds to the flat dispersion at the zone boundary of the magnetic Brillouin zone (MBZ). The dispersion starts out linearly from $\boldsymbol{k} = \boldsymbol{0}$ in the isotropic case, whereas the anisotropic dispersion starts out like a paraboloid shifted upwards by $\varepsilon_{\min}$. The energy gap can be seen in the anisotropic DOS.

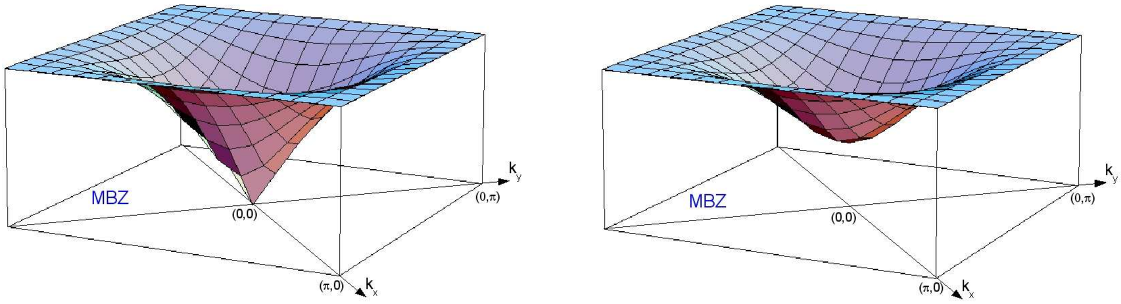

Abbildung 2.3. Dimensionless Dispersion $\varepsilon_{\boldsymbol{k}} \in [0,1]$ for $\boldsymbol{k} \in$ MBZ, where MBZ is the magnetic Brillouin zone (see Fig. 2.1). Left panel: $\Delta = 1.0$. Right panel: $\Delta = 1.1$.

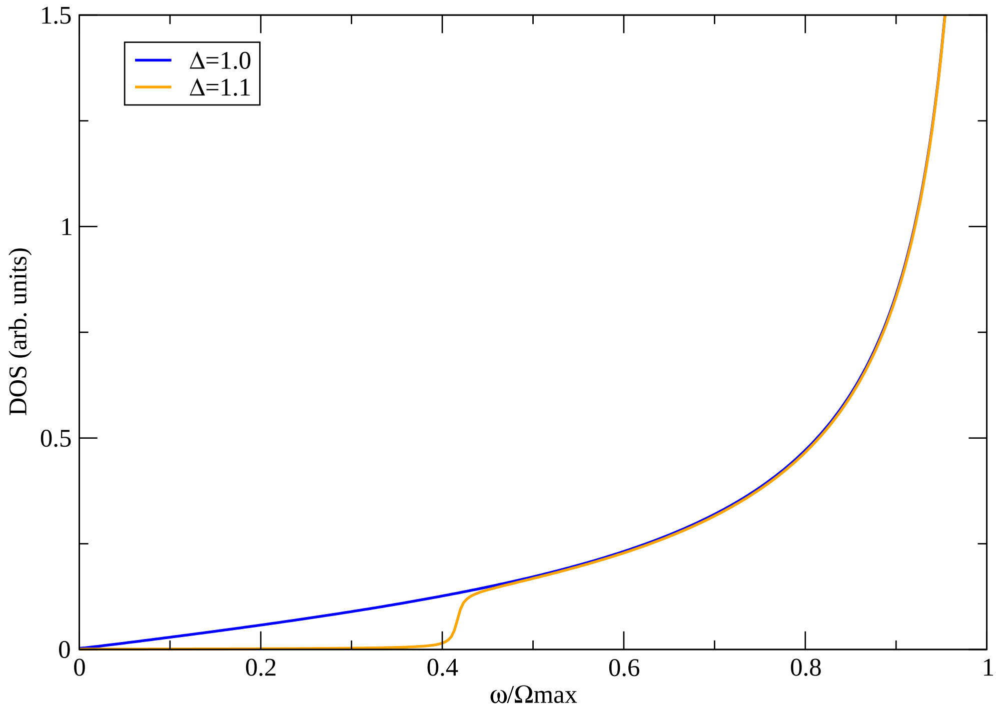

Abbildung 2.4. Noninteracting-magnon DOS for the $d = 2$ HAFM with anisotropy parameter $\Delta = 1.0$ (isotropic) and $\Delta = 1.1$ (anisotropic).

This concludes the analysis of the spin-wave treatment of the Heisenberg antiferromagnet. Our next task is to define the terms *spin currents* and *spin conductivity* by means of linear-response theory, which will be one of the main purposes of Chapter 3.

KAPITEL 3

Linear-Response Theory for Spin Currents

In this chapter we will give a definition of the spin conductivity and derive an expression for its calculation. Before we start, we have a look at the optical conductivity, i. e., the conductivity for charge transport, and its implications for important system properties.

The conductivity is defined as the linear current response to a uniform, frequency-dependent, current-driving, external force field, e.g., an electric field in the case of charge transport or a gradient of the z-component of the magnetic field for spin transport. One can classify solids into three categories, according to the low-frequency behavior of the optical conductivity $\sigma(\omega) = \sigma'(\omega) + i\sigma''(\omega)$ at $T = 0$ [**28**, **29**]:

$$\begin{aligned} \sigma'_{xx}(\omega) &= D\delta(\omega) + \sigma^{\text{reg}}_{xx}(\omega) && \text{ideal conductors,} \\ \lim_{\omega\to 0} \sigma'_{xx}(\omega) &= \sigma_0 && \text{non-ideal conductors,} \\ \lim_{\omega\to 0} \sigma'_{xx}(\omega) &= 0 && \text{insulators.} \end{aligned} \tag{3.1}$$

Ideal conductors are characterized by a delta-function contribution at zero frequency. The prefactor D is called the Drude weight or charge stiffness [**30**]. The delta function implies that currents do not decay to zero once they have been induced − a fact that will be addressed in Section 3.3. If there is scattering off crystal impurities, which smears out the delta function to a Lorentzian, the conductivity has a finite zero-frequency limit σ_0. This is the characteristic of non-ideal conductors. Insulators are defined by a vanishing dc conductivity.

So far, the spin conductivity in Heisenberg magnets (see, e. g., [**6**]) has been derived by analogy to the charge case [**30**], which we now review. Consider an electronic Hamiltonian, namely the kinetic energy

$$K = -t \sum_{\langle ij\rangle s} (c^\dagger_{is} c_{js} + c^\dagger_{js} c_{is}). \tag{3.2}$$

Here, $c_{is}^\dagger$ creates an electron of spin s on site i of a lattice, and t is the one-electron overlap between nearest-neighbor Wannier or atomic orbitals. In the presence of a vector potential $A_x(l,t)$ – where (l,t) denote lattice site and time, respectively – the hopping term $c_{l+x,s}^\dagger c_{ls}$ is modified [**31**] by a phase factor $e^{ieA_x(l)}$ ($\hbar = c = a = 1$). An expansion of these phase factors leads to the vector-potential-dependent kinetic-energy term

$$K_A = K - \sum_l \left[e j_x^P(l) A_x(l) + \frac{e^2 K_x(l)}{2} A_x^2(l) \right], \tag{3.3}$$

where ej_x^P is the x-component of the paramagnetic current density

$$j_x^P(l) = it \sum_s (c_{l+x,s}^\dagger c_{ls} - c_{ls}^\dagger c_{l+x,s}), \tag{3.4}$$

and $K_x(l)$ is the kinetic-energy density associated with the x-oriented links

$$K_x(l) = -t \sum_s (c_{l+x,s}^\dagger c_{ls} + c_{ls}^\dagger c_{l+x,s}). \tag{3.5}$$

The total current density $j_x(l)$ is obtained from the derivative of the kinetic-energy term with respect to the vector potential:

$$j_x(l) = -\frac{\delta K}{\delta A_x(l)} = e j_x^P(l) + e^2 K_x(l) A_x(l). \tag{3.6}$$

Linear-response theory then leads to the relation

$$\langle j_x(\boldsymbol{q},\omega)\rangle = -e^2 \left[\langle -K_x\rangle - \Lambda_{xx}(\boldsymbol{q},\omega)\right] A_x(\boldsymbol{q},\omega), \tag{3.7}$$

where $\Lambda_{xx}(\boldsymbol{q},\omega)$ is the retarded current-current Green function and $K_x = \sum_l K_x(l)$ is the total kinetic energy in x-direction. Setting $A_x(\boldsymbol{q}=\boldsymbol{0},\omega) = E_x(\boldsymbol{q}=\boldsymbol{0},\omega)/i(\omega + i0^+)$, the longitudinal conductivity for a uniform, frequency-dependent electric field is given by

$$\boxed{\sigma_{xx}(\omega) = -e^2 \frac{\langle -K_x\rangle - \Lambda_{xx}(\boldsymbol{q}=\boldsymbol{0},\omega)}{i(\omega + i0^+)}.} \tag{3.8}$$

An analogous formula can be derived for the spin conductivity defined as the linear spin-current response to a static twist in the boundary conditions (see, e. g., Ref. [**6**]). Unlike in the electronic case, where the phase factors are directly connected to the vector potential [**31**] and thus to an electric field, the relation between the "twist conductivity" and the response to an inhomogeneous magnetic field is not clear. Therefore, our first task in this chapter is to exhibit this relation.

3.1. Spin-Current Operator in Heisenberg Magnets

Consider a general XXZ Heisenberg Hamiltonian in the presence of an external magnetic field $h \equiv g\mu_B B$:

$$\mathcal{H} = \sum_{\langle i,j \rangle} J_{ij} \left[\Delta S_i^z S_j^z + \frac{1}{2}(S_i^+ S_j^- + S_i^- S_j^+) \right] - \sum_l \boldsymbol{S}_l \cdot \boldsymbol{h}_l, \tag{3.9}$$

where the sum $\langle i,j \rangle$ counts bonds (no double counting of pairs i, j). We use the Heisenberg equation of motion, $i\hbar\partial_t \boldsymbol{S}_i = [\boldsymbol{S}_i, \mathcal{H}]$, and obtain

$$\partial_t S_i^z + \frac{1}{\hbar} \left[\sum_j J_{ij} \left[\frac{i}{2}(S_i^+ S_j^- - S_i^- S_j^+) \right] + (\boldsymbol{h}_i \times \boldsymbol{S}_i)^z \right] = 0. \tag{3.10}$$

We have restricted ourselves to the transport of S^z. For a magnetic field only in the z-direction, the field-dependent term is 0 and we have

$$\partial_t S_i^z + \sum_j j_{i\to j} = 0, \tag{3.11}$$

which can be interpreted as the discrete lattice version of the equation of continuity for spin currents transporting magnetization $\langle S^z \rangle$. The operator for the spin current from site i to site j is thus defined as

$$\boxed{j_{i\to j} \equiv \frac{i}{2\hbar} J_{ij}(S_i^+ S_j^- - S_i^- S_j^+).} \tag{3.12}$$

In general (for the transport of $\boldsymbol{S}$), we would have the equation of motion

$$\partial_t \boldsymbol{S}_i + \frac{1}{\hbar} \left[\sum_j J_{ij} \left[\boldsymbol{S}_i \times \boldsymbol{S}_j^{(\Delta)} \right] + \boldsymbol{h}_i \times \boldsymbol{S}_i \right] = 0, \tag{3.13}$$

where $\boldsymbol{S}^{(\Delta)} = (S^x, S^y, \Delta S^z)$. In this case, it is not that easy to obtain a spin-current operator, since the field-dependent term has to be interpreted as the lattice divergence of the field-dependent part of the current operator. Note that a current-operator for $\boldsymbol{S}$-transport is a $d\times 3$-tensor due to the fact that a vector quantity (3 spin components) is transported in d spatial dimensions. Also note that the anisotropy parameter Δ enters the general expression for the spin-current operator.

3.2. Spin-Current Operator in Bosonic Representation

We will now derive a bosonic representation for the spin-current operator using the transformations introduced in Section 2.2.2. This representation shall serve for the discussion of the symmetry properties of the spin-current operator (Section 3.6). The second expression for the current operator (based on the standard transformations of Section 2.2.1) will be used for our further calculations.

We start from the current operator in terms of spin operators,

$$j_x \equiv \sum_l j_x(l) = \frac{i}{2} J \sum_l \left(S_l^+ S_{l+x}^- - S_l^- S_{l+x}^+ \right). \tag{3.14}$$

Using the leading-order terms of the Dyson-Maleev transformation,

$$S_i^+ = \sqrt{2S} a_i, \tag{3.15}$$

$$S_i^- = \sqrt{2S} a_i^\dagger, \tag{3.16}$$

for sublattice A, and

$$S_j^+ = \sqrt{2S} b_j^\dagger, \tag{3.17}$$

$$S_j^- = \sqrt{2S} b_j, \tag{3.18}$$

for sublattice B, we can transform the current-operator as follows:

$$j_x = 2JS\frac{i}{2}\left[\sum_{l\in A}(a_l b_{l+x} - a_l^\dagger b_{l+x}^\dagger) + \sum_{l\in B}(b_l^\dagger a_{l+x}^\dagger - b_l a_{l+x})\right]. \tag{3.19}$$

Using the "same-sign" Fourier transformation

$$a_i = \sqrt{\frac{2}{N}} \sum_{\boldsymbol{k}} e^{+i\boldsymbol{k}\cdot\boldsymbol{R}_i} a_{\boldsymbol{k}}, \tag{3.20}$$

$$b_j = \sqrt{\frac{2}{N}} \sum_{\boldsymbol{k}} e^{+i\boldsymbol{k}\cdot\boldsymbol{R}_j} b_{\boldsymbol{k}}, \tag{3.21}$$

we get for example

$$\sum_{l\in A} a_l b_{l+x} = \frac{2}{N} \sum_{l\in A} \sum_{\boldsymbol{kq}} e^{i(\boldsymbol{k}+\boldsymbol{q})\boldsymbol{R}_l} e^{iq_x} a_{\boldsymbol{k}} b_{\boldsymbol{q}} = \sum_{\boldsymbol{k}} e^{-ik_x} a_{\boldsymbol{k}} b_{-\boldsymbol{k}}. \tag{3.22}$$

Putting all the terms together, we obtain

$$j_x = 2JS \sum_{\boldsymbol{k}} \sin(k_x)(a^\dagger_{\boldsymbol{k}} b^\dagger_{-\boldsymbol{k}} + a_{\boldsymbol{k}} b_{-\boldsymbol{k}}). \tag{3.23}$$

Here the "same-sign" Fourier transformation is useful to recognize the momentum-conserving structure of the current operator. Otherwise, the indices for the b-operators would have $+$-signs.

The appropriate Bogoliubov transformation reads

$$a_{\boldsymbol{k}} = u_{\boldsymbol{k}} \alpha_{\boldsymbol{k}} - v_{\boldsymbol{k}} \beta^\dagger_{-\boldsymbol{k}}, \tag{3.24}$$

$$b_{\boldsymbol{k}} = u_{\boldsymbol{k}} \beta_{\boldsymbol{k}} - v_{\boldsymbol{k}} \alpha^\dagger_{-\boldsymbol{k}}, \tag{3.25}$$

with the formerly-derived relations

$$\lambda_{\boldsymbol{k}} = \sqrt{\Delta^2 - \gamma^2_{\boldsymbol{k}}}, \tag{3.26}$$

$$u_{\boldsymbol{k}} = \sqrt{\frac{\Delta + \lambda_{\boldsymbol{k}}}{2\lambda_{\boldsymbol{k}}}}, \tag{3.27}$$

$$v_{\boldsymbol{k}} = -\mathrm{sgn}(\gamma_{\boldsymbol{k}}) \sqrt{\frac{\Delta - \lambda_{\boldsymbol{k}}}{2\lambda_{\boldsymbol{k}}}}. \tag{3.28}$$

The inclusion of quartic terms and their normal-ordering again yields the Oguchi correction factor $\alpha(S)$, and the final result is

$$j_x = 2JS\alpha(S) \sum_{\boldsymbol{k}} \sin(k_x) \left[\frac{\gamma_{\boldsymbol{k}}}{\lambda_{\boldsymbol{k}}} (\alpha^\dagger_{\boldsymbol{k}} \alpha_{\boldsymbol{k}} - \beta^\dagger_{\boldsymbol{k}} \beta_{\boldsymbol{k}}) + \frac{\Delta}{\lambda_{\boldsymbol{k}}} (\alpha^\dagger_{\boldsymbol{k}} \beta^\dagger_{-\boldsymbol{k}} + \alpha_{\boldsymbol{k}} \beta_{-\boldsymbol{k}}) \right]. \tag{3.29}$$

For a detailed discussion of the symmetry properties of this operator see Section 3.6.

We can perform the same steps using the transformations of Section 2.2.1. The result is

$$\boxed{j_x = 2JS\alpha(S) \sum_{\boldsymbol{k}} \sin(k_x) \left[\frac{\gamma_{\boldsymbol{k}}}{\lambda_{\boldsymbol{k}}} (\alpha^\dagger_{\boldsymbol{k}} \alpha_{\boldsymbol{k}} + \beta^\dagger_{\boldsymbol{k}} \beta_{\boldsymbol{k}}) - \frac{\Delta}{\lambda_{\boldsymbol{k}}} (\alpha^\dagger_{\boldsymbol{k}} \beta^\dagger_{\boldsymbol{k}} + \alpha_{\boldsymbol{k}} \beta_{\boldsymbol{k}}) \right].} \tag{3.30}$$

We will use this expression for the calculation of the spin conductivity (Chapter 4).

3.3. Kubo Formula for the Spin Conductivity

In this section we derive a formula that describes the spin current response to an external magnetic field $h^z(l,t)$, where $h \equiv g\mu_B B$. The procedure shall be as follows:

The starting point is a time-dependent Hamiltonian $\mathcal{H}(t) = \mathcal{H} - \mathcal{V}(t)$, where $\mathcal{H}$ describes the XXZ Heisenberg system and $\mathcal{V}(t)$ is a Zeeman term which describes the coupling of the spins to the external field. Standard linear-response theory is used to calculate the spin current response, which is expressed by a susceptibility χ_{jS}. We transform this susceptibility to obtain a formula of the type $\langle \boldsymbol{j} \rangle = \sigma \nabla h^z$, where σ is the spin conductivity[1].

The time-dependent Hamiltonian reads

$$\mathcal{H}(t) = \mathcal{H} - \sum_l S^z(l) h^z(l,t). \tag{3.31}$$

Let us assume that the system is in thermal equilibrium at $t = -\infty$ and the external perturbation is switched on adiabatically. The current response linear in the external field is

$$\langle j_x(l,t) \rangle = \sum_j \int_{-\infty}^{\infty} dt'\ \chi_{jS}(l,j;t-t') h^z(j,t'), \tag{3.32}$$

where the susceptibility is defined as

$$\chi_{jS}(l,j;t-t') \equiv i\Theta(t-t') \langle [j_x(l,t), S^z(j,t')] \rangle. \tag{3.33}$$

The expectation values are

$$\langle A(t)B(t') \rangle \equiv \frac{\mathrm{Tr}[e^{-\beta\mathcal{H}} e^{i\mathcal{H}t} A e^{-i\mathcal{H}t} e^{i\mathcal{H}t'} B e^{-i\mathcal{H}t'}]}{\mathrm{Tr}\ e^{-\beta\mathcal{H}}}, \tag{3.34}$$

where Tr $\mathcal{A} = \sum_n \mathcal{A}_{nn}$ denotes the trace of an operator $\mathcal{A}$, i. e., the sum of its diagonal elements in a matrix representation. Note that the expectation values are defined with $\mathcal{H}$ and *not* $\mathcal{H}(t)$, which is one of the main advantages of linear-response theory. Since we are dealing with equilibrium quantities ($\mathcal{H}$ is time-independent), the susceptibility is only a function of $(t-t')$. Hence, it is convenient to work with the Fourier transforms in time,

$$A(\omega) \equiv \int_{-\infty}^{\infty} dt\ e^{i\omega t} A(t), \quad A(t) \equiv \int_{-\infty}^{\infty} \frac{d\omega}{2\pi} e^{-i\omega t} A(\omega). \tag{3.35}$$

[1] Actually, the spin conductivity should be defined with B^z instead of h^z. We use h^z here for brevity. See Appendix A.

As usual, the convolution in t transforms into a product in ω and yields

$$\langle j_x(l,\omega)\rangle = \sum_j \chi_{jS}(l,j;\omega) h^z(j,\omega) \tag{3.36}$$

with

$$\chi_{jS}(l,j;\omega) \equiv i\int_0^\infty dt\; e^{i(\omega+i0^+)t}\langle [j_x(l,t), S^z(j,0)]\rangle. \tag{3.37}$$

As the unperturbed system is invariant with respect to translations by a lattice vector, the susceptibility is only a function of $(\boldsymbol{l}-\boldsymbol{j})$. The spatial Fourier transforms are

$$A(\boldsymbol{q}) \equiv \sum_{\boldsymbol{l}} e^{-i\boldsymbol{q}\cdot\boldsymbol{l}} A(l), \quad A(l) \equiv \frac{1}{N}\sum_{\boldsymbol{q}} e^{i\boldsymbol{q}\cdot\boldsymbol{l}} A(\boldsymbol{q}). \tag{3.38}$$

Performing this transformation we obtain for the current response

$$\langle j_x(\boldsymbol{q},\omega)\rangle = \chi_{jS}(\boldsymbol{q},\omega) h^z(\boldsymbol{q},\omega), \tag{3.39}$$

where the frequency- and wave-vector-dependent susceptibility is given by

$$\chi_{jS}(\boldsymbol{q},\omega) \equiv \frac{i}{N}\int_0^\infty dt\; e^{i(\omega+i0^+)t}\langle [j_x(\boldsymbol{q},t), S^z(-\boldsymbol{q},0)]\rangle. \tag{3.40}$$

In order to derive a formula for the spin conductivity, we need the equation of continuity for the spin current:

$$\dot{S}^z(\boldsymbol{q},t) + i\boldsymbol{q}\cdot\boldsymbol{j}(\boldsymbol{q},t) = 0. \tag{3.41}$$

By a partial integration χ_{jS} can be transformed as follows:

$$\begin{aligned}
\chi_{jS}(\boldsymbol{q},\omega) &= \frac{i}{N}\int_0^\infty dt\, \frac{1}{i(\omega+i0^+)}\left[\frac{d}{dt}e^{i(\omega+i0^+)t}\right]\langle [j_x(\boldsymbol{q},t), S^z(-\boldsymbol{q},0)]\rangle \\
&= \frac{i}{N}\frac{1}{i(\omega+i0^+)}\Bigg[e^{i(\omega+i0^+)t}\langle [j_x(\boldsymbol{q},t), S^z(-\boldsymbol{q},0)]\rangle\Big|_0^\infty \\
&\quad - \int_0^\infty dt\; e^{i(\omega+i0^+)t}\frac{d}{dt}\langle [j_x(\boldsymbol{q},t), S^z(-\boldsymbol{q},0)]\rangle\Bigg].
\end{aligned}$$

The equation of continuity is used to substitute the time derivative in the second term:

$$\frac{d}{dt}\langle [j_x(\boldsymbol{q},t), S^z(-\boldsymbol{q},0)]\rangle = -\langle [j_x(\boldsymbol{q},t), \dot{S}^z(-\boldsymbol{q},0)]\rangle = -\langle [j_x(\boldsymbol{q},t), iq_x j_x(-\boldsymbol{q},0)]\rangle.$$

The last replacement is correct because the expectation value of the commutator of j_x and j_y vanishes due to the discrete rotational symmetry of the unperturbed system. Hence, no current should flow along the y-direction unless this symmetry is broken (see Section 3.7 for the case of broken inversion symmetry).

We arrive at

$$\begin{aligned}\chi_{jS}(\boldsymbol{q},\omega) &= \frac{i}{N}\frac{1}{i(\omega+i0^+)}\Bigg[iq_x\int_0^\infty dt\; e^{i(\omega+i0^+)t}\langle[j_x(\boldsymbol{q},t),j_x(-\boldsymbol{q},0)]\rangle \\ &\quad -\langle[j_x(\boldsymbol{q},0),S^z(-\boldsymbol{q},0)]\rangle\Bigg].\end{aligned}$$

By means of the representation of the spin current operator in terms of spin operators (see Eq. 3.14),

$$j_x(l) = \frac{i}{2}\sum_x J_{l,l+x}\left(S_l^+S_{l+x}^- - S_l^-S_{l+x}^+\right), \tag{3.42}$$

where the sum over x is defined as the sum over x-oriented links, one can transform the second term as

$$\langle[j_x(\boldsymbol{q},0),S^z(-\boldsymbol{q},0)]\rangle = \frac{i}{2}\sum_{l,x} J_{l,l+x}\left(e^{iq_x}-1\right)\langle S_l^+S_{l+x}^- + S_l^-S_{l+x}^+\rangle.$$

In the long-wavelength $q_x \to 0$ limit the susceptibility $\chi_{jS}(\boldsymbol{q},\omega)$ is thus proportional to iq_x and we can write

$$\boxed{\langle j_x(\boldsymbol{q},\omega)\rangle = -\frac{\langle -K_x\rangle - \Lambda_{xx}(\boldsymbol{q},\omega)}{i(\omega+i0^+)}iq_x h^z(\boldsymbol{q},\omega),} \tag{3.43}$$

where we call K_x the kinetic energy (cf. Section 3.5) per site divided by the number of lattice dimensions,

$$\langle K_x\rangle \equiv \frac{1}{2}\frac{1}{N}\sum_{l,x} J_{l,l+x}\langle S_l^+S_{l+x}^- + S_l^-S_{l+x}^+\rangle, \tag{3.44}$$

and Λ_{xx} is the current-response function,

$$\Lambda_{xx}(\boldsymbol{q},\omega) \equiv \frac{i}{N}\int_0^\infty dt\; e^{i(\omega+i0^+)t}\langle[j_x(\boldsymbol{q},t),j_x(-\boldsymbol{q},0)]\rangle. \tag{3.45}$$

Equation (3.43) exhibits the desired structure $\langle \boldsymbol{j}\rangle = \sigma\nabla h^z$. We can now write down a formula for the spin conductivity defined as the linear spin-current response to a uniform, $\boldsymbol{q} = 0$, frequency-dependent gradient of the magnetic field (see Figure 3.1):

$$\boxed{\sigma_{xx}(\omega) = -\frac{\langle -K_x\rangle - \Lambda_{xx}(\boldsymbol{q}=\boldsymbol{0},\omega)}{i(\omega + i0^+)}.} \tag{3.46}$$

This complex expression can be decomposed into its real and imaginary parts:

$$\sigma_{xx}(\omega) = \sigma'_{xx}(\omega) + i\sigma''_{xx}(\omega), \tag{3.47}$$

where

$$\sigma'_{xx}(\omega) = \pi[\langle -K_x\rangle - \Lambda'_{xx}(\boldsymbol{q}=\boldsymbol{0},\omega\to 0)]\delta(\omega) + \frac{\Lambda''_{xx}(\boldsymbol{q}=\boldsymbol{0},\omega)}{\omega} \tag{3.48}$$

and

$$\sigma''_{xx}(\omega) = \pi[-\Lambda''_{xx}(\boldsymbol{q}=\boldsymbol{0},\omega\to 0)]\delta(\omega) + \frac{\langle -K_x\rangle - \Lambda'_{xx}(\boldsymbol{q}=\boldsymbol{0},\omega)}{\omega}. \tag{3.49}$$

Since $\Lambda_{xx}(\boldsymbol{q}=\boldsymbol{0},\omega\to 0)$ is a susceptibility (a "retarded commutator") and thus the Fourier transform in time of a real function, we know that its real part is an even function of ω and its imaginary part is an odd function of ω. As long as the odd function Λ''_{xx} has no singularity at $\omega = 0$, we know that $\Lambda''_{xx}(\boldsymbol{q}=\boldsymbol{0},\omega\to 0) = 0$ and the first term contributing to σ''_{xx} vanishes.

In general, the $\boldsymbol{q}=\boldsymbol{0}$ conductivity at $T = 0$ may be written as

$$\boxed{\sigma'_{xx}(\omega) = D\delta(\omega) + \sigma^{\mathrm{reg}}_{xx}(\omega).} \tag{3.50}$$

The coefficient D of the delta function is the Drude weight as defined in Eq. (3.1). We have already mentioned that the Drude weight provides information about the possibility of persistent currents in the system. In order to understand this connection,

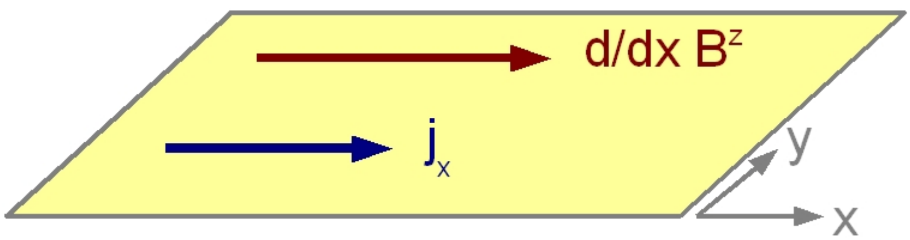

ABBILDUNG 3.1. Setup for a spin current driven along a magnetic-field gradient.

let us rewrite Eq. (3.43) introducing a force $f_x(\boldsymbol{q},\omega) \equiv iq_x h^z(\boldsymbol{q},\omega)$:

$$\langle j_x(\boldsymbol{q},\omega)\rangle = \sigma_{xx}(\omega) f_x(\boldsymbol{q},\omega). \tag{3.51}$$

Taking the limit $\boldsymbol{q} = \boldsymbol{0}$, assuming a delta-shaped force in time,

$$f_x(t) = f_0\delta(t) \Rightarrow f_x(\omega) = f_0, \tag{3.52}$$

and using Eq. 3.50, the real part of the current's expectation value becomes

$$\mathrm{Re}\langle j_x(\omega)\rangle = Df_0\delta(\omega) + f_0\sigma_{xx}^{\mathrm{reg}}(\omega). \tag{3.53}$$

The inverse Fourier transform, $\mathrm{Re}\langle j_x(t)\rangle = \mathrm{Re}\int \frac{d\omega}{2\pi}\langle j_x(\omega)\rangle e^{-i\omega t}$, reads

$$\mathrm{Re}\langle j_x(t)\rangle = \frac{Df_0}{2\pi} + \mathrm{Re}\int \frac{d\omega}{2\pi} f_0\sigma_{xx}^{\mathrm{reg}}(\omega)e^{-i\omega t}. \tag{3.54}$$

The first term, $\frac{Df_0}{2\pi}$, is constant in time. This exhibits the connection between the Drude weight D and the possibility of persistent currents.

From Equation (3.48), we can see that the real part of the spin conductivity will contain such a delta function contribution with

$$\boxed{\frac{D}{\pi} = \langle -K_x\rangle - \Lambda'_{xx}(\boldsymbol{q}=\boldsymbol{0},\omega\to 0).} \tag{3.55}$$

The regular part is given by

$$\boxed{\sigma_{xx}^{\mathrm{reg}}(\omega) = \frac{\Lambda''_{xx}(\boldsymbol{q}=\boldsymbol{0},\omega)}{\omega}.} \tag{3.56}$$

Here, we should emphasize the fact that these expressions look completely analogous to the case of charge transport [**30**]. This result is noteworthy since, in the theory of spin transport, we cannot resort to a gauge theory like the electrodynamical gauge theory connecting the vector potential with the electric field. In the charge-transport case, one usually starts from a Hamiltonian where the vector potential couples to the current operator and calculates the linear current response to the vector potential. One then uses the relation between the vector potential and the electric field to obtain the Kubo formula for the optical conductivity.

Here, we have used the standard Zeeman term in the Hamiltonian and the definition of spin currents via the continuity equation. The connection to the gradient of the z-component of the magnetic field (i. e., to the external perturbation coupling to S^z, our transport quantity) emerged quite naturally, without introducing any "vector potential". Nevertheless, the conductivity consisting of the kinetic-energy term and the current-response function is in perfect analogy with the optical conductivity. This can be understood by looking at another representation of the Heisenberg model, namely in terms of the Jordan-Wigner fermions, which will be disussed in Section 3.5.

3.4. Sum Rule for the Spin Conductivity

3.4.1. Derivation using a generating Operator. In general, sum rules are expressions for frequency integrals of spectral functions. We would like to derive a sum rule for the spin conductivity. This can be accomplished by first identifying a generating operator for the $\boldsymbol{q} = \mathbf{0}$ spin current operator,

$$j_x \equiv \sum_l j_x(l) = \frac{i}{2} J \sum_l \left(S_l^+ S_{l+x}^- - S_l^- S_{l+x}^+ \right) , \tag{3.57}$$

where $l+x$ labels the lattice site next to site l in the x-direction and J is the nearest-neighbor exchange coupling as before. The spin current was defined by the lattice version of the equation of continuity and thus by the commutator of the Heisenberg Hamiltonian and the z-component of the spin operator,

$$i[S_l^z, \mathcal{H}] = \sum_m j_{l \to m} = j_{l \to l+x} - j_{l-x \to l} = j_x(l) - j_x(l-x), \tag{3.58}$$

where the notation $j_x(l) \equiv j_{l \to l+x}$ is used. Denoting by x_l the x-coordinate of lattice site l the spin-current operator is rewritten

$$\begin{aligned} j_x \equiv \sum_l j_x(l) = \sum_l (1 + x_l - x_l) j_x(l) = \sum_l (1 + x_{l-x}) j_x(l-x) - \sum_l x_l j_x(l) \\ = -\sum_l x_l [j_x(l) - j_x(l-x)] = -i \sum_l x_l [S_l^z, \mathcal{H}]. \end{aligned}$$

Thus, the spin-current operator can be expressed as

$$j_x = -i[X, \mathcal{H}], \tag{3.59}$$

where the generating operator X is

$$X \equiv \sum_l x_l S_l^z. \tag{3.60}$$

Let $|n\rangle$ be the eigenstates of $\mathcal{H}$ and E_n the corresponding eigenvalues. The commutation relation (3.59) yields

$$\langle 0|j_x|n\rangle = -i(E_n - E_0)\langle 0|X|n\rangle, \tag{3.61}$$

where $|0\rangle$ is the ground state of the system and it is assumed that this ground state is unique. We apply this relation to the $\boldsymbol{q} = \mathbf{0}$ current-response function,

$$\Lambda_{xx}(\omega) \equiv \frac{i}{N}\int_0^\infty dt\; e^{i(\omega+i0^+)t}\langle[j_x(t), j_x(0)]\rangle. \tag{3.62}$$

We use its Lehmann representation

$$\begin{aligned} \Lambda_{xx}(\omega) &= \frac{1}{N}\sum_n^{E_n \neq E_0} |\langle 0|j_x|n\rangle|^2 \\ &\times \left[\frac{1}{\omega + (E_n - E_0) + i0^+} - \frac{1}{\omega - (E_n - E_0) + i0^+}\right] \end{aligned} \tag{3.63}$$

to write the regular part of the spin conductivity, $\Lambda''_{xx}(\omega)/\omega$, as follows:

$$\frac{\Lambda''_{xx}(\omega)}{\omega} = \frac{\pi}{N}\sum_n^{E_n \neq E_0} |\langle 0|j_x|n\rangle|^2 \left[\frac{\delta(\omega + (E_n - E_0))}{E_n - E_0} + \frac{\delta(\omega - (E_n - E_0))}{E_n - E_0}\right]. \tag{3.64}$$

Since $E_n > E_0$, only the last term contributes for $\omega \geq 0$ and we have

$$\begin{aligned} \int_0^\infty d\omega\; \sigma'_{xx}(\omega) &= \int_0^\infty d\omega\; \frac{\pi}{N}\sum_n^{E_n \neq E_0} |\langle 0|j_x|n\rangle|^2 \frac{\delta(\omega - (E_n - E_0))}{E_n - E_0} \\ &= \frac{\pi}{N}\sum_n^{E_n \neq E_0} |\langle 0|j_x|n\rangle|^2 \frac{1}{E_n - E_0}. \end{aligned}$$

We can now use Equation (3.61) to transform the matrix elements of the spin-current operator,

$$\begin{aligned} |\langle 0|j_x|n\rangle|^2 &= \frac{1}{2}[\langle 0|j_x|n\rangle\langle n|j_x|0\rangle + \langle 0|j_x|n\rangle\langle n|j_x|0\rangle] \\ &= -i(E_n - E_0)\frac{1}{2}[\langle 0|X|n\rangle\langle n|j_x|0\rangle - \langle 0|j_x|n\rangle\langle n|X|0\rangle]. \end{aligned}$$

Hence,

$$\frac{2}{\pi}\int_0^\infty d\omega\ \sigma'_{xx}(\omega) = \frac{i}{N}\langle 0|[j_x, X]|0\rangle. \tag{3.65}$$

Using expression (3.57) for the spin-current operator, we can calculate the commutator

$$[j_x, X] = \frac{i}{2}J\sum_l \left(S_l^+ S_{l+x}^- + S_l^- S_{l+x}^+\right). \tag{3.66}$$

Now we can see that the sum rule contains the familiar expression $\langle K_x\rangle$ defined in Equation (3.44):

$$\boxed{\frac{2}{\pi}\int_0^\infty d\omega\ \sigma'_{xx}(\omega) = \langle -K_x\rangle.} \tag{3.67}$$

Equation (3.67) is the sum rule for the spin conductivity. Here, we have been following a derivation by Maldague [**32**]. From this derivation it is not entirely clear how to interpret the integral $\int_0^\infty d\omega$. In other words: How do we handle the possible delta peak at $\omega = 0$? Should it be included completely, only by one half or even be left out? This is apparently ambiguous, and we will resolve this question in the following subsection.

3.4.2. Derivation using the Kramers-Kronig Relations for the Current-Response Function. Here, we are going to use the complete expression for the real part of the spin conductivity, namely

$$\sigma'_{xx}(\omega) = D\delta(\omega) + \sigma^{\mathrm{reg}}_{xx}(\omega), \tag{3.68}$$

with the Drude weight

$$\frac{D}{\pi} = \langle -K_x\rangle - \Lambda'_{xx}(\boldsymbol{q} = \boldsymbol{0}, \omega \to 0). \tag{3.69}$$

Any retarded function (analytic in the upper half-plane) obeys the Kramers-Kronig relations connecting its real and imaginary parts. These relations are given by

$$\Lambda'_{xx}(\omega) = ⨍_{-\infty}^{\infty} \frac{d\omega'}{\pi}\, \frac{\Lambda''_{xx}(\omega')}{\omega' - \omega}, \tag{3.70}$$

$$\Lambda''_{xx}(\omega) = -⨍_{-\infty}^{\infty} \frac{d\omega'}{\pi}\, \frac{\Lambda'_{xx}(\omega')}{\omega' - \omega}, \tag{3.71}$$

where the dashed integral symbol denotes the principal value of the integral. We use the first one of these relations and the fact that the imaginary part of the current-response function is an odd function of the frequency:

$$\begin{aligned} \Lambda'_{xx}(\omega \to 0) &= \frac{1}{\pi} \fint_{-\infty}^{\infty} d\omega' \left. \frac{\Lambda''_{xx}(\omega')}{\omega' - \omega} \right|_{\omega \to 0} = \frac{2}{\pi} \int_0^{\infty} d\omega' \, \frac{\Lambda''_{xx}(\omega')}{\omega'} \\ &= \frac{2}{\pi} \int_0^{\infty} d\omega' \, \sigma_{xx}^{\mathrm{reg}}(\omega'). \end{aligned} \tag{3.72}$$

We can then write

$$\begin{aligned} \frac{1}{\pi} \fint_{-\infty}^{\infty} \sigma'_{xx}(\omega) d\omega &= \frac{1}{\pi} \left[D + \fint_{-\infty}^{\infty} \sigma_{xx}^{\mathrm{reg}}(\omega) d\omega \right] \\ &= [\langle -K_x \rangle - \Lambda'_{xx}(\omega \to 0)] + \frac{2}{\pi} \int_0^{\infty} d\omega \, \sigma_{xx}^{\mathrm{reg}}(\omega) \\ &= [\langle -K_x \rangle - \Lambda'_{xx}(\omega \to 0)] + \Lambda'_{xx}(\omega \to 0) \\ &= \langle -K_x \rangle, \end{aligned} \tag{3.73}$$

where (3.69) and (3.72) were used.

It is now clear how the usual sum rule,

$$\frac{2}{\pi} \int_0^{\infty} d\omega \, \sigma'_{xx}(\omega) = \langle -K_x \rangle, \tag{3.74}$$

has to be interpreted: The integral must contain $\frac{1}{2}$ of the Drude peak at $\omega = 0$. This is consistent with the fact that the sum rule for the optical conductivity is used to determine a metal-superconductor phase transition. The optical conductivity is suppressed at low energy since there is an energy gap in the superconducting phase. Some of the spectral weight suppressed below the gap can reappear as a Drude peak at $\omega = 0$ [**33**], depending on the value of the kinetic energy above and below T_C.

Furthermore, we point out that the measurement of the imaginary part of the spin conductivity also permits the determination of the Drude weight:

$$\sigma''_{xx}(\omega) = \pi[-\Lambda''_{xx}(\boldsymbol{q} = \boldsymbol{0}, \omega \to 0)]\delta(\omega) + \frac{\langle -K_x \rangle - \Lambda'_{xx}(\boldsymbol{q} = \boldsymbol{0}, \omega)}{\omega}. \tag{3.75}$$

If we multiply this by ω and take the $\omega \to 0$-limit, we can see that

$$\lim_{\omega \to 0} \omega \sigma''_{xx}(\omega) = \langle -K_x \rangle - \Lambda'_{xx}(\boldsymbol{q} = \boldsymbol{0}, \omega \to 0) = \frac{D}{\pi}. \tag{3.76}$$

Thus, the Drude weight can be calculated from

$$\boxed{D = \pi \lim_{\omega \to 0} \omega \sigma''_{xx}(\omega).} \tag{3.77}$$

If there is a $1/\omega$-behavior of the imaginary part of the conductivity for small frequencies the Drude weight is finite. Of course, we should emphasize that we still have to calculate $\langle -K_x \rangle$. Apparently, complete information about the Drude weight cannot be obtained from computing $\Lambda_{xx}(\boldsymbol{q} = \mathbf{0}, \omega)$ alone. We will come back to this point in Chapter 5.

3.5. Jordan-Wigner Mapping

In Section 2.2 we have seen that the spin Hamiltonian can be mapped onto bosonic Hamiltonians. We now consider a mapping onto fermionic degrees of freedom. The Jordan-Wigner mapping [**34**] is most easily performed in $d = 1$, but it can also be used in $d = 2$ [**35**, **36**]. We want to concentrate on the fact that the mapping can help us to understand the analogy between the spin conductivity and the optical conductivity.

Consider the XXZ chain ($d = 1$) in the presence of a magnetic field,

$$\mathcal{H} = \mathcal{H}_{\mathrm{XY}} + J\Delta \sum_i S_i^z S_{i+1}^z - \sum_i h_i^z S_i^z. \tag{3.78}$$

The Jordan-Wigner mapping introduces fermionic operators c_i and $c_i^\dagger$ preserving the spin algebra of the original spin operators:

$$\begin{aligned} S_i^z &= c_i^\dagger c_i - \frac{1}{2}, \\ S_i^- &= \exp\left[i\pi \sum_{l<i} c_l^\dagger c_l \right] c_i, \\ S_i^+ &= (S_i^-)^\dagger. \end{aligned} \tag{3.79}$$

The disadvantage of the Jordan-Wigner representation is that the anticommutator algebra of the fermions requires long-range phase factors $\exp\left[i\pi \sum_{l<i} c_l^\dagger c_l \right]$, which make sure that any two fermion operators on different sites anticommute even though the corresponding spin operators commute. The Jordan-Wigner mapping transforms the XXZ chain into the following fermionic Hamiltonian – note that the phase factors

drop out, which is the case only in $d = 1$:

$$\mathcal{H} = \sum_i \left[\frac{J}{2}(c_i^\dagger c_{i+1} + c_i c_{i+1}^\dagger) + J\Delta n_i n_{i+1} - \mu_i c_i^\dagger c_i \right], \tag{3.80}$$

where we have introduced the chemical potential

$$\mu_i = h_i^z + J\Delta. \tag{3.81}$$

The XY part of the Heisenberg Hamiltonian maps onto the nearest-neighbor hopping term, i. e., the kinetic energy. For this reason we have used the expression "kinetic energy" in the discussion of the spin conductivity. The density-density interaction of neighboring fermion sites corresponds to the Ising term of the spin Hamiltonian.

The chemical potential is connected to the magnetic field. This explains that the current-generating force $\nabla\mu$ in the charge case maps onto the spin-current generating force ∇h^z in the spin case.

In the evaluation of the spin conductivity (for $d = 2$), we will use the Dyson-Maleev bosonic representation and consider the regime $\Delta \geq 1$. For the Drude weight, we expect $D = 0$ for $\Delta > 1$ (gapped regime, "spin insulator"). On the other hand, it is tempting to assume that the Jordan-Wigner mapping suggests $D > 0$ for $\Delta = 0$ ("spin liquid" or "spin metal") even though this is not as clear in two dimensions as it is in $d = 1$. We will come back to this point in the discussion of our results in Chapter 5.

3.6. Selection Rules

In this section we derive a set of selection rules for the spin-current operator. In general, selection rules are statements about matrix elements of an operator. These rules allow us to conclude which matrix elements are zero without explicitly calculating them.

We start from the Lehmann representation of the current-response function,

$$\begin{aligned} \Lambda_{xx}(\omega) &= \frac{1}{N} \sum_n^{E_n \neq E_0} |\langle 0|j_x|n\rangle|^2 \\ &\quad \times \left[\frac{1}{\omega + (E_n - E_0) + i0^+} - \frac{1}{\omega - (E_n - E_0) + i0^+} \right]. \end{aligned} \tag{3.82}$$

The selection rules for the spin conductivity can be derived from the matrix elements $\langle 0|j_x|n\rangle$ and the symmetry properties of the spin-current operator j_x. We first look at the current operator in terms of spin operators,

$$j_x = \frac{i}{2} J \sum_l \left(S_l^+ S_{l+x}^- - S_l^- S_{l+x}^+ \right) . \tag{3.83}$$

It is obvious that $j_x \to -j_x$ under spatial inversion, which means that the current operator has negative parity. Thus, the matrix elements $\langle 0|j_x|n\rangle$ are nonzero for states of opposite parity (even↔odd, odd↔even)[2].

From the lattice-translational invariance of the spin-current operator it follows directly that the total lattice momentum $\boldsymbol{K}_{\text{tot}}$ has to be conserved. Since the ground state has zero total momentum the matrix elements will be nonzero if $|n\rangle$ also has $\boldsymbol{K}_{\textbf{tot}} = \boldsymbol{0}$.

Finally, it is clear that the total spin z-component S^z_{tot} is conserved when applying the spin-current operator. A measurement of the the spin conductivity therefore probes the $S^z_{\text{tot}} = 0$-sector of the system.

We can summarize these selection rules as follows:

$$\boxed{\begin{aligned} \text{Parity}: &\quad P_0 P_n = -1, \\ \text{Momentum}: &\quad \Delta \boldsymbol{K}_{\text{tot}} = 0, \\ \text{Spin}: &\quad \Delta S^z_{\text{tot}} = 0. \end{aligned}} \tag{3.84}$$

We can also check these symmetry properties for the spin-wave approximation of the spin-current operator. The Dyson-Maleev-transformed operator with the same sign for the momentum-Fourier transformation on the two sublattices reads

$$j_x = 2JS\alpha(S) \sum_{\boldsymbol{k}} \sin(k_x) \left[\frac{\gamma_{\boldsymbol{k}}}{\lambda_{\boldsymbol{k}}} (\alpha^\dagger_{\boldsymbol{k}} \alpha_{\boldsymbol{k}} - \beta^\dagger_{\boldsymbol{k}} \beta_{\boldsymbol{k}}) + \frac{\Delta}{\lambda_{\boldsymbol{k}}} (\alpha^\dagger_{\boldsymbol{k}} \beta^\dagger_{-\boldsymbol{k}} + \alpha_{\boldsymbol{k}} \beta_{-\boldsymbol{k}}) \right] . \tag{3.85}$$

The negative parity of this operator is due to the $\sin(k_x)$-factor indicating that we ask for the current flowing in the x-direction. The total momentum is conserved since in the first two terms there are only magnon number operators, and in the third and fourth term two particles are created (or annihilated, respectively) with opposite

[2] It is important to note that this argument only holds if the Hamiltonian commutes with the operator of consideration, which is the parity operator P in this case. Otherwise, the eigenstates of the Hamiltonian are not necessarily states of definite parity. See also Sec. 3.8.1.

momenta. The conservation of S^z_{tot} is due to the fact that α- and β-magnons carry opposite S^z, namely -1 and +1. This can be seen by calculating the expectation values of the S^z_{tot}-operator for the states with one α-magnon and one β-magnon, respectively. Therefore, we transform the S^z_{tot}-operator into its Dyson-Maleev form,

$$S^z_{\mathrm{tot}} = \sum_{i\in A} S^z_i + \sum_{j\in B} S^z_j = \sum_{\boldsymbol{k}} (\beta^\dagger_{\boldsymbol{k}}\beta_{\boldsymbol{k}} - \alpha^\dagger_{\boldsymbol{k}}\alpha_{\boldsymbol{k}}), \tag{3.86}$$

to see that

$$\langle\Psi_0|\alpha_{\boldsymbol{k}} S^z_{\mathrm{tot}} \alpha^\dagger_{\boldsymbol{k}}|\Psi_0\rangle = -1, \tag{3.87}$$

and

$$\langle\Psi_0|\beta_{\boldsymbol{k}} S^z_{\mathrm{tot}} \beta^\dagger_{\boldsymbol{k}}|\Psi_0\rangle = +1. \tag{3.88}$$

Hence, the current operator does not change the S^z_{tot}-eigenvalue when applied to a state.

3.7. Coupling to an external electric Field

So far we have discussed the coupling to an external magnetic field via a Zeeman term. We shall now investigate the reaction of a Heisenberg system to an electric field breaking the inversion symmetry of the system. It is well known that the combination of low symmetry and spin-orbit coupling gives rise to an anisotropic exchange interaction, which can be described by a Dzyaloshinskii-Moriya (DzM) term in the spin Hamiltonian [**37**,**38**]. Katsura et al. [**39**] have pointed out that the electric field can act as a gauge field or vector potential to the spin current via the Dzyaloshinskii-Moriya vector. The gauge field, however, has no gauge degrees of freedom since the electric field is the (measurable) physical field, so the term “gauge” is based on the formal analogy to the case of charge transport. In this section, we show that this vector potential leads to a linear-response relation in complete analogy to the case of charge transport.

We start from an electric field $\boldsymbol{E} = (0, E_y, 0)$. This field induces a Dzyaloshinskii-Moriya vector $\boldsymbol{D}_{ij} \propto \boldsymbol{E} \times \boldsymbol{e}_{ij}$, which was suggested from symmetry considerations by Shiratori and Kita [**40**]. Here, $\boldsymbol{e}_{ij}$ is the unit vector connecting the two sites i and j. We consider only nearest-neighbor couplings with a proportionality constant

α. Thus, we have for the x- and y-directions ($d = 2$) of the Dzyaloshinskii-Moriya vector

$$\boldsymbol{D}_{i,i+x} = \alpha \boldsymbol{E} \times \boldsymbol{e}_x = \begin{pmatrix} 0 \\ 0 \\ -\alpha E_y \end{pmatrix}, \quad \boldsymbol{D}_{i,i+y} = \boldsymbol{0}. \tag{3.89}$$

The Dzyaloshinskii-Moriya (DzM) Hamiltonian is given by

$$\mathcal{H}_{\mathrm{DzM}} = \sum_{\langle ij \rangle} \boldsymbol{D}_{ij} \cdot (\boldsymbol{S}_i \times \boldsymbol{S}_j). \tag{3.90}$$

The spin-current operator from site i to site j of the unperturbed system (no external fields) is $\boldsymbol{j}_{i \to j} = J_{ij} \boldsymbol{S}_i \times \boldsymbol{S}_j^{(\Delta)}$, where $\boldsymbol{S}_j^{(\Delta)}$ is defined below Eq. (3.13). In our case, the DzM vector points in the z-direction in spin space, $\boldsymbol{D}_{ij} = D_{ij}\, \boldsymbol{e}_z$, and we have

$$\mathcal{H}_{\mathrm{DzM}} = \sum_{\langle ij \rangle} \frac{D_{ij}}{J_{ij}} j_{i \to j}, \tag{3.91}$$

where the spin-current tensor is again reduced to a real-space vector current for the transport of magnetization. We can rewrite the DzM Hamiltonian,

$$\mathcal{H}_{\mathrm{DzM}} = -\sum_{l} A_x(l,t) j_x(l), \tag{3.92}$$

where (as before) $j_x(l) = \sum_x j_{l \to l+x} = j_{l \to l+x}$ (for only nearest-neighbor exchange couplings J), and the vector potential is given by

$$\boxed{A_x(l,t) = \frac{2\alpha E_y(l,t)}{J}.} \tag{3.93}$$

In order to use linear-response theory, we have to find the current operator in the presence of the external perturbation. We must apply the Heisenberg equation of motion, $i\partial_t \boldsymbol{S}_i = [\boldsymbol{S}_i, \mathcal{H}_{\mathrm{DzM}}]$, to the DzM Hamiltonian. For the general form, $\mathcal{H}_{\mathrm{DzM}} = \sum_{\langle ij \rangle} \boldsymbol{D}_{ij} \cdot (\boldsymbol{S}_i \times \boldsymbol{S}_j)$, a straightforward calculation yields

$$[\boldsymbol{S}_i, \mathcal{H}_{\mathrm{DzM}}] = i \sum_j \left[(\boldsymbol{S}_i \cdot \boldsymbol{S}_j)(\boldsymbol{D}_{ij} - \boldsymbol{D}_{ji}) + ((\boldsymbol{D}_{ji} - \boldsymbol{D}_{ij}) \cdot \boldsymbol{S}_i) \boldsymbol{S}_j \right]. \tag{3.94}$$

For a DzM vector in the z-direction in spin space, this leads to a DzM spin-current operator

$$j_{i\to j}^{\mathrm{DzM}} = (D_{ji} - D_{ij})\frac{1}{2}(S_i^+ S_j^- + S_i^- S_j^+). \tag{3.95}$$

With this expression, the spin-current operator in the presence of the external field can be written as

$$j_x(l; A) = j_x(l; A = 0) + K_x(l)A_x(l), \tag{3.96}$$

where $K_x(l) = \frac{J}{2}(S_l^+ S_{l+x}^- + S_l^- S_{l+x}^+)$ is the usual kinetic energy term.

At this point, we recognize the perfect analogy to the charge transport formulae [**30**] for the current operator in the presence of the vector potential as well as for the perturbation Hamiltonian (3.92). This means that we can directly write down the linear-response relation for the spin current,

$$\boxed{\langle j_x(\boldsymbol{q}, \omega)\rangle = -\left[\langle -K_x\rangle - \Lambda_{xx}(\boldsymbol{q}, \omega)\right] A_x(\boldsymbol{q}, \omega),} \tag{3.97}$$

with the same notation as in Section 3.3.

Now it is obvious that we could also write this as the response to the time derivative of the vector potential and would again obtain our formula for the longitudinal spin conductivity. The question is: What is the physical interpretation? Let us assume an electric field $\boldsymbol{E} = (E_x, E_y, E_z)$. Taking the vector-potential idea seriously, we can write $[\boldsymbol{D}_{ij}]^z = \alpha[\boldsymbol{E} \times \boldsymbol{e}_{ij}]^z$ and obtain for the vector potential (defined by "the field which couples to the current operator in the Hamiltonian")

$$\boxed{\boldsymbol{A}(l, t) = \frac{2\alpha}{J}\begin{pmatrix} E_y(l, t) \\ -E_x(l, t) \\ 0 \end{pmatrix}.} \tag{3.98}$$

The time-derivative of this vector potential is a current-driving force analogous to the charge case (see Figure 3.2). Now consider the microscopic Maxwell equation

$$\mathrm{rot}\boldsymbol{B} = \frac{4\pi}{c}\boldsymbol{j} + \frac{1}{c}\frac{\partial \boldsymbol{E}}{\partial t}. \tag{3.99}$$

In the absence of any charge currents, rot$\boldsymbol{B}$ is directly related to $\frac{\partial \boldsymbol{E}}{\partial t}$. Assume a magnetic field only in the z-direction (which is the component coupling to the magnetization). The equation then simplifies to

$$\begin{pmatrix} \partial_y B^z \\ -\partial_x B^z \\ 0 \end{pmatrix} = \frac{1}{c} \begin{pmatrix} \partial_t E_x \\ \partial_t E_y \\ \partial_t E_z \end{pmatrix}, \tag{3.100}$$

and we have, e. g., for the x-direction,

$$\partial_x B^z = \frac{-J}{2\alpha c} \partial_t A_x, \tag{3.101}$$

which displays the connection between the time derivative of the vector potential and the current-driving force.

3.8. Transversal Spin Response

Meier and Loss [**41**] have pointed out the possibility of a spin-current effect analogous to the Hall effect for charge currents[3]. Consider a magnetic field gradient along the x-axis, driving a spin-current j_x. As we have seen in the previous subsection, the magnetic field gradient in x-direction can be connected to a time-dependent x-component of the vector potential. We now add a static y-component to the vector potential. This corresponds either to an x-directed external electric field ($A_y = -\frac{2\alpha}{J} E_x$) or to an intrinsic lowering of the crystal symmetry, which both lead to a nonvanishing DzM vector in the presence of spin-orbit coupling.

[3]The name *Spin Hall Effect* is already used for an effect in semiconducting devices, where, due to spin-orbit coupling, an electric current flowing in some direction can lead to spin transport in a perpendicular direction [**42**]. A possible name for the effect described here might be *Heisenberg-Spin Hall Effect*, since it involves magnetization transport through a system of localized Heisenberg spins.

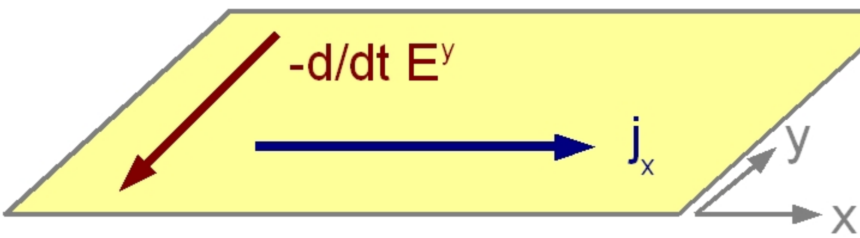

ABBILDUNG 3.2. Setup for a spin current driven by a time-dependent electric field.

3.8.1. Extrinsic Effect. Consider an external electric field coupled to the Heisenberg system via the DzM term. For charge currents the Hall effect can be described by the quadratic response to a current-driving electric and a current-deflecting magnetic field (see, e. g., Ref. [**43**]):

$$j_\alpha = \sigma_{\alpha\beta} E_\beta + \sigma_{\alpha\beta\gamma} E_\beta B_\gamma. \tag{3.102}$$

In order to obtain the mixed term (linear in A_x and A_y, respectively) of the quadratic response we have to start from the equation of motion for the density matrix. The Hamiltonian reads

$$\mathcal{H}(t) = \mathcal{H} - \sum_l j_x(l) A_x(l,t) - \sum_m j_y(m) A_y(m,t) = \mathcal{H} - \mathcal{V}(t), \tag{3.103}$$

where $\mathcal{H}$ describes the Heisenberg system. The von Neumann equation of motion for the density matrix

$$\varrho(t) \equiv \frac{e^{-\beta\mathcal{H}(t)}}{\mathrm{Tr}\; e^{-\beta\mathcal{H}(t)}} \tag{3.104}$$

in the Schrödinger picture with respect to $\mathcal{H}(t)$ is

$$\dot{\varrho}(t) = -i[\mathcal{H}(t), \varrho(t)]. \tag{3.105}$$

In the interaction picture, where the time evolution of operators is $O(t) = e^{i\mathcal{H}t} O e^{-i\mathcal{H}t}$ and the density matrix is $\varrho_W(t) = e^{i\mathcal{H}t} \varrho(t) e^{-i\mathcal{H}t}$, the equation of motion for the density matrix reads

$$\begin{aligned} \dot{\varrho}_W(t) &= i e^{i\mathcal{H}t} [\mathcal{V}(t), \varrho(t)] e^{-i\mathcal{H}t} \\ &= i \sum_l A_x(l,t) [j_x(l,t), \varrho_W(t)] + i \sum_m A_y(m,t) [j_y(l,t), \varrho_W(t)]. \end{aligned} \tag{3.106}$$

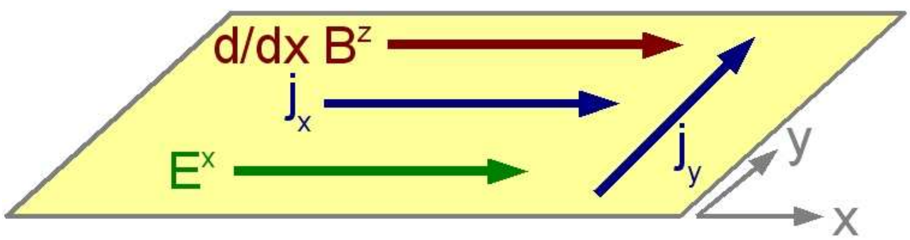

ABBILDUNG 3.3. Possible setup for the extrinsic *Heisenberg-Spin Hall Effect*.

The system is in equilibrium for $t \to -\infty$ and thus described by the equilibrium density matrix

$$\varrho_W(-\infty) = \varrho_0 \equiv \frac{e^{-\beta\mathcal{H}}}{\mathrm{Tr}\; e^{-\beta\mathcal{H}}}. \tag{3.107}$$

The perturbation $\mathcal{V}(t)$ is switched on adiabatically ($\boldsymbol{A}(t) \to \boldsymbol{A}(t)e^{\alpha t}$ for $t < 0$ with $\alpha \to 0^+$). The solution of the equation of motion can be obtained by iteration:

$$\begin{aligned} \varrho_W(t) &= \varrho_0 + i\int_{-\infty}^{t} dt'[\mathcal{V}(t'), \varrho_0] \\ &\quad -\frac{1}{2}\int_{-\infty}^{t} dt' \int_{-\infty}^{t} dt''[\mathcal{V}(t'), [\mathcal{V}(t''), \varrho_0]] + \mathcal{O}(\mathcal{V}^3). \end{aligned} \tag{3.108}$$

We multiply this equation with $j_y(i,t)$ and take the trace. Note that $\mathrm{Tr}A[B,[C,\varrho_0]] = \mathrm{Tr}[[A,B],C]\varrho_0 = \langle[[A,B],C]\rangle$. We separate from $\langle j_y(i,t)\rangle$ the mixed bilinear term which involves A_x and A_y, i. e.,

(3.109)

$$\begin{aligned} \langle j_y(i,t)\rangle_{\text{mixed,I}} &= -\frac{1}{2}\sum_{lm}\int_{-\infty}^{\infty} dt' \int_{-\infty}^{\infty} dt''\Theta(t-t')\Theta(t-t'') \\ &\quad \times\Big[\langle[[j_y(i,t), j_x(l,t')], j_y(m,t'')]\rangle + \langle[[j_y(i,t), j_y(m,t'')], j_x(l,t')]\rangle\Big] \\ &\quad \times A_x(l,t')A_y(m,t'') \\ &= -\frac{1}{2}\sum_{lm}\int_{-\infty}^{\infty} dt' \int_{-\infty}^{\infty} dt''\Theta(t-t')\Theta(t-t'') \\ &\quad \times\Big[\langle[[j_y(i,t-t'), j_x(l,0)], j_y(m,t''-t')]\rangle \\ &\qquad +\langle[[j_y(i,t-t''), j_y(m,0)], j_x(l,t'-t'')]\rangle\Big] \\ &\quad \times A_x(l,t')A_y(m,t''), \end{aligned}$$

where the field-independent versions of the current operators have to be used.

Let us focus on the situation where A_y is homogeneous in space and constant in time. A Fourier transformation $\langle j_y(i,\omega)\rangle = \int dt e^{i\omega t}\langle j_y(i,t)\rangle$ yields

$$\langle j_y(i,\omega)\rangle_{\text{mixed,I}} = \sum_{lm}\Lambda_{yxy}(i,l,m;\omega)A_x(l,\omega)A_y, \tag{3.110}$$

with

(3.111)

$$\Lambda_{yxy}(i,l,m;\omega) = -\frac{1}{2}\int_0^\infty dt' \int_0^\infty dt'' e^{i(\omega+i0^+)t'} \langle [[j_y(i,t'), j_x(l,0)], j_y(m,-t'')]\rangle.$$

In order to prove this result, we use the identity $\int dt' \int dt'' \Theta(t-t')\Theta(t-t'') = \int dt' \int dt'' \Theta(t-t')\Theta(t'-t'')$ and write the time-dependent Equation (3.109) schematically as follows:

$$A(t) = \int dt' \int dt'' B(t-t', t'-t'') D(t') E, \tag{3.112}$$

where $E(t'') = E$ due to the assumed time-independence of A_y. The Fourier transform is

$$\begin{aligned} A(\omega) &= \int dt e^{i\omega t} A(t) \\ &= \int dt \int dt' \int dt'' e^{i\omega t} B(t-t', t'-t'') D(t') E \\ &= \int dt \int dt' \int dt'' e^{i\omega(t-t')} B(t-t', t'-t'') e^{i\omega t'} D(t') E. \end{aligned} \tag{3.113}$$

Substituting $t - t' = \tau'$ and $t' - t'' = \tau''$ (note that $\int dt'' = \int_{-\infty}^{\infty} dt'' = -\int_{\infty}^{-\infty} d\tau'' = +\int_{-\infty}^{\infty} d\tau''$) yields

$$\begin{aligned} A(\omega) &= \int d\tau' \int d\tau'' \int dt' e^{i\omega\tau'} B(\tau', \tau'') e^{i\omega t'} D(t') E \\ &= \int d\tau' \int d\tau'' e^{i\omega\tau'} B(\tau', \tau'') D(\omega) E. \end{aligned} \tag{3.114}$$

This proves the Equations (3.110) and (3.111), where $\omega \to \omega + i0^+$ as before.

A spatial Fourier transformation making use of the lattice translational invariance leads to

$$\langle j_y(\boldsymbol{q},\omega)\rangle_{\text{mixed,I}} = \Lambda_{yxy}(\boldsymbol{q},\omega) A_x(\boldsymbol{q},\omega) A_y, \tag{3.115}$$

with the definition

(3.116)

$$\boxed{\Lambda_{yxy}(\boldsymbol{q},\omega) = -\frac{1}{2N}\int_0^\infty dt' \int_0^\infty dt'' e^{i(\omega+i0^+)t'} \langle [[j_y(\boldsymbol{q},t'), j_x(-\boldsymbol{q},0)], j_y(\boldsymbol{q}=\boldsymbol{0},-t'')]\rangle,}$$

where the field-independent current operators have to be used.

In addition, there is another mixed bilinear term contributing to $\langle j_y \rangle$. The field-dependent current operator (see Eq. 3.96) reads

$$j_y(l; A) = j_y(l; A = 0) + K_y(l) A_y(l). \tag{3.117}$$

Therefore,

$$\langle j_y(\boldsymbol{q}, \omega) \rangle_{\text{mixed,II}} = \frac{i}{N} \langle\langle [K_y(\boldsymbol{q}, t), j_x(-\boldsymbol{q}, 0)] \rangle\rangle_\omega A_y A_x(\boldsymbol{q}, \omega),$$

where

$$\langle\langle O(t) \rangle\rangle_\omega \equiv \int_0^\infty dt\, e^{i(\omega + i0^+)t} \langle O(t) \rangle. \tag{3.118}$$

The time-derivative of A_x is the current-driving force. We use the formerly derived relations (Eqns. (3.98) and (3.101))

$$A_x(\boldsymbol{q}, \omega) = \frac{2\alpha c}{J} \frac{1}{i(\omega + i0^+)} i q_x B^z(\boldsymbol{q}, \omega), \tag{3.119}$$

$$A_y = \frac{-2\alpha}{J} E_x, \tag{3.120}$$

where E_x is a homogeneous and constant electric field. Putting everything together yields

$$\langle j_y(\boldsymbol{q}, \omega) \rangle_{\text{mixed}} = \left[\Lambda_{yxy}(\boldsymbol{q}, \omega) + \frac{i}{N} \langle\langle [K_y(\boldsymbol{q}, t), j_x(-\boldsymbol{q}, 0)] \rangle\rangle_\omega \right] A_x(\boldsymbol{q}, \omega) A_y, \tag{3.121}$$

or

$$\boxed{\langle j_y(\boldsymbol{q}, \omega) \rangle_{\text{mixed}} = \sigma_{yxy}(\boldsymbol{q}, \omega) i q_x B^z(\boldsymbol{q}, \omega) E_x} \tag{3.122}$$

with

(3.123)

$$\boxed{\sigma_{yxy}(\boldsymbol{q}, \omega) = -\frac{4\alpha^2}{J^2 c} \frac{1}{i(\omega + i0^+)} \left[\Lambda_{yxy}(\boldsymbol{q}, \omega) + \frac{i}{N} \langle\langle [K_y(\boldsymbol{q}, t), j_x(-\boldsymbol{q}, 0)] \rangle\rangle_\omega \right].}$$

The three-current response function Λ_{yxy} is difficult to compute. We can at least derive its Lehmann representation in order to study its structure with regard to matrix elements and selection rules. The expression of interest is

$$\Lambda_{yxy}(\boldsymbol{q}=\boldsymbol{0},\omega) = -\frac{1}{2N}\int_0^\infty dt' \int_0^\infty dt'' e^{i(\omega+i0^+)t'} \langle [[j_y(t'), j_x(0)], j_y(-t'')] \rangle. \tag{3.124}$$

We focus on $T=0$, which allows us to replace thermal averages by ground-state expectation values. Making use of the completeness relation $1=\sum_n |n\rangle\langle n|$ for the basis of eigenstates of $\mathcal{H}_{\mathrm{HAFM}}$ yields

$$\begin{aligned} \langle 0|j_y(t')j_x(0)j_y(-t'')|0\rangle &= \sum_{nm} \langle 0|j_y(t')|n\rangle\langle n|j_x(0)|m\rangle\langle m|j_y(-t'')|0\rangle \\ &= \sum_{nm} e^{i[(E_0-E_n)t'+(E_0-E_m)t'']}\langle 0|j_y|n\rangle\langle n|j_x|m\rangle\langle m|j_y|0\rangle. \end{aligned} \tag{3.125}$$

An analogous representation can easily be derived for the other terms contributing to Λ_{yxy}. The time integrals require another $i0^+$-term for convergence, and the final result reads

$$\begin{aligned} \Lambda_{yxy}(\boldsymbol{q}=\boldsymbol{0},\omega) = -\frac{i}{2N}\sum_{nm} & \left[\frac{\langle 0|j_y|n\rangle\langle n|j_x|m\rangle\langle m|j_y|0\rangle}{(\omega-(E_n-E_0)+i0^+)(E_0-E_m+i0^+)} \right. \\ & - \frac{\langle 0|j_x|n\rangle\langle n|j_y|m\rangle\langle m|j_y|0\rangle}{(\omega-(E_m-E_n)+i0^+)(E_0-E_m+i0^+)} \\ & - \frac{\langle 0|j_y|n\rangle\langle n|j_y|m\rangle\langle m|j_x|0\rangle}{(\omega-(E_m-E_n)+i0^+)(E_n-E_0+i0^+)} \\ & \left. + \frac{\langle 0|j_y|n\rangle\langle n|j_x|m\rangle\langle m|j_y|0\rangle}{(\omega-(E_0-E_m)+i0^+)(E_n-E_0+i0^+)} \right]. \end{aligned} \tag{3.126}$$

The selection rule for the parity (Section 3.6) implies that this expression is zero for any finite frequency. Consider, e. g., the matrix elements $\langle 0|j_y|n\rangle\langle n|j_x|m\rangle\langle m|j_y|0\rangle$. The first one, $\langle 0|j_y|n\rangle$, can only be nonzero if the states $|0\rangle$ and $|n\rangle$ have opposite parity. The second one, $\langle n|j_x|m\rangle$, requires $|n\rangle$ and $|m\rangle$ to be of opposite parity. Therefore, $|0\rangle$ and $|m\rangle$ must have the same parity and thus $\langle m|j_y|0\rangle = 0$.[4]

The parity selection rule, on the other hand, may only be applied as long as the Hamiltonian has inversion symmetry. This symmetry is broken if the external electric field E_x is taken to be part of the system. In the case of charge transport,

[4]By means of analogous considerations, the second term of the long-wavelength limit of the transversal conductivity (3.123) can be shown to be zero for any finite frequencies, since the kinetic-energy operator K_y has nonzero matrix elements only between states of equal parity.

one therefore encounters a more careful definition of the Hall coefficient R_H [**44**]:

$$R_H(\omega) = \lim_{B\to 0} R_H(B,\omega) = \lim_{B\to 0} \frac{\sigma_{xy}(\omega)}{B\sigma_{xx}^2(\omega)}. \tag{3.127}$$

The difference from our ansatz is that the magnetic field (corresponding to A_y or E_x in our case) is incorporated in the system's Hamiltonian. Therefore, one has to use the B-dependent eigenstates[5] in a Lehmann representation. The Hall coefficient is obtained from the limit $B \to 0$. Hence, we conclude that the linear-response procedure has to be applied with caution for any kind of Hall effect, and the above derivation has to be reconsidered in this respect.

3.8.2. Intrinsic Effect. Consider a crystal with broken inversion symmetry. The Dzyaloshinskii-Moriya term is then a part of the system's Hamiltonian. Prominent examples for such a system are the cuprates, like La_2CuO_4 [**45**]. The Hamiltonian (system plus time-dependent perturbation) reads

$$\mathcal{H}(t) = \mathcal{H}_{\mathrm{HAFM}} + \mathcal{H}_{\mathrm{DzM}} - \sum_l j_x(l) A_x^{(ext)}(l,t), \tag{3.128}$$

where we use the superscript in $A_x^{(ext)}$ to distinguish between external and internal perturbations with respect to $\mathcal{H}_{\mathrm{HAFM}}$. There is an intrinsic *Heisenberg-Spin Hall Effect* if a spin current driven along the x-direction is deflected in y-direction by the system's DzM term. The spin-current operator is a function of the DzM vector. Its y-component reads

$$j_y(l) = j_y(l; D=0) + \sum_y j_{l\to l+y}^{\mathrm{DzM}}, \tag{3.129}$$

where

$$j_{i\to j}^{\mathrm{DzM}} = (D_{ji} - D_{ij})\frac{1}{2}(S_i^+ S_j^- + S_i^- S_j^+). \tag{3.130}$$

In order to determine if a transverse spin current can exist in such a system, one could now use a Dyson-Maleev representation for $\mathcal{H}_{\mathrm{HAFM}} + \mathcal{H}_{\mathrm{DzM}}$, similar to the case of only $\mathcal{H}_{\mathrm{HAFM}}$, and calculate the response of j_y linear in $A_x^{(ext)}$.

[5] In an electron system these states differ considerably from the states at $B = 0$, since the electrons are forced to occupy Landau levels.

The problem we have encountered in the previous subsection, namely whether the transversal component of the vector potential should be considered a part of the system, does not occur here. The (possibly) current-deflecting term $\mathcal{H}_{\mathrm{DzM}}$ belongs to the system and expectation values have to be calculated with respect to $\mathcal{H}_{\mathrm{HAFM}} + \mathcal{H}_{\mathrm{DzM}}$.

However, such calculations are outside the scope of this thesis. Instead, we are going to focus on the computation of the longitudinal spin conductivity (3.46), which is the main goal of Chapter 4.

KAPITEL 4

Calculation of the Spin Conductivity

In this chapter the Kubo formula is evaluated using many-body techniques for magnon propagators. We define the basic propagators (one-magnon Green functions) and examine the current correlation function that enters the spin conductivity. It is dominated by a certain two-magnon propagator. We first study the noninteracting-magnon approximation and include magnon scattering in a ladder approximation afterwards.

4.1. Basic Propagators for the Antiferromagnet

We define the basic propagators for the HAFM [**16**, **27**]

$$G_{\alpha\alpha}(\boldsymbol{k}, t-t') \equiv -i\langle\psi_0|\mathcal{T}\alpha_{\boldsymbol{k}}(t)\alpha^\dagger_{\boldsymbol{k}}(t')|\psi_0\rangle, \tag{4.1}$$

$$G_{\beta\beta}(\boldsymbol{k}, t-t') \equiv -i\langle\psi_0|\mathcal{T}\beta^\dagger_{\boldsymbol{k}}(t)\beta_{\boldsymbol{k}}(t')|\psi_0\rangle, \tag{4.2}$$

$$G_{\alpha\beta}(\boldsymbol{k}, t-t') \equiv -i\langle\psi_0|\mathcal{T}\alpha_{\boldsymbol{k}}(t)\beta_{\boldsymbol{k}}(t')|\psi_0\rangle, \tag{4.3}$$

$$G_{\beta\alpha}(\boldsymbol{k}, t-t') \equiv -i\langle\psi_0|\mathcal{T}\beta^\dagger_{\boldsymbol{k}}(t)\alpha^\dagger_{\boldsymbol{k}}(t')|\psi_0\rangle. \tag{4.4}$$

The Fourier representations are defined by

$$G_{\mu\nu}(\boldsymbol{k}, \omega) \equiv \int_{-\infty}^{\infty} d(t-t')e^{i\omega(t-t')}G_{\mu\nu}(\boldsymbol{k}, t-t'), \tag{4.5}$$

where μ and ν can take the values α and β. The unperturbed Green functions are

$$G^{(0)}_{\alpha\alpha}(\boldsymbol{k}, t-t') = -i\Theta(t-t')e^{-i\Omega_{\boldsymbol{k}}(t-t')}, \tag{4.6}$$

$$G^{(0)}_{\beta\beta}(\boldsymbol{k}, t-t') = -i\Theta(t'-t)e^{i\Omega_{\boldsymbol{k}}(t-t')}, \tag{4.7}$$

$$G^{(0)}_{\alpha\beta}(\boldsymbol{k}, t-t') = 0, \tag{4.8}$$

$$G^{(0)}_{\beta\alpha}(\boldsymbol{k}, t-t') = 0. \tag{4.9}$$

The Fourier transforms of the unperturbed Green functions are

$$G^{(0)}_{\alpha\alpha}(\boldsymbol{k},\omega) = \frac{1}{\omega - \Omega_{\boldsymbol{k}} + i\eta}, \tag{4.10}$$

$$G^{(0)}_{\beta\beta}(\boldsymbol{k},\omega) = \frac{-1}{\omega + \Omega_{\boldsymbol{k}} - i\eta}. \tag{4.11}$$

The symbols asscociated with the basic propagators are displayed in Figure 4.1.

The Green functions satisfy a matrix Dyson equation, namely

$$G_{\mu\nu}(\boldsymbol{k},\omega) = G^{(0)}_{\mu\nu}(\boldsymbol{k},\omega) + \sum_{\gamma,\delta=\alpha,\beta} G^{(0)}_{\mu\gamma}(\boldsymbol{k},\omega)\Sigma_{\gamma\delta}(\boldsymbol{k},\omega)G_{\delta\nu}(\boldsymbol{k},\omega), \tag{4.12}$$

where $\Sigma_{\gamma\delta}(\boldsymbol{k},\omega)$ is the magnon self-energy.

4.2. Spin-Current Correlation Function

We now obtain the spin-current correlation function that is needed for the spin conductivity at $T = 0$. For real $\omega > 0$ the following relation holds:

$$\sigma'_{xx}(\omega) = \frac{\Lambda''_{xx}(\boldsymbol{q} = \boldsymbol{0},\omega)}{\omega} = -\frac{1}{\omega}G''_j(\omega). \tag{4.13}$$

The time-ordered Green function for the spin current is

$$G_j(t) \equiv -\frac{i}{N}\langle\psi_0|\mathcal{T} j_x(t) j_x(0)|\psi_0\rangle \tag{4.14}$$

and its Fourier transform reads

$$G_j(\omega) = \int_{-\infty}^{\infty} dt\; e^{i\omega t} G_j(t). \tag{4.15}$$

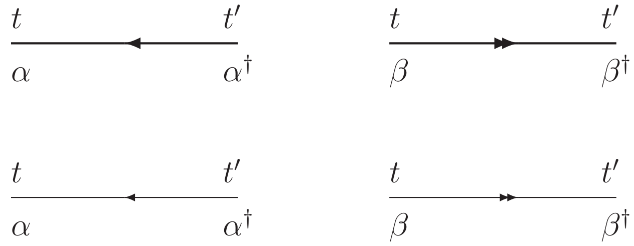

ABBILDUNG 4.1. Diagrammatic representation of the α and β propagators. A boldface line with a single arrow oriented from t' to t represents $G_{\alpha\alpha}(\boldsymbol{k}, t - t')$, a boldface line with a double arrow oriented from t to t' represents $G_{\beta\beta}(\boldsymbol{k}, t - t')$. Light lines represent the unperturbed propagators $G^{(0)}$.

For the calculation of $G_j(\omega)$, we will use the quadratic part of the spin-current operator in Dyson-Maleev representation (see Eq. 3.30),

$$j_x = 2JS\alpha(S)\sum_{\boldsymbol{k}}\sin(k_x)\left[\frac{\gamma_{\boldsymbol{k}}}{\lambda_{\boldsymbol{k}}}(\alpha^\dagger_{\boldsymbol{k}}\alpha_{\boldsymbol{k}}+\beta^\dagger_{\boldsymbol{k}}\beta_{\boldsymbol{k}})-\frac{\Delta}{\lambda_{\boldsymbol{k}}}(\alpha^\dagger_{\boldsymbol{k}}\beta^\dagger_{\boldsymbol{k}}+\alpha_{\boldsymbol{k}}\beta_{\boldsymbol{k}})\right]. \tag{4.16}$$

By multiplying out $j_x(t)j_x(0)$, we obtain the spin-current correlation function $G_j(\omega)$ consisting of 16 terms, each of which contains four magnon operators. Following Canali and Girvin [**16**], who have calculated similar quantities in their study of the Raman-scattering line shape of the HAFM, we will neglect 14 of those terms. Two arguments support our approximations. First, the terms containing factors $\gamma_{\boldsymbol{k}}/\lambda_{\boldsymbol{k}}$ are small due to the fact that $|\gamma_{\boldsymbol{k}}/\lambda_{\boldsymbol{k}}| \approx 0$ near the zone boundary, where dominant contributions from two-magnon scattering are expected from phase-space considerations. Second, there are only two terms which have a nonzero contribution in the noninteracting case. We will thus focus our attention on the following part of the spin-current correlation function $G_j(\omega)$:

$$G_j(\omega) \approx G_j^+(\omega) + G_j^+(-\omega), \tag{4.17}$$

where

$$G_j^+(\omega) \equiv [2JS\alpha(S)]^2\,\frac{1}{N}\sum_{\boldsymbol{k},\boldsymbol{k}'}\sin(k_x)\sin(k'_x)\frac{\Delta^2}{\lambda_{\boldsymbol{k}}\lambda_{\boldsymbol{k}'}}\Pi_{\boldsymbol{k}\boldsymbol{k}'}(\omega). \tag{4.18}$$

Here, we have defined the correlation function

$$\Pi_{\boldsymbol{k}\boldsymbol{k}'}(t) \equiv -i\langle\psi_0|\mathcal{T}\alpha_{\boldsymbol{k}}(t)\beta_{\boldsymbol{k}}(t)\alpha^\dagger_{\boldsymbol{k}'}(0)\beta^\dagger_{\boldsymbol{k}'}(0)|\psi_0\rangle. \tag{4.19}$$

We will now focus on this two-magnon Green function.

4.3. Bethe-Salpeter Equation

The diagrammatic representation of $\Pi_{\boldsymbol{k}\boldsymbol{k}'}(\omega)$ is

$$\Pi_{\boldsymbol{k}\boldsymbol{k}'}(\omega) = i\int_{-\infty}^{\infty}\frac{d\omega'}{2\pi}G_{\alpha\alpha}(\boldsymbol{k},\omega+\omega')G_{\beta\beta}(\boldsymbol{k},\omega')\Gamma_{\boldsymbol{k}\boldsymbol{k}'}(\omega,\omega'). \tag{4.20}$$

This equation is depicted in Figure 4.2.

The vertex function $\Gamma_{\boldsymbol{kk}'}(\omega,\omega')$ satisfies the Bethe-Salpeter equation

$$
\begin{aligned}
(4.21)\quad \Gamma_{\boldsymbol{kk}'}(\omega,\omega') \;=\;& \delta_{\boldsymbol{kk}'} + \Delta J \frac{z}{4}\frac{2}{N}\left[\frac{-i}{\hbar}\right]\sum_{\boldsymbol{k}_1}\int_{-\infty}^{\infty}\frac{d\omega_1}{2\pi} \\
&\times \mathcal{V}^{\alpha\beta}_{\boldsymbol{kk}_1\boldsymbol{k}_1\boldsymbol{k}}(\omega',\omega_1) G_{\alpha\alpha}(\boldsymbol{k}_1,\omega+\omega_1) G_{\beta\beta}(\boldsymbol{k}_1,\omega_1)\Gamma_{\boldsymbol{k}_1\boldsymbol{k}'}(\omega,\omega_1),
\end{aligned}
$$

which is represented in Figure 4.3.

Here, $\mathcal{V}^{\alpha\beta}_{\boldsymbol{kk}_1\boldsymbol{k}_1\boldsymbol{k}}(\omega',\omega_1)$ is the sum of all the irreducible interaction parts.

Instead of solving these coupled equations, we write down a set of equations for the spin-current correlation directly. Using Equation (4.18) yields

$$
\begin{aligned}
(4.22)\quad G_j^{+}(\omega) \;=\;& [2JS\alpha(S)]^2\,\frac{i}{N} \\
&\times \int_{-\infty}^{\infty}\frac{d\omega'}{2\pi}\sum_{\boldsymbol{k}}\frac{\sin(k_x)}{\lambda_{\boldsymbol{k}}/\Delta} G_{\alpha\alpha}(\boldsymbol{k},\omega+\omega') G_{\beta\beta}(\boldsymbol{k},\omega')\Gamma_{\boldsymbol{k}}(\omega,\omega'),
\end{aligned}
$$

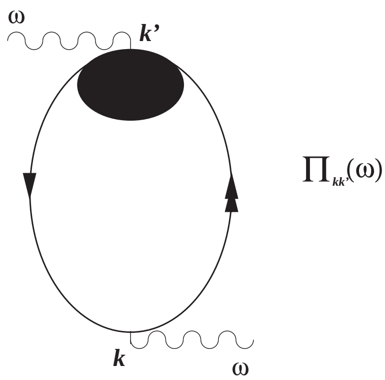

ABBILDUNG 4.2. Diagrammatic representation of the correlation function $\Pi_{\boldsymbol{kk}'}(\omega)$. The solid lines are the α and β propagators. The solid circle represents the vertex function $\Gamma_{\boldsymbol{kk}'}(\omega,\omega')$.

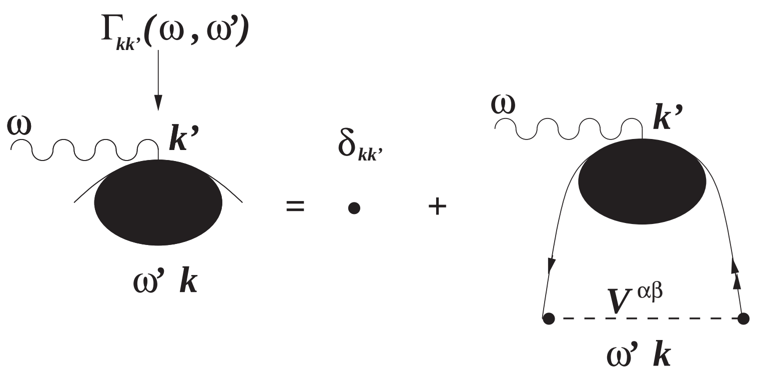

ABBILDUNG 4.3. Bethe-Salpeter equation.

where

$$\Gamma_{\boldsymbol{k}}(\omega, \omega') \equiv \sum_{\boldsymbol{k}'} \frac{\sin(k'_x)}{\lambda_{\boldsymbol{k}'}/\Delta} \Gamma_{\boldsymbol{k}\boldsymbol{k}'}(\omega, \omega'). \tag{4.23}$$

The new vertex function $\Gamma_{\boldsymbol{k}}(\omega, \omega')$ satisfies the equation

$$\begin{aligned} \Gamma_{\boldsymbol{k}}(\omega, \omega') &= \frac{\sin(k_x)}{\lambda_{\boldsymbol{k}}/\Delta} + \Delta J \frac{z}{4} \frac{2}{N} \left[\frac{-i}{\hbar}\right] \sum_{\boldsymbol{k}_1} \int_{-\infty}^{\infty} \frac{d\omega_1}{2\pi} \\ &\times \mathcal{V}^{\alpha\beta}_{\boldsymbol{k}\boldsymbol{k}_1\boldsymbol{k}_1\boldsymbol{k}}(\omega', \omega_1) G_{\alpha\alpha}(\boldsymbol{k}_1, \omega + \omega_1) G_{\beta\beta}(\boldsymbol{k}_1, \omega_1) \Gamma_{\boldsymbol{k}_1}(\omega, \omega_1). \end{aligned} \tag{4.24}$$

4.4. Noninteracting Magnons

The solution of the coupled Equations (4.22) and (4.24) requires certain simplifications. The lowest approximation is to replace the magnon propagators $G_{\alpha\alpha}$ and $G_{\beta\beta}$ by the free propagators $G^{(0)}_{\alpha\alpha}$ and $G^{(0)}_{\beta\beta}$ and to set $\Gamma_{\boldsymbol{k}} = \sin(k_x)/(\lambda_{\boldsymbol{k}}/\Delta)$. Magnon interactions are completely neglected at this level.

We then have

$$\begin{aligned} G^{+}_{j}(\omega) &= [2JS\alpha(S)]^2 \, \frac{i}{N} \\ &\times \int_{-\infty}^{\infty} \frac{d\omega'}{2\pi} \sum_{\boldsymbol{k}} \frac{\sin(k_x)}{\lambda_{\boldsymbol{k}}/\Delta} G^{(0)}_{\alpha\alpha}(\boldsymbol{k}, \omega + \omega') G^{(0)}_{\beta\beta}(\boldsymbol{k}, \omega') \frac{\sin(k_x)}{\lambda_{\boldsymbol{k}}/\Delta}. \end{aligned} \tag{4.25}$$

The ω'-integration is carried out first,

$$i \int_{-\infty}^{\infty} \frac{d\omega'}{2\pi} G^{(0)}_{\alpha\alpha}(\boldsymbol{k}, \omega + \omega') G^{(0)}_{\beta\beta}(\boldsymbol{k}, \omega') = i \int_{-\infty}^{\infty} \frac{d\omega'}{2\pi} \frac{1}{\omega + \omega' - \Omega_{\boldsymbol{k}} + i\eta} \frac{-1}{\omega' + \Omega_{\boldsymbol{k}} - i\eta}.$$

The integrand has a pole in the upper half-plane at $\omega' = -\Omega_{\boldsymbol{k}} + i\eta$. We close the integral in the upper half-plane and obtain

$$i \int_{-\infty}^{\infty} \frac{d\omega'}{2\pi} G^{(0)}_{\alpha\alpha}(\boldsymbol{k}, \omega + \omega') G^{(0)}_{\beta\beta}(\boldsymbol{k}, \omega') = \frac{1}{\omega - 2\Omega_{\boldsymbol{k}} + i\eta}.$$

We thus get, for the noninteracting case at $T = 0$,

$$G^{+}_{j}(\omega) = [2JS\alpha(S)]^2 \, \frac{1}{N} \sum_{\boldsymbol{k}} \frac{(\sin(k_x))^2}{(\lambda_{\boldsymbol{k}}/\Delta)^2} \frac{1}{\omega - 2\Omega_{\boldsymbol{k}} + i\eta}. \tag{4.26}$$

It is convenient to introduce the dimensionless frequency

$$\widetilde{\omega} \equiv \omega/\Omega_{\max}, \tag{4.27}$$

where $\Omega_{\max}$ is defined in Eq. (2.41), and to use the normalized dispersion $\varepsilon_{\boldsymbol{k}} = \lambda_{\boldsymbol{k}}/\Delta$. We define the functions

$$
\begin{aligned}
L^{(m)}(\omega) &\equiv i\int_{-\infty}^{\infty}\frac{d\omega'}{2\pi}\frac{2}{N}\sum_{\boldsymbol{k}}\frac{(\sin(k_x))^2}{(\varepsilon_{\boldsymbol{k}})^m}G^{(0)}_{\alpha\alpha}(\boldsymbol{k},\omega+\omega')G^{(0)}_{\beta\beta}(\boldsymbol{k},\omega') \\
&= \frac{2}{N}\sum_{\boldsymbol{k}}\frac{(\sin(k_x))^2}{(\lambda_{\boldsymbol{k}}/\Delta)^m}\frac{1}{\omega-2\Omega_{\boldsymbol{k}}+i\eta} \\
&= \frac{2}{N\Omega_{\max}}\sum_{\boldsymbol{k}}\frac{(\sin(k_x))^2}{(\varepsilon_{\boldsymbol{k}})^m}\frac{1}{\widetilde{\omega}-2\varepsilon_{\boldsymbol{k}}+i\eta}
\end{aligned}
\tag{4.28}
$$

and

$$
\ell^{(m)}(\widetilde{\omega}) \equiv \Omega_{\max}L^{(m)}(\omega) = \frac{2}{N}\sum_{\boldsymbol{k}}\frac{(\sin(k_x))^2}{(\varepsilon_{\boldsymbol{k}})^m}\frac{1}{\widetilde{\omega}-2\varepsilon_{\boldsymbol{k}}+i\eta}. \tag{4.29}
$$

We can now write

$$
G_j^{+}(\omega) = [2JS\alpha(S)]^2\,\frac{1}{2}L^{(2)}(\omega) = [2JS\alpha(S)]^2\,\frac{1}{2}\frac{\ell^{(2)}(\widetilde{\omega})}{\Omega_{\max}}. \tag{4.30}
$$

The spin conductivity for $\omega > 0$ without any magnon interactions is thus

$$
\begin{aligned}
\sigma'_{xx}(\omega) &= -\frac{1}{\omega}(G_j^{+})''(\omega) = -\,[2JS\alpha(S)]^2\,\frac{1}{2}\frac{1}{\widetilde{\omega}\Omega_{\max}}\frac{(\ell^{(2)})''(\widetilde{\omega})}{\Omega_{\max}} \\
&= \frac{1}{\omega}\,[2JS\alpha(S)]^2\,\frac{1}{\Omega_{\max}}\frac{1}{N}\sum_{\boldsymbol{k}}\frac{(\sin(k_x))^2}{(\varepsilon_{\boldsymbol{k}})^2}\pi\delta(\widetilde{\omega}-2\varepsilon_{\boldsymbol{k}}).
\end{aligned}
\tag{4.31}
$$

This function has a cutoff at the maximum energy a two-magnon state can have, $\widetilde{\omega} = 2$ or $\omega = 2\Omega_{\max}$, respectively, where there is a van-Hove type of singularity similar to the free-magnon density of states. This singularity is unphysical and due to the neglect of magnon scattering. In fact, the magnon interactions cannot be neglected since the two magnons of consideration are created close to each other in real space [**46**].

In (4.31) we also recognize the selection rules discussed in Section 3.6. The delta function implies that we deal with two-magnon excitations. Hence, momentum conservation is fulfilled as long as the two magnons have opposite momenta. They can still have the same energy, of course, since $\varepsilon_{\boldsymbol{k}} = \varepsilon_{-\boldsymbol{k}}$. The conservation of magnetization is fulfilled by a two-magnon excitation since α and β magnons carry opposite spin ("particle-hole"-like excitation).

4.5. Ladder Approximation: Two-Magnon Scattering

We now take into account magnon interactions to lowest order. Therefore, we approximate $\mathcal{V}^{\alpha\beta}$ by its first-order irreducible interaction part,

$$\mathcal{V}^{\alpha\beta}_{\boldsymbol{k}\boldsymbol{k}_1\boldsymbol{k}_1\boldsymbol{k}}(\omega', \omega_1) = V^{(4)}_{\boldsymbol{k}\boldsymbol{k}_1\boldsymbol{k}_1\boldsymbol{k}}. \tag{4.32}$$

The diagram for this two-magnon scattering process is depicted in Figure 4.4. We have to correct the magnon propagators by the first-order self-energy. For the isotropic case, $\Delta = 1$, Canali and Girvin [**16**] have shown that the first-order magnon self-energy vanishes at $T = 0$. Therefore, we will use the bare expressions $G^{(0)}_{\alpha\alpha}$ and $G^{(0)}_{\beta\beta}$ in Equation (4.22).

4.5.1. Calculation of the Interaction Vertex. Before we go on to solve the set of Equations (4.22) and (4.24), we have to calculate the vertex function $V^{(4)}_{\boldsymbol{k}\boldsymbol{k}_1\boldsymbol{k}_1\boldsymbol{k}}$ explicitly. We go back to Section 2.2.1 and the magnon-interaction part in Dyson-Maleev representation,

$$V'_{\mathrm{DM}} = -J \sum_{\langle ij \rangle} \left[\Delta a_i^\dagger a_i b_j^\dagger b_j + \frac{1}{2} \left(a_i^\dagger a_i a_i b_j + a_i^\dagger b_j^\dagger b_j^\dagger b_j \right) \right]. \tag{4.33}$$

We choose the origin in real space to be on sublattice A. Any vector $\boldsymbol{R}_j$ of sublattice B can be written in the form $\boldsymbol{R}_j = \boldsymbol{R}_i + \delta$, where $\boldsymbol{R}_i$ is a vector of sublattice A. We

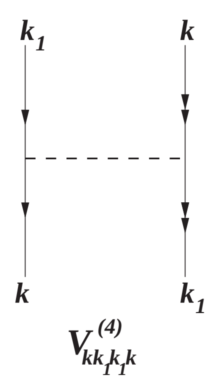

ABBILDUNG 4.4. Magnon interaction.

take the Fourier transforms,

$$a_i = \sqrt{\frac{2}{N}} \sum_{\boldsymbol{k}} e^{-i\boldsymbol{k}\cdot\boldsymbol{R}_i} a_{\boldsymbol{k}}, \tag{4.34}$$

$$b_j = \sqrt{\frac{2}{N}} \sum_{\boldsymbol{k}} e^{+i\boldsymbol{k}\cdot\boldsymbol{R}_j} b_{\boldsymbol{k}}, \tag{4.35}$$

and obtain, writing $1, 2, 3, 4$ for $\boldsymbol{k}_1, \boldsymbol{k}_2, \boldsymbol{k}_3, \boldsymbol{k}_4$,

$$\begin{aligned} V'_{\mathrm{DM}} &= -J\frac{z}{4}\frac{2}{N} \sum_{(1234)} \delta_{\boldsymbol{G}}(1+2-3-4) \\ &\times \Big[\Delta(\gamma_{2-4} a_1^\dagger a_3 b_4^\dagger b_2 + \gamma_{1-4} a_2^\dagger a_3 b_4^\dagger b_1 + \gamma_{2-3} a_1^\dagger a_4 b_3^\dagger b_2 + \gamma_{1-3} a_2^\dagger a_4 b_3^\dagger b_1) \\ &\quad + \gamma_2 a_1^\dagger a_3 a_4 b_2 + \gamma_1 a_2^\dagger a_3 a_4 b_1 + \gamma_{2-3-4} a_1^\dagger b_3^\dagger b_4^\dagger b_2 + \gamma_{1-3-4} a_2^\dagger b_3^\dagger b_4^\dagger b_1\Big]. \end{aligned} \tag{4.36}$$

The Kronecker delta has to be interpreted as in Equation (2.42), and we have used

$$\frac{2}{N} \sum_i e^{-i(\boldsymbol{k}_1+\boldsymbol{k}_2-\boldsymbol{k}_3-\boldsymbol{k}_4)\boldsymbol{R}_i} = \delta_{\boldsymbol{G}}(1+2-3-4). \tag{4.37}$$

We now perform the Bogoliubov transformation,

$$a_{\boldsymbol{k}} = u_{\boldsymbol{k}} \alpha_{\boldsymbol{k}} + v_{\boldsymbol{k}} \beta_{\boldsymbol{k}}^\dagger, \tag{4.38}$$

$$b_{\boldsymbol{k}} = u_{\boldsymbol{k}} \beta_{\boldsymbol{k}} + v_{\boldsymbol{k}} \alpha_{\boldsymbol{k}}^\dagger. \tag{4.39}$$

The normal-ordered part of V'_{DM} is given in Equation (2.35). We want to compute the vertex function $V^{(4)}_{(1234)}$. First, we have to collect all the terms leading to the combination $\alpha_1^\dagger \alpha_3 \beta_4^\dagger \beta_2$ after normal-ordering. The prefactors of this combination in terms of u's and v's combine to

$$\begin{aligned} \frac{\Delta}{4} V^{(4)}_{(1234)} &= \Delta(u_1 u_2 u_3 u_4 \gamma_{2-4} + v_1 v_2 u_3 u_4 \gamma_{1-4} + u_1 u_2 v_3 v_4 \gamma_{2-3} + v_1 v_2 v_3 v_4 \gamma_{1-3}) \\ &\quad + u_1 u_2 u_3 v_4 \gamma_2 + v_1 v_2 u_3 v_4 \gamma_1 + u_1 u_2 v_3 u_4 \gamma_{2-3-4} + v_1 v_2 v_3 u_4 \gamma_{1-3-4}. \end{aligned} \tag{4.40}$$

Using the explicit expressions for the u's and v's (see Eqns. (2.21) and (2.22)) we can finally calculate the interaction vertex $V^{(4)}_{\boldsymbol{k}\boldsymbol{k}_1\boldsymbol{k}_1\boldsymbol{k}}$,

$$\begin{aligned} \frac{1}{4} V^{(4)}_{\boldsymbol{k}\boldsymbol{k}_1\boldsymbol{k}_1\boldsymbol{k}} &= \left[\frac{1}{2}\gamma_{\boldsymbol{k}-\boldsymbol{k}_1}\left[\frac{\Delta^2}{\lambda_{\boldsymbol{k}}\lambda_{\boldsymbol{k}_1}} + 1\right] - \frac{1}{2}\gamma_{\boldsymbol{k}}\gamma_{\boldsymbol{k}_1}\frac{1}{\lambda_{\boldsymbol{k}}\lambda_{\boldsymbol{k}_1}}\right] \\ &= \frac{1}{2}\gamma_{\boldsymbol{k}-\boldsymbol{k}_1}\left[\frac{1}{\varepsilon_{\boldsymbol{k}}\varepsilon_{\boldsymbol{k}_1}} + 1\right] - \frac{1}{2}\gamma_{\boldsymbol{k}}\gamma_{\boldsymbol{k}_1}\frac{1}{\lambda_{\boldsymbol{k}}\lambda_{\boldsymbol{k}_1}}, \end{aligned} \tag{4.41}$$

where we have used $\varepsilon_{\boldsymbol{k}} \equiv \lambda_{\boldsymbol{k}}/\Delta = \sqrt{1-(\gamma_{\boldsymbol{k}}/\Delta)^2}$.

4.5.2. Solution of the Ladder Bethe-Salpeter Equation. The next step is to solve the Equations (4.22) and (4.24) in the approximation that uses $G^{(0)}_{\alpha\alpha}$ and $G^{(0)}_{\beta\beta}$ for the single-particle propagators and $V^{(4)}_{\boldsymbol{k}\boldsymbol{k}_1\boldsymbol{k}_1\boldsymbol{k}}$ for the interaction vertex.

In order to find an analytic solution, we will need the following relations to decouple $\boldsymbol{k}$-sums:

$$\sum_{\boldsymbol{k}} \sin(k_x)\gamma_{\boldsymbol{k}} g_{\boldsymbol{k}} = 0, \tag{4.42}$$

$$\sum_{\boldsymbol{k}} \sin(k_x)\gamma_{\boldsymbol{k}-\boldsymbol{k}_1} g_{\boldsymbol{k}} = \frac{2}{z}\sin(k_{1,x})\sum_{\boldsymbol{k}}(\sin(k_x))^2 g_{\boldsymbol{k}}. \tag{4.43}$$

Here $g_{\boldsymbol{k}}$ is any function having the symmetry of the square lattice, i. e., discrete $90°$-rotational symmetry, and we have used $z = 2d$.

The basic equations are

$$G^+_j(\omega) = Ci\int_{-\infty}^{\infty}\frac{d\omega'}{2\pi}\frac{2}{N}\sum_{\boldsymbol{k}}\frac{\sin(k_x)}{\varepsilon_{\boldsymbol{k}}}G^{(0)}_{\alpha\alpha}(\boldsymbol{k},\omega+\omega')G^{(0)}_{\beta\beta}(\boldsymbol{k},\omega')\Gamma_{\boldsymbol{k}}(\omega,\omega') \tag{4.44}$$

and

$$\begin{aligned}\Gamma_{\boldsymbol{k}}(\omega,\omega') &= \frac{\sin(k_x)}{\varepsilon_{\boldsymbol{k}}} + \Delta Jz\frac{2}{N}\left[\frac{-i}{\hbar}\right]\sum_{\boldsymbol{k}_1}\int_{-\infty}^{\infty}\frac{d\omega_1}{2\pi} \\ &\times\frac{1}{4}V^{(4)}_{\boldsymbol{k}\boldsymbol{k}_1\boldsymbol{k}_1\boldsymbol{k}}G^{(0)}_{\alpha\alpha}(\boldsymbol{k}_1,\omega+\omega_1)G^{(0)}_{\beta\beta}(\boldsymbol{k}_1,\omega_1)\Gamma_{\boldsymbol{k}_1}(\omega,\omega_1),\end{aligned} \tag{4.45}$$

where $C = \frac{1}{2}\left[2JS\alpha(S)\right]^2$. Note that, in this approximation, $\Gamma_{\boldsymbol{k}}(\omega,\omega')$ is not a function of ω' anymore, since $V^{(4)}_{\boldsymbol{k}\boldsymbol{k}_1\boldsymbol{k}_1\boldsymbol{k}}$ is frequency-independent.

Substituting Equation (4.45) into Equation (4.44) results in

$$G^+_j(\omega) = CL^{(2)}(\omega) + \mathcal{A}_1(\omega), \tag{4.46}$$

where $L^{(2)}(\omega)$ is defined in Equation (4.28). The new function $\mathcal{A}_1(\omega)$ is defined by

$$\begin{aligned}\mathcal{A}_1(\omega) &\equiv Ci\int_{-\infty}^{\infty}\frac{d\omega'}{2\pi}\frac{2}{N}\sum_{\boldsymbol{k}}\frac{\sin(k_x)}{\varepsilon_{\boldsymbol{k}}}G^{(0)}_{\alpha\alpha}(\boldsymbol{k},\omega+\omega')G^{(0)}_{\beta\beta}(\boldsymbol{k},\omega') \\ &\times\Delta Jz\left[\frac{-i}{\hbar}\right]\frac{2}{N}\sum_{\boldsymbol{k}_1}\int_{-\infty}^{\infty}\frac{d\omega_1}{2\pi}\frac{1}{4}V^{(4)}_{\boldsymbol{k}\boldsymbol{k}_1\boldsymbol{k}_1\boldsymbol{k}}G^{(0)}_{\alpha\alpha}(\boldsymbol{k}_1,\omega+\omega_1) \\ &\times G^{(0)}_{\beta\beta}(\boldsymbol{k}_1,\omega_1)\Gamma_{\boldsymbol{k}_1}(\omega,\omega_1).\end{aligned} \tag{4.47}$$

We use the explicit expression of $V^{(4)}_{\boldsymbol{k}\boldsymbol{k}_1\boldsymbol{k}_1\boldsymbol{k}}$ in order to compute $\mathcal{A}_1(\omega)$,

$$\begin{aligned}\mathcal{A}_1(\omega) &= Ci\int_{-\infty}^{\infty}\frac{d\omega'}{2\pi}\frac{2}{N}\sum_{\boldsymbol{k}}\frac{\sin(k_x)}{\varepsilon_{\boldsymbol{k}}}G^{(0)}_{\alpha\alpha}(\boldsymbol{k},\omega+\omega')G^{(0)}_{\beta\beta}(\boldsymbol{k},\omega') \\ &\times\Delta Jz\left[\frac{-i}{\hbar}\right]\frac{2}{N}\sum_{\boldsymbol{k}_1}\int_{-\infty}^{\infty}\frac{d\omega_1}{2\pi} \\ &\times\left[\frac{1}{2}\gamma_{\boldsymbol{k}-\boldsymbol{k}_1}\left[\frac{1}{\varepsilon_{\boldsymbol{k}}\varepsilon_{\boldsymbol{k}_1}}+1\right]-\frac{1}{2}\gamma_{\boldsymbol{k}}\gamma_{\boldsymbol{k}_1}\frac{1}{\lambda_{\boldsymbol{k}}\lambda_{\boldsymbol{k}_1}}\right] \\ &\times G^{(0)}_{\alpha\alpha}(\boldsymbol{k}_1,\omega+\omega_1)G^{(0)}_{\beta\beta}(\boldsymbol{k}_1,\omega_1)\Gamma_{\boldsymbol{k}_1}(\omega,\omega_1).\end{aligned} \tag{4.48}$$

Carrying out $\sum_{\boldsymbol{k}}$ using Equations (4.42) and (4.43) yields

$$\begin{aligned}\mathcal{A}_1(\omega) &= C\Delta Jz\left[\frac{-i}{\hbar}\right]\frac{2}{N}\sum_{\boldsymbol{k}_1}\int_{-\infty}^{\infty}\frac{d\omega_1}{2\pi} \\ &\times G^{(0)}_{\alpha\alpha}(\boldsymbol{k}_1,\omega+\omega_1)G^{(0)}_{\beta\beta}(\boldsymbol{k}_1,\omega_1)\Gamma_{\boldsymbol{k}_1}(\omega,\omega_1)i\int_{-\infty}^{\infty}\frac{d\omega'}{2\pi} \\ &\times\frac{2}{N}\underbrace{\sum_{\boldsymbol{k}}\frac{\sin(k_x)}{\varepsilon_{\boldsymbol{k}}}\left[\frac{1}{2}\gamma_{\boldsymbol{k}-\boldsymbol{k}_1}\left[\frac{1}{\varepsilon_{\boldsymbol{k}}\varepsilon_{\boldsymbol{k}_1}}+1\right]\right]G^{(0)}_{\alpha\alpha}(\boldsymbol{k},\omega+\omega')G^{(0)}_{\beta\beta}(\boldsymbol{k},\omega')}_{\overset{(4.43)}{=}\frac{2}{z}\sin(k_{1,x})\sum_{\boldsymbol{k}}\frac{(\sin(k_x))^2}{\varepsilon_{\boldsymbol{k}}}\left[\frac{1}{2}\left[\frac{1}{\varepsilon_{\boldsymbol{k}}\varepsilon_{\boldsymbol{k}_1}}+1\right]\right]G^{(0)}_{\alpha\alpha}(\boldsymbol{k},\omega+\omega')G^{(0)}_{\beta\beta}(\boldsymbol{k},\omega')}.\end{aligned} \tag{4.49}$$

We rewrite this in the following way:

$$\begin{aligned}\mathcal{A}_1(\omega) &= C\Delta Jz\left[\frac{-i}{\hbar}\right]\frac{2}{N}\sum_{\boldsymbol{k}_1}\int_{-\infty}^{\infty}\frac{d\omega_1}{2\pi}\frac{1}{z}\sin(k_{1,x}) \\ &\times G^{(0)}_{\alpha\alpha}(\boldsymbol{k}_1,\omega+\omega_1)G^{(0)}_{\beta\beta}(\boldsymbol{k}_1,\omega_1)\Gamma_{\boldsymbol{k}_1}(\omega,\omega_1)i\int_{-\infty}^{\infty}\frac{d\omega'}{2\pi} \\ &\times\frac{2}{N}\sum_{\boldsymbol{k}}\frac{(\sin(k_x))^2}{\varepsilon_{\boldsymbol{k}}}\left[\frac{1}{\varepsilon_{\boldsymbol{k}}\varepsilon_{\boldsymbol{k}_1}}+1\right]G^{(0)}_{\alpha\alpha}(\boldsymbol{k},\omega+\omega')G^{(0)}_{\beta\beta}(\boldsymbol{k},\omega').\end{aligned} \tag{4.50}$$

Recalling our basic Equation (4.44) and the definition of the L-functions,

$$L^{(m)}(\omega)\equiv i\int_{-\infty}^{\infty}\frac{d\omega'}{2\pi}\frac{2}{N}\sum_{\boldsymbol{k}}\frac{(\sin(k_x))^2}{(\varepsilon_{\boldsymbol{k}})^m}G^{(0)}_{\alpha\alpha}(\boldsymbol{k},\omega+\omega')G^{(0)}_{\beta\beta}(\boldsymbol{k},\omega'), \tag{4.51}$$

this can be summarized as follows:

$$\mathcal{A}_1(\omega)=\Delta\left[\frac{-J}{\hbar}\right]G^{+}_{j}(\omega)L^{(2)}(\omega)+\mathcal{A}_2(\omega), \tag{4.52}$$

where

$$\begin{aligned}(4.53)\qquad \mathcal{A}_2(\omega) &\equiv L^{(1)}(\omega)C\Delta J\left[\frac{-i}{\hbar}\right]\frac{2}{N}\sum_{\boldsymbol{k}_1}\int_{-\infty}^{\infty}\frac{d\omega_1}{2\pi}\sin(k_{1,x})\\ &\quad\times G^{(0)}_{\alpha\alpha}(\boldsymbol{k}_1,\omega+\omega_1)G^{(0)}_{\beta\beta}(\boldsymbol{k}_1,\omega_1)\Gamma_{\boldsymbol{k}_1}(\omega,\omega_1).\end{aligned}$$

We can now put expression (4.45) into Equation (4.53),

$$\begin{aligned}(4.54)\qquad \mathcal{A}_2(\omega) &= L^{(1)}(\omega)C\Delta J\left[\frac{-i}{\hbar}\right]\frac{2}{N}\sum_{\boldsymbol{k}_1}\int_{-\infty}^{\infty}\frac{d\omega_1}{2\pi}\sin(k_{1,x})\\ &\quad\times G^{(0)}_{\alpha\alpha}(\boldsymbol{k}_1,\omega+\omega_1)G^{(0)}_{\beta\beta}(\boldsymbol{k}_1,\omega_1)\\ &\quad\times\Bigg[\frac{\sin(k_{1,x})}{\varepsilon_{\boldsymbol{k}_1}}+\Delta Jz\frac{2}{N}\left[\frac{-i}{\hbar}\right]\sum_{\boldsymbol{k}_2}\int_{-\infty}^{\infty}\frac{d\omega_2}{2\pi}\frac{1}{4}V^{(4)}_{\boldsymbol{k}_1\boldsymbol{k}_2\boldsymbol{k}_2\boldsymbol{k}_1}\\ &\quad\times G^{(0)}_{\alpha\alpha}(\boldsymbol{k}_2,\omega+\omega_2)G^{(0)}_{\beta\beta}(\boldsymbol{k}_2,\omega_2)\Gamma_{\boldsymbol{k}_2}(\omega,\omega_2)\Bigg].\end{aligned}$$

We get three terms, one of them coming from the $\sin(k_{1,x})/\varepsilon_{\boldsymbol{k}_1}$ -term and another two from the interaction vertex. The first one reads

$$\begin{aligned}(4.55)\qquad \mathcal{A}^{(I)}_2(\omega) &= L^{(1)}(\omega)C\Delta J\left[\frac{-i}{\hbar}\right]\frac{2}{N}\sum_{\boldsymbol{k}_1}\int_{-\infty}^{\infty}\frac{d\omega_1}{2\pi}\sin(k_{1,x})\\ &\quad\times G^{(0)}_{\alpha\alpha}(\boldsymbol{k}_1,\omega+\omega_1)G^{(0)}_{\beta\beta}(\boldsymbol{k}_1,\omega_1)\frac{\sin(k_{1,x})}{\varepsilon_{\boldsymbol{k}_1}}\\ &= C\Delta\left[\frac{-J}{\hbar}\right]L^{(1)}(\omega)L^{(1)}(\omega).\end{aligned}$$

For the second and third term, the explicit expression for the interaction vertex is put into the equation, and again Equations (4.42) and (4.43) are used to disentangle the two sums. Therefore, we rewrite those terms,

(4.56)

$$\begin{aligned}\mathcal{A}_2(\omega) &= \mathcal{A}^{(I)}_2(\omega)+L^{(1)}(\omega)C\Delta^2 z\left[\frac{J}{\hbar}\right]^2\frac{2}{N}\sum_{\boldsymbol{k}_2}i\int_{-\infty}^{\infty}\frac{d\omega_2}{2\pi}\\ &\quad\times G^{(0)}_{\alpha\alpha}(\boldsymbol{k}_2,\omega+\omega_2)G^{(0)}_{\beta\beta}(\boldsymbol{k}_2,\omega_2)\Gamma_{\boldsymbol{k}_2}(\omega,\omega_2)i\int_{-\infty}^{\infty}\frac{d\omega_1}{2\pi}\frac{2}{N}\\ &\quad\times\underbrace{\sum_{\boldsymbol{k}_1}\sin(k_{1,x})\left[\frac{1}{2}\gamma_{\boldsymbol{k}_1-\boldsymbol{k}_2}\left[\frac{1}{\varepsilon_{\boldsymbol{k}_1}\varepsilon_{\boldsymbol{k}_2}}+1\right]\right]G^{(0)}_{\alpha\alpha}(\boldsymbol{k}_1,\omega+\omega_1)G^{(0)}_{\beta\beta}(\boldsymbol{k}_1,\omega_1).}_{\overset{(4.43)}{=}\frac{2}{z}\sin(k_{2,x})\sum_{\boldsymbol{k}_1}\sin^2(k_{1,x})\left[\frac{1}{2}\left[\frac{1}{\varepsilon_{\boldsymbol{k}_1}\varepsilon_{\boldsymbol{k}_2}}+1\right]\right]G^{(0)}_{\alpha\alpha}(\boldsymbol{k}_1,\omega+\omega_1)G^{(0)}_{\beta\beta}(\boldsymbol{k}_1,\omega_1)}\end{aligned}$$

The result is

$$
\begin{aligned}
\mathcal{A}_2(\omega) &= \mathcal{A}_2^{(I)}(\omega) + L^{(1)}(\omega) C\Delta^2 \left[\frac{J}{\hbar}\right]^2 \frac{2}{N} \sum_{\boldsymbol{k}_2} i \int_{-\infty}^{\infty} \frac{d\omega_2}{2\pi} \sin(k_{2,x}) \\
&\times G^{(0)}_{\alpha\alpha}(\boldsymbol{k}_2, \omega+\omega_2) G^{(0)}_{\beta\beta}(\boldsymbol{k}_2, \omega_2) \Gamma_{\boldsymbol{k}_2}(\omega, \omega_2) i \int_{-\infty}^{\infty} \frac{d\omega_1}{2\pi} \frac{2}{N} \\
&\times \sum_{\boldsymbol{k}_1} \sin^2(k_{1,x}) \left[\frac{1}{\varepsilon_{\boldsymbol{k}_1}\varepsilon_{\boldsymbol{k}_2}} + 1\right] G^{(0)}_{\alpha\alpha}(\boldsymbol{k}_1, \omega+\omega_1) G^{(0)}_{\beta\beta}(\boldsymbol{k}_1, \omega_1).
\end{aligned} \tag{4.57}
$$

The term coming from the 1 in $\left[\frac{1}{\varepsilon_{\boldsymbol{k}_1}\varepsilon_{\boldsymbol{k}_2}} + 1\right]$ then reads

$$
\mathcal{A}_2^{(III)}(\omega) = \Delta \left[\frac{-J}{\hbar}\right] L^{(0)}(\omega) \mathcal{A}_2(\omega), \tag{4.58}
$$

and the other one is

$$
\mathcal{A}_2^{(II)}(\omega) = \Delta^2 \left[\frac{J}{\hbar}\right]^2 L^{(1)}(\omega) L^{(1)}(\omega) G_j^+(\omega). \tag{4.59}
$$

Summarizing this, we can write $\mathcal{A}_2(\omega)$ in the following way:

$$
\begin{aligned}
\mathcal{A}_2(\omega) &= \mathcal{A}_2^{(I)}(\omega) + \mathcal{A}_2^{(II)}(\omega) + \mathcal{A}_2^{(III)}(\omega) \\
&= C\Delta \left[\frac{-J}{\hbar}\right] L^{(1)}(\omega) L^{(1)}(\omega) + \Delta^2 \left[\frac{J}{\hbar}\right]^2 L^{(1)}(\omega) L^{(1)}(\omega) G_j^+(\omega) \\
&\quad + \Delta \left[\frac{-J}{\hbar}\right] L^{(0)}(\omega) \mathcal{A}_2(\omega).
\end{aligned} \tag{4.60}
$$

Here, we can substitute $\mathcal{A}_2(\omega)$ using Equation (4.52) and drop all the ω-arguments for simplicity. We obtain

$$
\begin{aligned}
\mathcal{A}_1 - \Delta \left[\frac{-J}{\hbar}\right] G_j^+ L^{(2)} &= C\Delta \left[\frac{-J}{\hbar}\right] L^{(1)} L^{(1)} + \Delta^2 \left[\frac{J}{\hbar}\right]^2 L^{(1)} L^{(1)} G_j^+ \\
&\quad + \Delta \left[\frac{-J}{\hbar}\right] L^{(0)} \left[\mathcal{A}_1 - \Delta \left[\frac{-J}{\hbar}\right] G_j^+ L^{(2)}\right].
\end{aligned} \tag{4.61}
$$

The next step is to use Equation (4.46) in order to eliminate $\mathcal{A}_1(\omega)$:

$$
\begin{aligned}
G_j^+ - CL^{(2)} - \Delta \left[\frac{-J}{\hbar}\right] G_j^+ L^{(2)} &= C\Delta \left[\frac{-J}{\hbar}\right] L^{(1)} L^{(1)} + \Delta^2 \left[\frac{J}{\hbar}\right]^2 L^{(1)} L^{(1)} G_j^+ \\
&\quad + \Delta \left[\frac{-J}{\hbar}\right] L^{(0)} \left[\left(G_j^+ - CL^{(2)}\right) - \Delta \left[\frac{-J}{\hbar}\right] G_j^+ L^{(2)}\right].
\end{aligned} \tag{4.62}
$$

We can now solve for G_j^+:

$$G_j^+ = C\left[\frac{L^{(2)} - \Delta(J/\hbar)[L^{(1)}L^{(1)} - L^{(0)}L^{(2)}]}{1 + \Delta(J/\hbar)[L^{(0)} + L^{(2)}] - \Delta^2(J/\hbar)^2[L^{(1)}L^{(1)} - L^{(0)}L^{(2)}]}\right]. \tag{4.63}$$

Replacing the abbreviation C and using the dimensionless ℓ-functions this can be retyped as

$$G_j^+ = \frac{1}{2}\frac{[2JS\alpha(S)]^2}{\Omega_{\max}}\left[\frac{\ell^{(2)} - \kappa[\ell^{(1)}\ell^{(1)} - \ell^{(0)}\ell^{(2)}]}{1 + \kappa[\ell^{(0)} + \ell^{(2)}] - \kappa^2[\ell^{(1)}\ell^{(1)} - \ell^{(0)}\ell^{(2)}]}\right], \tag{4.64}$$

where

$$\kappa \equiv \Delta J/\hbar\Omega_{\max}. \tag{4.65}$$

Note that Oguchi's corrections enter the spin conductivity in a nontrivial way. Apart from renormalizing the energy scale, $\alpha(S)$ (which is indeed also a function of the anisotropy Δ, a fact that we have suppressed in our equations for brevity) also changes the shape of the curves via $\Omega_{\max} \propto \alpha(S)$.

We can compare our result with the solution for the noninteracting case,

$$G_j^+\big|_{\text{nonint.}} = \frac{1}{2}\frac{[2JS\alpha(S)]^2}{\Omega_{\max}}\,\ell^{(2)}. \tag{4.66}$$

It corresponds to considering just the first terms in the enumerator and the denominator of the "interacting" solution. The singularities of van-Hove type disappear once magnon interactions are included.

The results are evaluated and discussed in more detail in Chapter 5.

KAPITEL 5

Results and Discussion

The equations we have obtained for the spin conductivity contain $\boldsymbol{k}$-sums over the antiferromagnetic Brillouin zone. We evaluate these sums numerically for a two-dimensional 15 000×15 000 lattice and a three-dimensional 600×600×600 lattice. The results are shown and discussed in this chapter. For comparison, we also perform analytical calculations (for the integrals corresponding to the sums in the thermodynamic limit) which are shown in Appendix B.

5.1. Spin Conductivity of the 2D Heisenberg Antiferromagnet

We first discuss the results for the 2D antiferromagnet focussing on the case $S = \frac{1}{2}$.

5.1.1. Noninteracting Magnons. Figure 5.1 shows the spin conductivity in the case of noninteracting magnons,

$$\boxed{\sigma'_{xx}(\omega) = \frac{1}{\omega}\left[2JS\alpha(S)\right]^2 \frac{1}{\Omega_{\max}} \frac{1}{N} \sum_{\boldsymbol{k}} \frac{(\sin(k_x))^2}{(\varepsilon_{\boldsymbol{k}})^2} \pi\delta(\omega/\Omega_{\max} - 2\varepsilon_{\boldsymbol{k}}).} \tag{5.1}$$

The curve has a cutoff at the maximum two-magnon energy. As mentioned before, there is a van-Hove type of singularity (square root and logarithmic, similar to the density of states) indicating the failure of the noninteracting-magnon approximation. The analytical solution is derived in Appendix B.

Some features of the interacting results are already included. The isotropic (gapless) curve has a finite $\omega \to 0$-limit. The anisotropic curve shows the characteristic energy gap of the system, showing that a minimum energy is required to get a finite value for the spin conductivity.

5.1.2. Drude Weight for noninteracting Magnons. In the case of noninteracting magnons, an explicit expression for the kinetic energy can be obtained at the same level of approximation as for the current-correlation function. Integrating by parts, one can show analytically that the Drude weight vanishes for all values $\Delta \geq 1$.

Therefore, we first calculate the kinetic energy

$$\langle K_x \rangle = \frac{J}{2}\frac{1}{N}\sum_l \langle S_l^+ S_{l+x}^- + S_l^- S_{l+x}^+ \rangle. \tag{5.2}$$

Performing a Dyson-Maleev transformation with subsequent Bogoliubov transformation including the normal-ordering of quartic terms, we obtain

$$\begin{aligned} \langle K_x \rangle &= -JS\alpha(S)\frac{2}{N}\sum_{\boldsymbol{k}} \cos(k_x)\frac{\gamma_{\boldsymbol{k}}}{\lambda_{\boldsymbol{k}}} \\ &\quad + JS\alpha(S)\frac{2}{N}\sum_{\boldsymbol{k}} \cos(k_x)\left[\frac{\Delta}{\lambda_{\boldsymbol{k}}}\langle \alpha_{\boldsymbol{k}}^\dagger \beta_{\boldsymbol{k}}^\dagger + \alpha_{\boldsymbol{k}}\beta_{\boldsymbol{k}}\rangle - \frac{\gamma_{\boldsymbol{k}}}{\lambda_{\boldsymbol{k}}}\langle \alpha_{\boldsymbol{k}}^\dagger \alpha_{\boldsymbol{k}} + \beta_{\boldsymbol{k}}^\dagger \beta_{\boldsymbol{k}}\rangle\right]. \end{aligned} \tag{5.3}$$

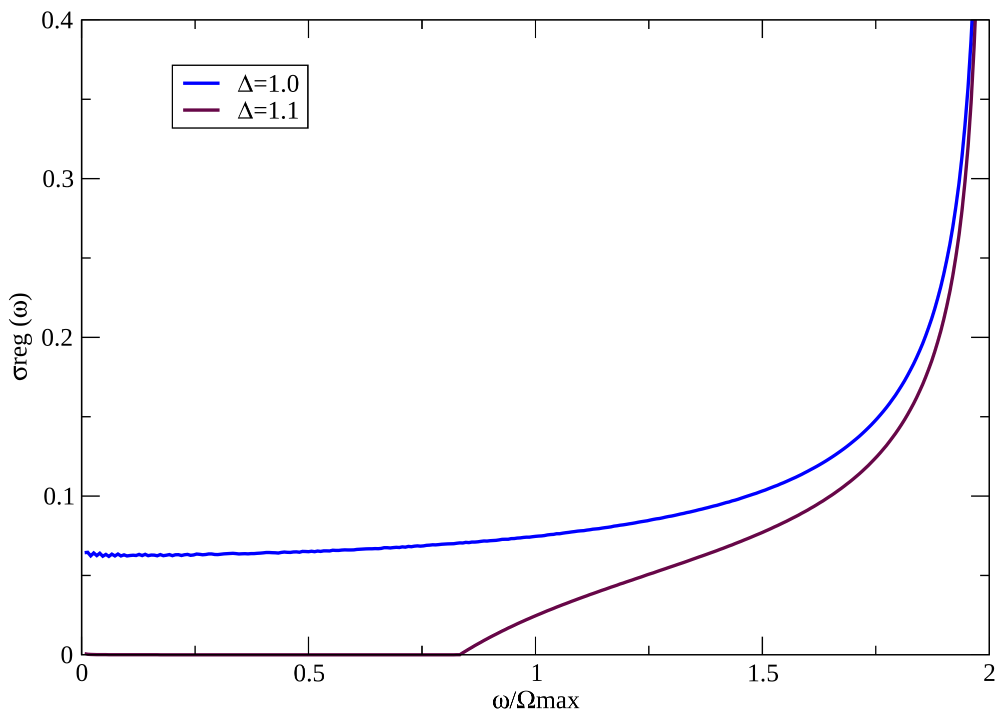

ABBILDUNG 5.1. Regular part of the spin conductivity for the $d = 2$, $S = \frac{1}{2}$ HAFM with anisotropy parameter $\Delta = 1.0$ (isotropic case) and $\Delta = 1.1$ (anisotropic case) for noninteracting magnons.

In the case of noninteracting magnons, the terms in the second line vanish (at $T = 0$), and we have

$$(5.4)\qquad \langle -K_x \rangle \;=\; 2JS\alpha(S)\frac{1}{N}\sum_{\boldsymbol{k}} \cos(k_x)\frac{\gamma_{\boldsymbol{k}}}{\Delta\varepsilon_{\boldsymbol{k}}}.$$

We can show that the Drude weight D,

$$(5.5)\qquad \frac{D}{\pi} = \langle -K_x \rangle - \Lambda'_{xx}(\omega \to 0),$$

is zero for noninteracting magnons in the regime $\Delta \geq 1$. In this case,

$$(5.6)\qquad \Lambda'_{xx}(\omega \to 0) = [2JS\alpha(S)]^2 \frac{1}{\Omega_{\max}}\frac{1}{N}\sum_{\boldsymbol{k}} \frac{(\sin(k_x))^2}{(\varepsilon_{\boldsymbol{k}})^2}\frac{1}{\varepsilon_{\boldsymbol{k}}}.$$

Note that we have used $\Lambda_{xx}(\omega) = -G_j(\omega) = -G_j^{+}(\omega) - G_j^{+}(-\omega)$ and the results of Section 4.4.

We claim that

$$(5.7)\qquad \sum_{\boldsymbol{k}} \cos(k_x)\frac{\gamma_{\boldsymbol{k}}}{\varepsilon_{\boldsymbol{k}}} = \frac{2}{z}\sum_{\boldsymbol{k}} \frac{(\sin(k_x))^2}{(\varepsilon_{\boldsymbol{k}})^3},$$

where, due to the symmetry of the integrands, the integrals can equally well be extended to the complete (not just the magnetic) Brillouin zone. Performing a partial integration with respect to k_x, we transform the left hand side as follows:

$$(5.8)\qquad \sum_{\boldsymbol{k}} \cos(k_x)\frac{\gamma_{\boldsymbol{k}}}{\varepsilon_{\boldsymbol{k}}} = \sum_{k_y} \sin(k_x)\frac{\gamma_{\boldsymbol{k}}}{\varepsilon_{\boldsymbol{k}}}\bigg|_{k_x=-\pi}^{k_x=\pi} - \sum_{\boldsymbol{k}} \sin(k_x)\frac{\partial}{\partial k_x}\frac{\gamma_{\boldsymbol{k}}}{\varepsilon_{\boldsymbol{k}}}.$$

The first term is zero for all $\Delta \geq 1$ since $\sum_{k_y} \sin(k_x)\frac{\gamma_{\boldsymbol{k}}}{\varepsilon_{\boldsymbol{k}}}$ is 2π-periodic with respect to k_x. Using $\partial\gamma_{\boldsymbol{k}}/\partial k_x = -\sin(k_x)/d = -2\sin(k_x)/z$, the second term becomes

$$(5.9)\qquad -\sum_{\boldsymbol{k}} \sin(k_x)\frac{\partial}{\partial k_x}\frac{\gamma_{\boldsymbol{k}}}{\varepsilon_{\boldsymbol{k}}} = \frac{1}{d}\sum_{\boldsymbol{k}}(\sin(k_x))^2\left[\frac{1}{\varepsilon_{\boldsymbol{k}}} + \frac{\gamma_{\boldsymbol{k}}^2}{\Delta^2\varepsilon_{\boldsymbol{k}}^3}\right] = \frac{2}{z}\sum_{\boldsymbol{k}} \frac{(\sin(k_x))^2}{(\varepsilon_{\boldsymbol{k}})^3},$$

which is just what we had to show. The result is

$$(5.10)\qquad \boxed{D = 0 \text{ for } \Delta \geq 1 \text{ and noninteracting magnons.}}$$

5.1.3. Interacting Magnons. Figure 5.2 shows the curves for noninteracting and interacting magnons. As derived in Chapter 4, the interacting solution is given by (see Eq. (4.64))

(5.11)

$$\boxed{\begin{aligned}\sigma'_{xx}(\omega) &= -\frac{1}{\omega}\frac{1}{2}\frac{[2JS\alpha(S)]^2}{\Omega_{\max}} \\ &\quad\times \mathrm{Im}\left[\frac{\ell^{(2)} - \kappa[\ell^{(1)}\ell^{(1)} - \ell^{(0)}\ell^{(2)}]}{1 + \kappa[\ell^{(0)} + \ell^{(2)}] - \kappa^2[\ell^{(1)}\ell^{(1)} - \ell^{(0)}\ell^{(2)}]}\right],\end{aligned}}$$

where the arguments $\widetilde{\omega} = \omega/\Omega_{\max}$ of the ℓ-functions,

$$\boxed{\ell^{(m)}(\widetilde{\omega}) = \frac{2}{N}\sum_{\boldsymbol{k}} \frac{(\sin(k_x))^2}{(\varepsilon_{\boldsymbol{k}})^m} \frac{1}{\widetilde{\omega} - 2\varepsilon_{\boldsymbol{k}} + i\eta},} \tag{5.12}$$

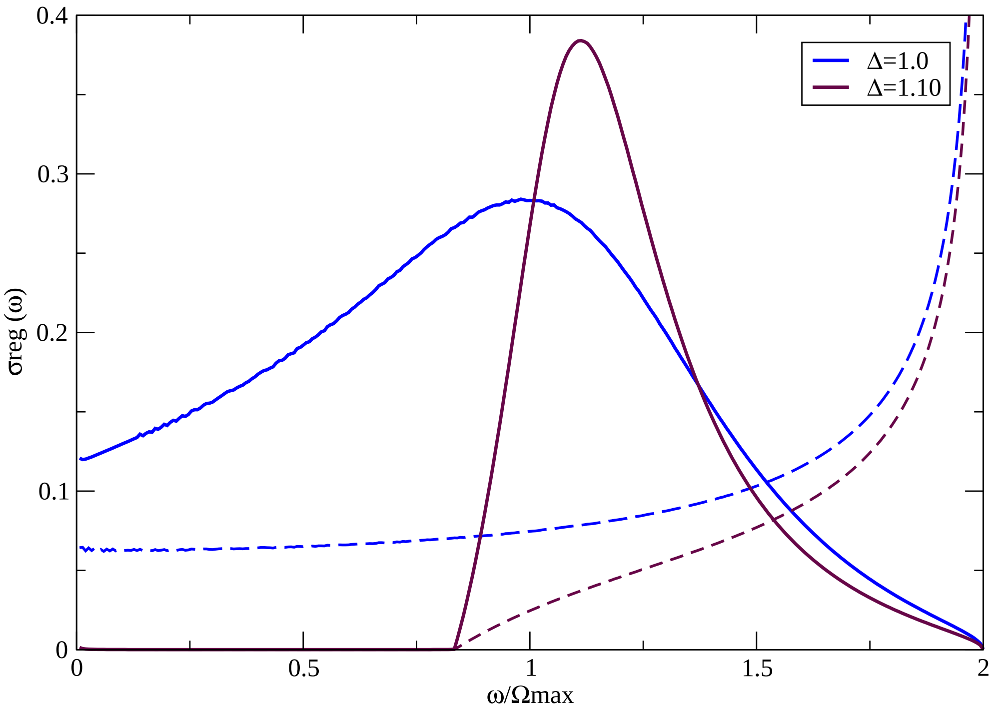

ABBILDUNG 5.2. Regular part of the spin conductivity for the $d = 2$, $S = \frac{1}{2}$ HAFM with anisotropy parameter $\Delta = 1.0$ (isotropic case) and $\Delta = 1.1$ (anisotropic case). Solid curves contain magnon interactions within the ladder approximation. Dashed curves are for noninteracting magnons.

TABELLE 5.1. Kramers-Kronig relation for interacting magnons.

Anisotropy Δ	Real Part Limit $\Lambda'_{xx}(\omega \to 0)$	Integral $\frac{2}{\pi}\int_0^\infty \sigma_{xx}^{\mathrm{reg}}(\omega)d\omega$	Oguchi $\alpha(S)$
1.0000	0.4863	0.4852	1.1579
1.0001	0.4766	0.4754	1.1579
1.0100	0.3978	0.3968	1.1530
1.0500	0.3131	0.3122	1.1371
1.1000	0.2638	0.2631	1.1216

are suppressed and κ is defined in Eq. (4.65). The unphysical singularities are removed once magnon interactions are included. The small-frequency behavior in the isotropic case will be discussed in detail below using a series expansion.

Figure 5.3 presents the interacting solution for several different values of Δ. The energy gap $\propto \sqrt{\Delta^2 - 1}$ is a characteristic feature of the spin conductivity. The dominant contribution to the spin conductivity is given by two-magnon processes

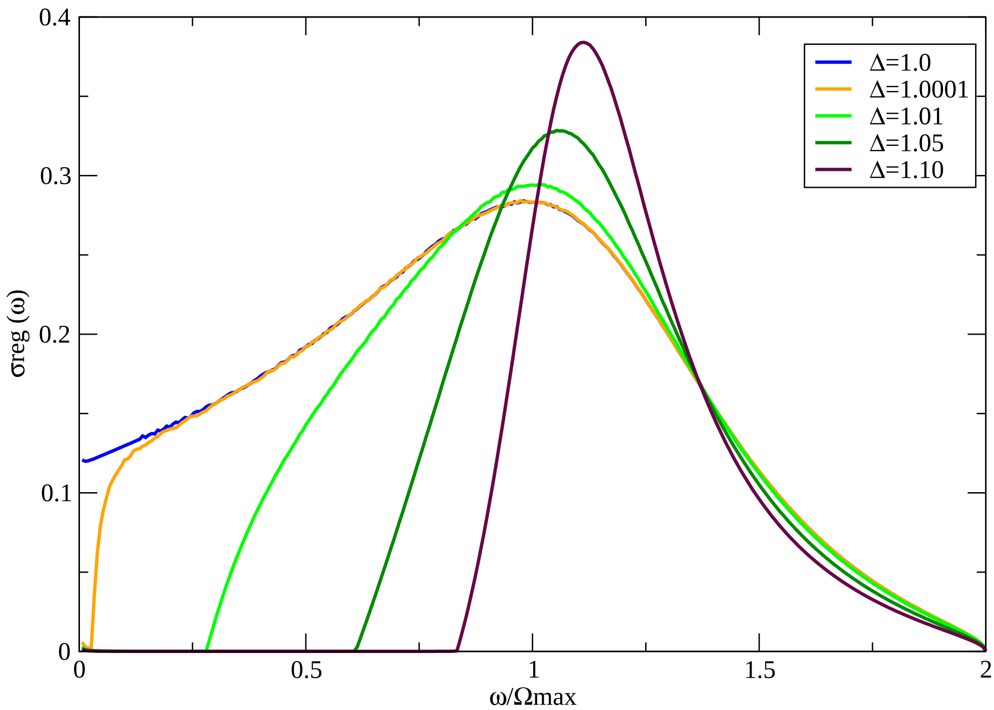

ABBILDUNG 5.3. Regular part of the spin conductivity for the $d = 2$, $S = \frac{1}{2}$ HAFM with anisotropy parameter $\Delta = 1.0$ (isotropic case) and several anisotropies.

TABELLE 5.2. Peak positions of the $d = 2$, $S = \frac{1}{2}$ spin conductivity.

Anisotropy Δ	Peak Frequency $\omega_0/\Omega_{\max}$	Peak Energy $\hbar\omega_0$
1.0000	0.98	2.27 J
1.0001	0.98	2.27 J
1.0100	1.02	2.38 J
1.0500	1.06	2.53 J
1.1000	1.12	2.76 J

(see Section 3.6), and a large part of the spectral weight is located at energies above the maximum one-magnon energy $\Omega_{\max}$. One could also take into account four-magnon processes (see, e. g., Ref. [**16**]) corresponding to quartic terms in the spin-current operator, which we have neglected except for their contribution to the Oguchi corrections.

Table 5.1 shows that the Kramers-Kronig relations given in Section 3.4.2 are indeed fulfilled for the current-correlation functions calculated in the ladder approximation within some numerical error arising from the finite energy resolution, especially at the upper band edge where the correlation functions diverge. Originally these calculations should be used to calculate the Drude weight by means of the sum rule. But as we have seen in Section 3.4.2 the $\boldsymbol{q} = \mathbf{0}$-current correlations alone do *not* seem to provide enough information for this task.

A significant feature of the spin conductivity is the peak position ω_0. Table 5.2 shows these frequencies and the corresponding energies in multiples of the exchange coupling energy J. The peak energy for the isotropic case, $2.27J$, is smaller than for analogous calculations of the Raman line shape [**16**], where the curve peaks at $3.38J$.

5.1.4. Small-frequency Expansion. In Appendix B the following small-frequency expansion is derived for the spin conductivity for interacting magnons within the ladder approximation:

(5.13)

$$\boxed{\sigma'_{xx}(\widetilde{\omega}) = 0.11605705 - 0.02173784\,\widetilde{\omega}\ln(\widetilde{\omega}) + 0.06946901\,\widetilde{\omega} + \mathcal{O}(\widetilde{\omega}^2\ln(\widetilde{\omega})),}$$

where $J = \hbar = 1$. The analytical calculations were performed in order to confirm the numerical data and to obtain a more accurate result for small frequencies. Figure

5.4 shows the result (5.13) in comparison to the numerical calculation. Note that the $\widetilde{\omega}\ln(\widetilde{\omega})$-term leads to a logarithmically diverging slope at $\widetilde{\omega} = 0$. The numerical curve cannot resolve this behavior, which is basically a problem of numerical accuracy when the imaginary part of the current-correlation function (which vanishes linearly in the zero-frequency limit) is divided by $\widetilde{\omega}$ and $\widetilde{\omega} \to 0$. The expansion demonstrates that the isotropic two-dimensional spin conductivity has a finite zero-frequency value.

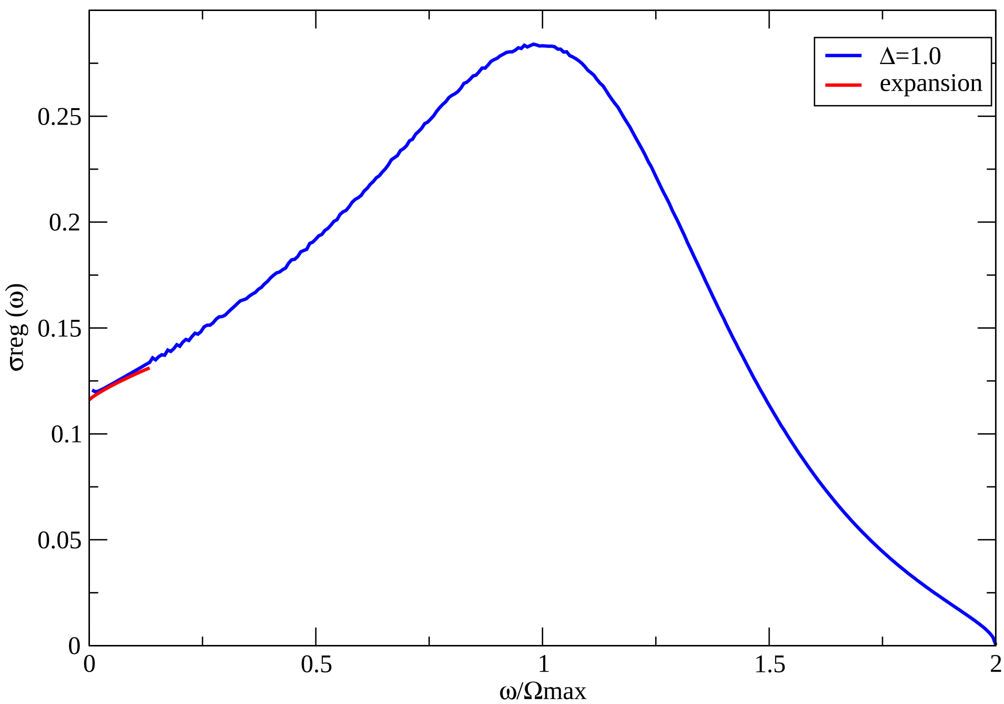

ABBILDUNG 5.4. Comparison of numerical data and the small-frequency expansion for the isotropic case.

5.1.5. The $S = 1$ Antiferromagnet. For $S = 1$ the physics of the Heisenberg system is different since each local spin can have three (instead of only two) different states: $S^z = 1$, 0 or -1. We can nevertheless use the formula for the spin conductivity changing just the value of S. The results (displayed in Figure 5.5) should be even better for $S = 1$ since the spin-wave expansion becomes more accurate with increasing S.

Apart from the change in the overall energy scale $\propto S\alpha(S)$, the line shape is different from the $S = \frac{1}{2}$-case. The peak position (see Table 5.3) is shifted to higher energies relative to the maximum two-magnon energy, as in the Raman spectra [**16**] of Heisenberg antiferromagnets. The relative peak positions of the isotropic and $\Delta = 1.1$-anisotropic cases do not differ as much (1.46 vs. 1.48) as for $S = \frac{1}{2}$ (0.98 vs. 1.12).

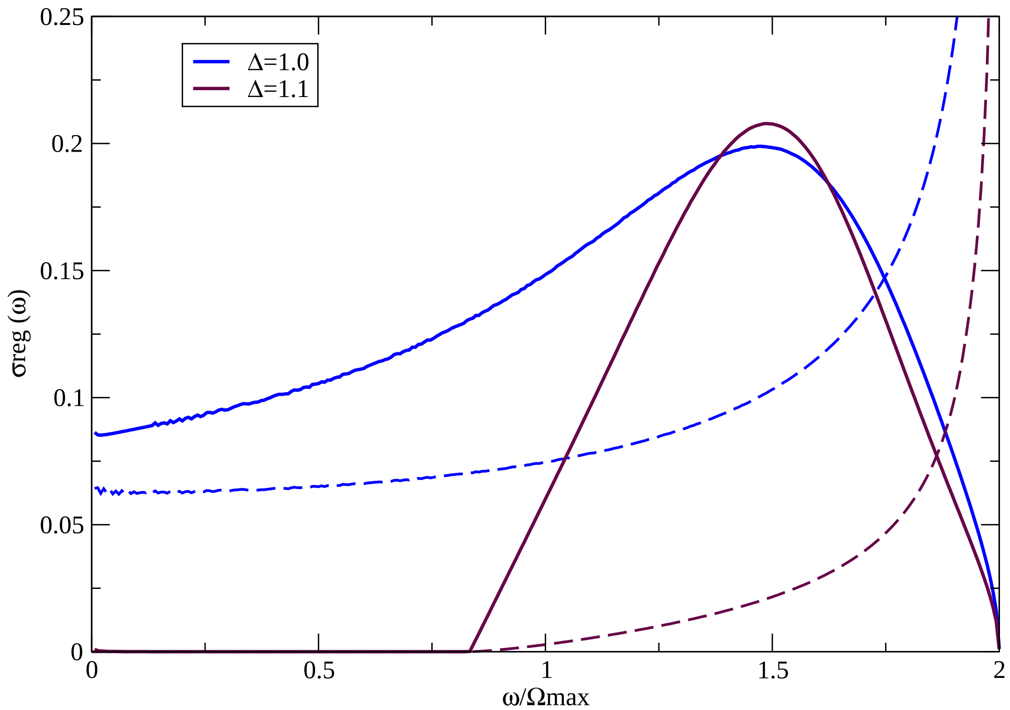

ABBILDUNG 5.5. Regular part of the spin conductivity for the $d = 2$, $S = 1$ HAFM.

TABELLE 5.3. Peak positions of the $d = 2$, $S = 1$ spin conductivity.

Anisotropy Δ	Peak Frequency $\omega_0/\Omega_{\text{max}}$	Peak Energy $\hbar\omega_0$
1.0000	1.46	6.76 J
1.1000	1.48	7.30 J

TABELLE 5.4. Peak positions of the $d = 3$, $S = \frac{1}{2}$ spin conductivity.

Anisotropy Δ	Peak Frequency $\omega_0/\Omega_{\text{max}}$	Peak Energy $\hbar\omega_0$
1.0000	1.47	5.11 J
1.1000	1.48	5.48 J

5.2. Spin Conductivity of the 3D Heisenberg Antiferromagnet

Figure 5.6 provides the spin conductivity for three-dimensional antiferromagnets. In contrast to $d = 2$, the zero-frequency limit of the isotropic curve is zero, which

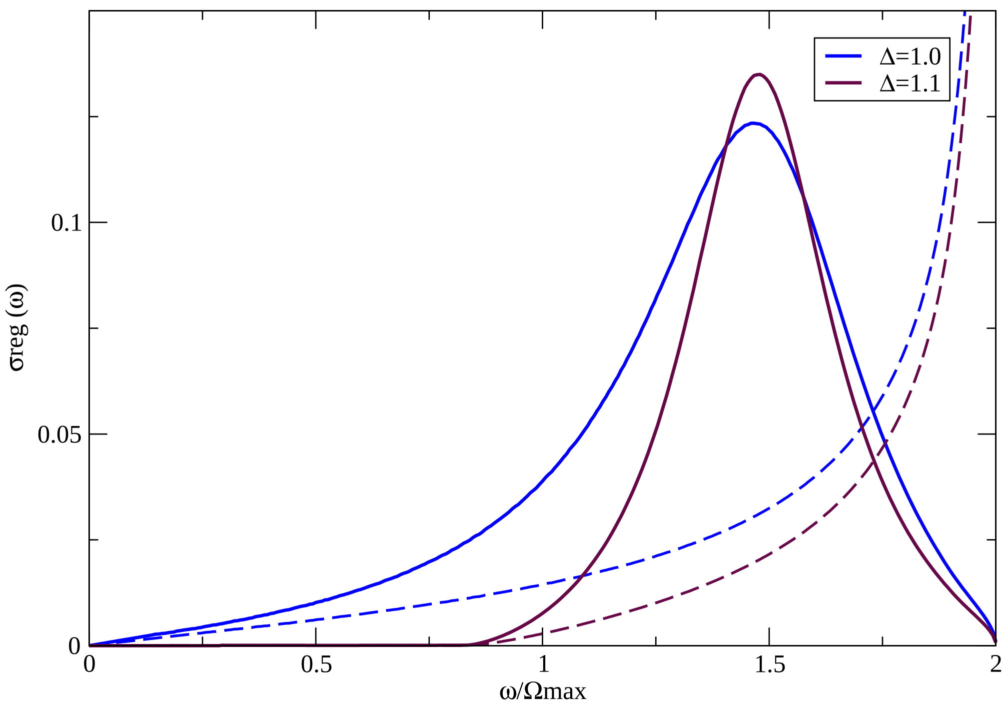

ABBILDUNG 5.6. Regular part of the spin conductivity for the $d = 3$, $S = \frac{1}{2}$ HAFM with anisotropy parameter $\Delta = 1.0$ (isotropic case) and $\Delta = 1.1$ (anisotropic case). Solid curves contain magnon interactions within the ladder approximation. Dashed curves are for noninteracting magnons.

is due to the dimension dependence of the $\boldsymbol{k}$-sums contributing to the l-functions. Moreover, the relative peak position depends only weakly on the anisotropy (1.47 vs. 1.48).

KAPITEL 6

Summary

In this work we have investigated spin-transport properties of Heisenberg antiferromagnets. Spin is transported via magnons, which are collective spin-flip excitations above the magnon vacuum. Spin currents flow along a gradient of the magnetic-field's z-component, or perpendicular to an electric field varying in time. The longitudinal spin conductivity is the linear spin-current response to a magnetic-field gradient. The dominant contributions are two-magnon processes, a fact that can be understood by analyzing the spin-current selection rules.

The inclusion of magnon scattering is crucial in order to obtain physical results without van-Hove singularities. As a function of frequency, the spin conductivity has a one-peak structure, where the peak energy is around one half of the maximum two-magnon energy. For the two-dimensional isotropic Heisenberg antiferromagnet, the regular part of the spin conductivity has a finite zero-frequency limit. The spin Drude weight is zero in the gapped regime as well as in the isotropic case for noninteracting magnons.

We have also discussed the possibility of transversal spin transport analogous to the Hall effect for charge currents. Such an effect might occur if an inhomogeneous magnetic field and an electric field are applied simultaneously, or in a Heisenberg system with a non-vanishing Dzyaloshinskii-Moriya vector. However, the calculation of the Heisenberg-spin Hall coefficient remains an unsolved problem.

ANHANG A

Dimensional Considerations

In this appendix we shall give the physical dimension of the spin conductivity, collecting some $\hbar$'s we have dropped along the way. First of all, we have defined the spin-current operator as

$$j_{i\to j} \equiv \frac{i}{2\hbar} J_{ij}(S_i^+ S_j^- - S_i^- S_j^+), \tag{A.1}$$

setting $\hbar = 1$ afterwards. Next we have used the linear-response relation

$$\chi_{jS}(l, j; t - t') \equiv i\Theta(t - t')\langle [j_x(l, t), S^z(j, t')]\rangle, \tag{A.2}$$

where there has to be $i/\hbar$ instead of the i. Furthermore, in the linear-response relation for the spin current,

$$\langle j_x(\boldsymbol{q}, \omega)\rangle = \sigma_{xx}(\boldsymbol{q}, \omega) i q_x h^z(\boldsymbol{q}, \omega), \tag{A.3}$$

we have defined the spin conductivity with the gradient of $h^z \equiv g\mu_B B^z$, although it should be the gradient of B^z. Thus, there has to be a prefactor $g\mu_B/\hbar^3$ in the spin conductivity formulae we have derived. For example, the formula (4.64) for interacting magnons has to be rewritten as

(A.4)

$$\begin{aligned}\sigma'_{xx}(\omega) &= -\frac{g\mu_B}{\hbar^3}\frac{1}{\omega}\frac{1}{2}\frac{[2JS\alpha(S)]^2}{\Omega_{\max}} \\ &\quad \times \mathrm{Im}\left[\frac{\ell^{(2)} - \kappa[\ell^{(1)}\ell^{(1)} - \ell^{(0)}\ell^{(2)}]}{1 + \kappa[\ell^{(0)} + \ell^{(2)}] - \kappa^2[\ell^{(1)}\ell^{(1)} - \ell^{(0)}\ell^{(2)}]}\right].\end{aligned}$$

The fraction is dimensionless and a function of $\widetilde{\omega}$. We can use $\omega = \widetilde{\omega}\Omega_{\max}$ and $\Omega_{\max} \sim J/\hbar$ and obtain

$$\sigma'_{xx}(\omega) \sim \frac{g\mu_B}{\hbar}. \tag{A.5}$$

We can check this result using the continuity equation (3.41) in its Fourier version. Note that momenta are measured in units of the inverse of the lattice constant a, which here we write explicitly for clarity. We focus on the frequency dependence here:

$$-i\omega S^z(\boldsymbol{q},\omega) + iq_x a j_x(\boldsymbol{q},\omega) = 0. \tag{A.6}$$

The spin operators are dimensionless, $S^z(\boldsymbol{q},\omega)$ has the dimension of a time (due to the Fourier transformation) and $\omega S^z(\boldsymbol{q},\omega)$ is dimensionless. Thus, $j_x(\boldsymbol{q},\omega)$ is also dimensionless.

The definition of the spin conductivity is

$$\langle j_x(\boldsymbol{q},\omega)\rangle = \sigma_{xx}(\boldsymbol{q},\omega) iq_x a B^z(\boldsymbol{q},\omega). \tag{A.7}$$

As $g\mu_B B^z(t)$ is an energy, $B^z(\boldsymbol{q},\omega)$ has the dimension of energy $\times$ time divided by $g\mu_B$. This means that $\sigma_{xx}(\boldsymbol{q},\omega)$ has the dimension of $g\mu_B$ divided by an action, i. e., magnetic moment divided by action. This is the case for $\frac{J}{\hbar\omega}\frac{g\mu_B}{\hbar}$.

When comparing this to Ref. [**41**] one finds a discrepancy. The spin conductance in $d = 1$ is quantized in units of order $(g\mu_B)^2/h$. The magnetic moment appears squared instead of just linearly as in our case. This is due to the fact that we have considered the transport of (dimensionless) spin instead of magnetization $m = g\mu_B\langle S^z\rangle$. This prefactor also enters the conductivity. Thus, the magnetization conductivity is of order

$$\sigma^{\mathrm{magn}}(\omega) \sim \frac{(g\mu_B)^2}{\hbar}. \tag{A.8}$$

One can also compare this to charge transport, where the quantum of conductance is given by e^2/h. The transport quantity "charge" is measured in multiples of e, whereas the transport quantity "magnetization" is measured in multiples of $g\mu_B$.

ANHANG B

Analytical Calculations

The 2D magnon density of states can be calculated analytically. The same is true for the 2D noninteracting-magnon spin conductivity. For interacting magnons, a small-frequency expansion of the spin conductivity may be obtained.

Below we evaluate $\boldsymbol{k}$-sums containing a delta function $\delta(x - \varepsilon_{\boldsymbol{k}})$. It can be rewritten as follows:

$$\begin{aligned} \text{(B.1)}\quad \delta(x - \varepsilon_{\boldsymbol{k}}) &= \delta\left(x - \sqrt{1 - (\gamma_{\boldsymbol{k}}/\Delta)^2}\right) \\ &= \Delta\frac{x}{\sqrt{1-x^2}}\left[\delta\left(\gamma_{\boldsymbol{k}} - \Delta\sqrt{1-x^2}\right) + \delta\left(\gamma_{\boldsymbol{k}} + \Delta\sqrt{1-x^2}\right)\right], \end{aligned}$$

where $x \in [\varepsilon_{\min}, 1]$ and $\varepsilon_{\min} = \sqrt{1 - 1/\Delta^2}$.

B.1. Density of States

The density of states for the dimensionless dispersion $\varepsilon_{\boldsymbol{k}}$ in d dimensions is

$$\text{(B.2)}\qquad \mathcal{N}_d(x) = \int\limits_{\text{BZ}} \frac{d^d k}{(2\pi)^d}\, \delta(x - \varepsilon_{\boldsymbol{k}}) = d\Delta\frac{x}{\sqrt{1-x^2}}\left[\mathcal{M}_d(y) + \mathcal{M}_d(-y)\right],$$

where $y = d\Delta\sqrt{1-x^2}$, and

$$\text{(B.3)}\qquad \mathcal{M}_d(y) = \int\limits_{\text{BZ}} \frac{d^d k}{(2\pi)^d}\, \delta(y + d\gamma_{\boldsymbol{k}}) = \int\limits_{\text{BZ}} \frac{d^d k}{(2\pi)^d}\, \delta\left(y + \sum_{\alpha=1}^{d} \cos(k_\alpha)\right).$$

In one dimension the integral can be easily computed and the result is

$$\text{(B.4)}\qquad \mathcal{M}_1(y) = \frac{1}{\pi\sqrt{1-y^2}}\Theta(|y| \leq 1),$$

where $\Theta(|y| \leq 1)$ is the step function being 1 for $|y| \leq 1$ and 0 otherwise. For higher dimensions there is a recursion relation, namely

$$\text{(B.5)}\qquad \mathcal{M}_{d+1}(y) = \int_0^\pi \frac{dk}{\pi}\, \mathcal{M}_d(y + \cos(k)) = \int_{-1}^{1} \frac{du}{\sqrt{1-u^2}}\, \mathcal{M}_d(y-u).$$

In $d = 2$ we have

$$\mathcal{M}_2(y) = \frac{1}{\pi^2}\int_{-1}^{1} du\, \frac{1}{\sqrt{1-u^2}\sqrt{1-(y-u)^2}}\Theta(|y-u| \leq 1). \tag{B.6}$$

Due to $\mathcal{M}_2(-y) = \mathcal{M}_2(y)$ it suffices to consider $y \geq 0$. The range of integration is given by

$$|u| \leq 1 \quad \text{and} \quad |y-u| \leq 1. \tag{B.7}$$

We want to take the Θ-function out of the integral. Therefore, we recombine these conditions as follows:

$$y \leq 2 \quad \text{and} \quad -1+y \leq u \leq 1. \tag{B.8}$$

This leads to

$$\mathcal{M}_2(y) = \frac{1}{\pi^2}\Theta(y \leq 2)\int_{-1+y}^{1} du\, \frac{1}{\sqrt{1-u^2}\sqrt{1-(y-u)^2}}. \tag{B.9}$$

We define $z \equiv 1 - y$. Because of $y \in [0, 2]$ we have $z \in [-1, 1]$. The integral becomes

$$\mathcal{M}_2(1-z) = \frac{1}{\pi^2}\Theta(|z| \leq 1)\int_{-z}^{1} du\, \frac{1}{\sqrt{1-u^2}\sqrt{z+u}\sqrt{2-z-u}}. \tag{B.10}$$

This can be rewritten using the complete elliptic integral of the first kind,

$$K(k) \equiv \int_0^{\pi/2} \frac{d\phi}{\sqrt{1-k^2\sin^2(\phi)}}, \tag{B.11}$$

namely

$$\mathcal{M}_2(1-z) = \frac{1}{\pi^2}\Theta(|z| \leq 1)\frac{4}{3-z}\ K\left(\frac{z+1}{3-z}\right), \tag{B.12}$$

or, for the original argument $y = 1 - z$,

$$\mathcal{M}_2(y) = \frac{4}{\pi^2}\Theta(y \leq 2)\frac{1}{y+2}\ K\left(\frac{2-y}{y+2}\right). \tag{B.13}$$

The density of states in two dimensions ($y = 2\Delta\sqrt{1-x^2}$) is

$$\mathcal{N}_2(x) = 4\Delta\frac{x}{\sqrt{1-x^2}}\mathcal{M}_2(2\Delta\sqrt{1-x^2}). \tag{B.14}$$

We thus obtain

$$\boxed{\begin{aligned}\mathcal{N}_2(x) &= \frac{8}{\pi^2}\frac{\Delta x}{\sqrt{1-x^2}(\Delta\sqrt{1-x^2}+1)} \\ &\quad \times K\left(\frac{1-\Delta\sqrt{1-x^2}}{\Delta\sqrt{1-x^2}+1}\right)\Theta\left(x\in[\varepsilon_{\min},1]\right).\end{aligned}} \tag{B.15}$$

The elliptic integral has a logarithmic singularity when its argument approaches 1, which is the case for $x \to 1$. Note that there is also a square-root singularity at this point coming from the prefactor.

B.2. Spin Conductivity for noninteracting Magnons

We now focus on the 2D ℓ-functions in the thermodynamic limit (where the lattice size $N \to \infty$),

$$\ell^{(m)}(\widetilde{\omega}) = \int\limits_{\mathrm{BZ}} \frac{d^2k}{(2\pi)^2}\frac{(\sin(k_x))^2}{(\varepsilon_{\boldsymbol{k}})^m}\frac{1}{\widetilde{\omega}-2\varepsilon_{\boldsymbol{k}}+i\eta}. \tag{B.16}$$

The integrals were extended over the complete Brillouin zone (BZ) due to the symmetry of the integrands. For simplicity we define new functions $f^{(m)}(x)$ by

$$f^{(m)}(x) = \int\limits_{\mathrm{BZ}} \frac{d^2k}{(2\pi)^2}\frac{(\sin(k_x))^2}{(\varepsilon_{\boldsymbol{k}})^m}\frac{1}{x-\varepsilon_{\boldsymbol{k}}+i\eta}, \tag{B.17}$$

such that $\ell^{(m)}(\widetilde{\omega}) = \frac{1}{2}f^{(m)}\left(\frac{\widetilde{\omega}}{2}\right)$.

The imaginary part is easier to handle. We define

$$\varrho_m(x) = -\frac{1}{\pi}f''^{(m)}(x) = \int\limits_{\mathrm{BZ}} \frac{d^2k}{(2\pi)^2}\frac{(\sin(k_x))^2}{(\varepsilon_{\boldsymbol{k}})^m}\delta(x-\varepsilon_{\boldsymbol{k}}) = \frac{1}{x^m}\varrho_0(x). \tag{B.18}$$

We can then get the real part of f using the Kramers-Kronig relation

$$f'^{(m)}(x) \equiv r_m(x) = ⨍_{\varepsilon_{\min}}^{1} dx'\,\frac{\varrho_m(x')}{x-x'}. \tag{B.19}$$

Using Equation (B.1) and the fact that $\gamma_{\boldsymbol{k}} \to -\gamma_{\boldsymbol{k}}$ when $k_\alpha \to \pi - k_\alpha$ results in

$$\boxed{\varrho_0(x) = \frac{2x\Delta}{\sqrt{1-x^2}}\mathrm{R}(\Delta\sqrt{1-x^2}),} \tag{B.20}$$

where

$$\mathrm{R}(z) = \int_0^\pi \frac{dk_x}{\pi} \int_0^\pi \frac{dk_y}{\pi} \sin^2(k_x)\delta(z - \gamma_{\boldsymbol{k}}) \tag{B.21}$$

and $z \in [0, 1]$. Observe that $\mathrm{R}(z)$ can be defined for $z \in [-1, 1]$, but $\mathrm{R}(-z) = \mathrm{R}(z)$, so we consider only $z \geq 0$. Substituting $x = \cos(k_x)$ and $y = \cos(k_y)$ we get

$$\begin{aligned} \mathrm{R}(z) &= \frac{2}{\pi^2} \int_{-1}^{1} \frac{dx}{\sqrt{1-x^2}}(1-x^2) \int_{-1}^{1} \frac{dy}{\sqrt{1-y^2}} \delta(2z - x - y) \\ &= \frac{2}{\pi^2} \int_{-1}^{1} \frac{dx\sqrt{1-x^2}}{\sqrt{1-(2z-x)^2}} \int_{-1}^{1} dy\ \delta(2z - x - y) \\ &= \frac{2}{\pi^2} \int_{\max(-1,2z-1)}^{\min(1,2z+1)} \frac{dx\sqrt{1-x^2}}{\sqrt{1-(2z-x)^2}} \\ &= \frac{2}{\pi^2} \int_{2z-1}^{1} \frac{dx\sqrt{1-x^2}}{\sqrt{1-(2z-x)^2}}. \end{aligned} \tag{B.22}$$

With $u = x - 2z$ and $a = 1 - 2z$ this can be rewritten,

$$\begin{aligned} \mathrm{R}(z) &= \frac{2}{\pi^2} \int_{-1}^{a} du \frac{\sqrt{a-u}\sqrt{2-a+u}}{\sqrt{1-u}\sqrt{1+u}} \\ &= \frac{2}{\pi^2} \left[2(a-1)K\left(\frac{a+1}{a-3}\right) + (3-a)E\left(\frac{a+1}{a-3}\right) \right], \end{aligned} \tag{B.23}$$

where E is the complete elliptic integral of the second kind defined as

$$E(k) \equiv \int_0^{\pi/2} d\phi\ \sqrt{1 - k^2 \sin^2(\phi)}. \tag{B.24}$$

Using $2(a-1) = -4z$, $3 - a = 2(z+1)$ and $\frac{a+1}{a-3} = \frac{z-1}{z+1}$ we finally obtain

$$\boxed{\mathrm{R}(z) = \frac{4}{\pi^2} \left[-2zK\left(\frac{1-z}{z+1}\right) + (z+1)E\left(\frac{1-z}{z+1}\right) \right],} \tag{B.25}$$

where $z \geq 0$ and $\mathrm{R}(-z) = \mathrm{R}(z)$ by definition.

The noninteracting spin conductivity in $d = 2$ can thus be expressed analytically.

B.3. Small-frequency Expansion for interacting Magnons

The small-frequency expansion for the interacting spin conductivity in the isotropic case $\Delta = 1$, Eq. (5.13), can be obtained as follows [**47**]. We expand $\varrho_0(x)$ in a series, exploiting the properties of the elliptic integrals:

$$\text{(B.26)} \qquad \begin{aligned} \varrho_0(x) &= \frac{2x}{\sqrt{1-x^2}} \mathrm{R}(\sqrt{1-x^2}) = \sum_{n\geq 3} a_n x^n \\ &= \frac{1}{\pi}\left(2x^3 + \frac{5}{4}x^5 + \frac{31}{32}x^7 + \frac{417}{512}x^9 + \frac{5853}{8192}x^{11} + \mathcal{O}(x^{13})\right). \end{aligned}$$

Therefore,

$$\text{(B.27)} \qquad \varrho_m(x) = \sum_{n\geq 3} a_n x^{n-m}$$

is regular for $m = 0, \ldots, 3$. The real part of the f-function then is

$$\text{(B.28)} \qquad \begin{aligned} r_m(x) &= \fint_0^1 dx' \frac{\varrho_m(x')}{x - x'} \\ &= \fint_0^1 dx' \frac{\varrho_m(x)}{x - x'} - \int_0^1 dx' \frac{\varrho_m(x) - \varrho_m(x')}{x - x'} \\ &= \varrho_m(x) \ln\left|\frac{x}{1-x}\right| - \int_0^1 dx' \frac{\varrho_m(x) - \varrho_m(x')}{x - x'}, \end{aligned}$$

where the integrand in the second integral is regular at $x = x'$. We rewrite this,

$$\text{(B.29)} \qquad r_m(x) = \varrho_m(x) \ln\left|\frac{x}{1-x}\right| - s_m(x),$$

where we have defined

$$\text{(B.30)} \qquad s_m(x) = \int_0^1 dx' \frac{\varrho_m(x) - \varrho_m(x')}{x - x'} = s_m(0) + \sum_{n\geq 1} \frac{s_m^{(n)}(0)}{n!} x^n,$$

and $s_m^{(n)}$ denotes the n-th derivative of s_m. The constant term is given by

$$\text{(B.31)} \qquad s_m(0) = \int_0^1 dx' \frac{\varrho_m(x') - \varrho_m(0)}{x'}.$$

For $n \geq 1$,

$$\begin{aligned}
\text{(B.32)} \quad \frac{s_m^{(n)}(x)}{n!} &= \frac{1}{n!}\int_0^1 dx' \frac{d^n}{dx^n}\frac{\varrho_m(x)-\varrho_m(x')}{x-x'} \\
&= \frac{1}{n!}\int_0^1 dx' \sum_{l=0}^{n}\binom{n}{l}\left(\varrho_m^{(l)}(x)-\delta_{l0}\varrho_m(x')\right)\frac{d^{n-l}}{dx^{n-l}}\frac{1}{x-x'} \\
&= \frac{1}{n!}\int_0^1 dx' \sum_{l=0}^{n}\binom{n}{l}\left(\varrho_m^{(l)}(x)-\delta_{l0}\varrho_m(x')\right)\frac{(-1)^{n-l}(n-l)!}{(x-x')^{n-l+1}} \\
&= -\int_0^1 dx' \sum_{l=0}^{n}\frac{1}{l!}\frac{\left(\varrho_m^{(l)}(x)-\delta_{l0}\varrho_m(x')\right)}{(x'-x)^{n-l+1}} \\
&= \int_0^1 dx' \frac{\varrho_m(x')-\sum_{l=0}^{n}\frac{\varrho_m^{(l)}(x)}{l!}(x'-x)^l}{(x'-x)^{n+1}},
\end{aligned}$$

and thus

$$\text{(B.33)} \qquad \frac{s_m^{(n)}(0)}{n!} = \int_0^1 dx' \frac{\varrho_m(x')-\sum_{l=0}^{n}\frac{\varrho_m^{(l)}(0)}{l!}(x')^l}{(x')^{n+1}}.$$

We can therefore express the expansion of s using the expansion of ϱ,

$$\text{(B.34)} \qquad s_m(x) = \sum_{n\geq 0} x^n \left[\int_0^1 \frac{dx'}{(x')^{n+1}}\left(\varrho_m(x') - \sum_{l=0}^{n}\frac{\varrho_m^{(l)}(0)}{l!}(x')^l\right)\right].$$

Consider the relevant m's, namely $m = 0, 1, 2$. We have

$$\text{(B.35)} \qquad \varrho_m(x) \;=\; \sum_{n\geq 3} a_n x^{n-m} = \sum_{l\geq 3-m} a_{l+m}x^l,$$

where

$$\text{(B.36)} \qquad a_{l+m} = \frac{\varrho_0^{(l+m)}(0)}{(l+m)!} = \frac{\varrho_m^{(l)}(0)}{l!}.$$

This yields

$$\begin{aligned}
\text{(B.37)} \quad \frac{\varrho_m(x')-\sum_{l=0}^{n}\frac{\varrho_m^{(l)}(0)}{l!}(x')^l}{(x')^{n+1}} &= \frac{\varrho_0(x')-\sum_{l=0}^{n}a_{l+m}(x')^{l+m}}{(x')^{m+n+1}} \\
&= \frac{\varrho_0(x')-\sum_{l=m}^{n+m}a_l(x')^l}{(x')^{m+n+1}} \\
&= \frac{\varrho_0(x')-\sum_{l=0}^{n+m}a_l(x')^l}{(x')^{m+n+1}},
\end{aligned}$$

where the last replacement may be performed for $m = 0, 1, 2$. The result reads

$$s_m(x) = \sum_{n \geq 0} b_{n+m} x^n, \tag{B.38}$$

where the coefficients are given by

$$\boxed{b_n = \int_0^1 \frac{dx'}{(x')^{n+1}} \left(\varrho_0(x') - \sum_{l=0}^{n} \frac{\varrho_0^{(l)}(0)}{l!} (x')^l \right).} \tag{B.39}$$

The first few coefficients are

$$\begin{aligned} b_0 &= 0.58180246, \\ b_1 &= 0.72676046, \\ b_2 &= 1.10230270, \\ b_3 &= 0.56423251, \\ b_4 &= 0.81011984. \end{aligned}$$

Putting all of this together we get

$$\boxed{r_m(x) = \frac{\varrho_0(x) \ln \left| \frac{x}{1-x} \right|}{x^m} - \sum_{n \geq 0} b_{n+m} x^n} \tag{B.40}$$

and

$$\boxed{f^{(m)}(x) = r_m(x) - i\pi \frac{\varrho_0(x)}{x^m}.} \tag{B.41}$$

Hence, the expansion for the f-functions (and for the spin conductivity) can be received from the boxed equations in this section. The small-frequency expansion for the $S = \frac{1}{2}$ isotropic spin conductivity in two dimensions is plotted in Section 5.1.4 and is given by

(B.42)

$$\boxed{\sigma'_{xx}(\widetilde{\omega}) = 0.11605705 - 0.02173784\, \widetilde{\omega} \ln(\widetilde{\omega}) + 0.06946901\, \widetilde{\omega} + \mathcal{O}(\widetilde{\omega}^2 \ln(\widetilde{\omega})),}$$

where $J = \hbar = 1$.

Abbildungsverzeichnis

Tabellenverzeichnis

Literaturverzeichnis

[1] S. A. Wolf et al., Science **294**, 1488 (2001).

[2] D. D. Awschalom, D. Loss, and N. Samarth, *Semiconductor Spintronics and Quantum Computations*, Springer, Berlin, 2002.

[3] I. Žutić, J. Fabian, and S. Das Sarma, Rev. Mod. Phys. **76**, 323 (2004).

[4] H. Akinaga and H. Ohno, IEEE T. Nanotechnol. **1**, 19 (2002).

[5] J. Bonča and J. Jaklič, Phys. Rev. B **51**, 16083 (1995).

[6] J. Alvarez and C. Gros, Phys. Rev. B **66**, 094403 (2002).

[7] F. Dyson, E. H. Lieb, and B. Simon, J. Stat. Phys. **18**, 335 (1978).

[8] T. Kennedy, E. H. Lieb, and B. S. Shastry, J. Stat. Phys. **53**, 1019 (1988).

[9] P. C. Hohenberg, Phys. Rev. **158**, 383 (1967).

[10] N. D. Mermin and H. Wagner, Phys. Rev. Lett. **17**, 1133 (1969).

[11] E. J. Neves and J. F. Perez, Phys. Lett. **114A**, 331 (1986).

[12] I. Affleck, T. Kennedy, E. H. Lieb, and H. Tasaki, Commun. Math. Phys. **115**, 447 (1988).

[13] E. Manousakis, Rev. Mod. Phys. **63**, 1 (1991).

[14] S. Chakravarty, B. I. Halperin, and D. R. Nelson, Phys. Rev. B **39**, 2344 (1989).

[15] L. Onsager, Phys. Rev. **65**, 117 (1944).

[16] C. M. Canali and S. M. Girvin, Phys. Rev. B **45**, 7127 (1992).

[17] A. A. Katanin and A. P. Kampf, Phys. Rev. B **67**, 100404 (2003).

[18] T. S. Nunner, *Spin Excitations in Low-Dimensional Quantum Antiferromagnets*, PhD thesis, Univ. Augsburg, 2003.

[19] J. B. Parkinson, J. Phys. C **2**, 2012 (1969).

[20] P. A. Fleury and H. J. Guggenheim, Phys. Rev. Lett. **24**, 1346 (1970).

[21] T. Holstein and H. Primakoff, Phys. Rev. **58**, 1098 (1940).

[22] P. W. Anderson, Phys. Rev. **86**, 694 (1952).

[23] R. Kubo, Phys. Rev. **87**, 568 (1952).

[24] T. Oguchi, Phys. Rev. **117**, 117 (1960).

[25] F. J. Dyson, Phys. Rev. **102**, 1217 (1956).

[26] S. V. Maleev, Zh. Eksp. Theor. Fiz. **30**, 1010 (1957), see also: Sov. Phys. JETP **64**, 654 (1958).

[27] A. B. Harris, D. Kumar, B. I. Halperin, and P. C. Hohenberg, Phys. Rev. B **3**, 961 (1971).

[28] W. Kohn, Phys. Rev. **133**, A171 (1964).

[29] I. Souza, T. Wilkens, and R. M. Martin, Phys. Rev. B **62**, 1666 (2000).

[30] D. J. Scalapino, S. R. White, and S. Zhang, Phys. Rev. B **47**, 7995 (1993).

[31] R. E. Peierls, Z. Phys. **80**, 763 (1933).

[32] P. F. Maldague, Phys. Rev. B **16**, 2437 (1977).

[33] P. L. Richards and M. Tinkham, Phys. Rev. Lett. **1**, 318 (1958).

[34] P. Jordan and E. Wigner, Z. Phys. **47**, 631 (1928).

[35] E. Fradkin, Phys. Rev. Lett. **63**, 322 (1989).

[36] D. Eliezer and G. W. Semenoff, Phys. Rev. B **286**, 118 (1992).

[37] I. Dzyaloshinskii, J. Phys. Chem. Solids **4**, 241 (1958).

[38] T. Moriya, Phys. Rev. Lett. **4**, 228 (1960).

[39] H. Katsura, N. Nagaosa, and A. V. Balatsky, Phys. Rev. Lett. **95**, 057205 (2005), see also: cond-mat/0412319 (2004).

[40] K. Shiratori and E. Kita, J. Phys. Soc. Jpn. **48**, 1443 (1980).

[41] F. Meier and D. Loss, Phys. Rev. Lett. **90**, 167204 (2003).

[42] H.-A. Engel, E. I. Rashba, and B. I. Halperin, cond-mat/0603306.

[43] P. B. Allen, W. E. Pickett, and H. Krakauer, Phys. Rev. B **37**, 7482 (1988).

[44] P. Majumdar and H. R. Krishnamurthy, cond-mat/9512151.

[45] D. Coffey, T. M. Rice, and F. C. Zhang, Phys. Rev. B **44**, 10112 (1991).

[46] R. J. Elliott and M. F. Thorpe, J. Phys. C **2**, 1630 (1969).

[47] M. Kollar, private communication.

Acknowledgements

First of all, I would like to thank my advisor Prof. Dr. Arno Kampf for introducing me to the fascinating subject of condensed matter physics and for the possibility to work in his group. I appreciate his guidance throughout this project and the valuable discussions we had.

Furthermore, I thank Dr. Marcus Kollar for the fruitful cooperation, for many precious hints and for his useful comments on my manuscript. Moreover, I wish to thank Markus Schmid for the technical support and for some of his coffee. Finally, I would like to say thank you to Michael Sekania, Martin Eckstein, Andreas Hackl and all the other members of Theoretical Physics III for the open and friendly atmosphere. I hope we will be more successful in next year's soccer cup.

I am much obliged to Wolfgang Krätschmer, not only for his comments on my manuscript, but also for lots of interesting discussions. I am *very* indebted to Liisa for motivating me in strenuous times and for her continuous support. And I should not forget to thank my aunt and parents for always sticking by me.

Last but not least, special thanks go to Prof. Dr. Thilo Kopp who kindly agreed to co-report on my thesis.